universität wien

MASTERARBEIT / MASTER'S THESIS

Titel der Masterarbeit / Title of the Master's Thesis

„Chemical Pathways in Protoplanetary Discs"

verfasst von / submitted by

Robert Pohl BSc

angestrebter akademischer Grad / in partial fulfilment of the requirements for the degree of

Master of Science (MSc)

Wien, 2016 / Vienna 2016

Studienkennzahl lt. Studienblatt / degree programme code as it appears on the student record sheet:	A 066 861
Studienrichtung lt. Studienblatt / degree programme as it appears on the student record sheet:	Astronomie UG 2002
Betreut von / Supervisor:	Univ.-Prof. Dr. Manuel Güdel

And God said, “Let there be lights in the vault of the sky to separate the day from the night, and let them serve as signs to mark sacred times, and days and years, and let them be lights in the vault of the sky to give light on the earth.” And it was so. God made two great lights—the greater light to govern the day and the lesser light to govern the night. He also made the **stars**. God set them in the vault of the sky to give light on the earth, to govern the day and the night, and to separate light from darkness. And God saw that it was good. And there was evening, and there was morning—the fourth day.

Genesis 1.14-19

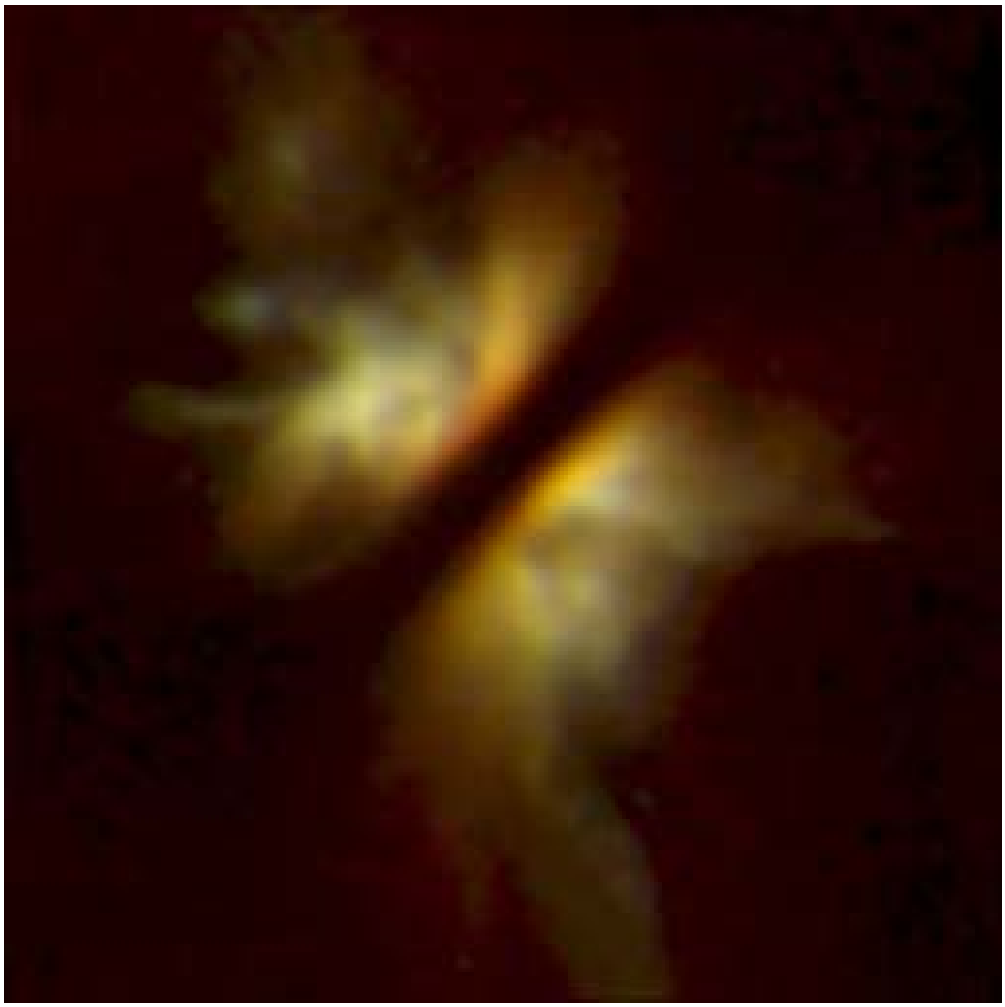

This image shows **IRAS 04302+2247**; the edge-on disk of dust and gas has a diameter of ~ 800 AU and a mass comparable to the Solar Nebula, which gave birth to Sun’s planetary system. Dark clouds and bright wisps above and below the disk suggest that it is still building up from infalling dust and gas.
(Credit: Caltech / NASA/ESA)

Acknowledgements :

I would like to thank Professor Dr. Manuel Güdel for the kind invitation to join his work group, for the help in choosing the right subject and for the thorough and inspiring correction of my thesis. I also thank Dr. Peter Woitke for the initial consultation on the thesis contents.
My sincere gratitude goes to Christian Rab MSc for supporting me in numerous stimulating discussions during my work, with the calculation programme and on the thesis itself. Last but not least, I express my gratitude to my wife Olga Barber, who made the wording British.

Contents

Frontispiece 3

A. Abstract 7
A. Zusammenfassung 8

B. Introduction 10

C. Aims and strategies of the thesis 15

D. Detailed description of chemical models 16
D.1. Stellar Disk properties 16
D.2. Calculation principles 16
D.3. Reaction sequences ('reaction trees' RT) 17

E. Design, implementation and screening of reactions 35
E.1. Specifications of models 35

F. Development of the models A – E 42
F.1. The principles of all models 42
F.2. Construction of the thesis models 43

G. Chemical reactions in reference and thesis models 47
G.1. Identification of important reactions in the models 47
G.2. Evaluation of the most important species reactions in the models 47
G.3. Compilation of model reactions 49
G.3.1. Sorting by species or by species group 49
G.3.2. Reactions present in all models 54
G.3.3. Verification of the RT reactions 56
G.3.4. Test calculation using the most important reactions 59

H. Comparison of models and discussion 60
H.1. General remarks 60
H.2. Comparing the concentration features of the models 60
H.2.1. Example log ε (CO) 61
H.2.2. Example log ε (HCO^+) 62
H.2.3. Example log ε (HCN) 63
H.3. Thermal balance of the models 64
H.4. Temperature distribution 65
H.5. Comparison of line fluxes 66
H.6. Chemical composition of the gas in the designed PPDs 68
H.6.1. Gas compositions 68
H.6.2. Chemical condensate / ice composition 69
H.6.3. Carbon distribution in the midplane 76

I. Conclusion and Outlook 78

K. Annexe 81
K.1. Annex B 81
K.2. Annex E 82
K.3. Annex F 85
K.4. Annex G 86

L. Methods and ProDiMo progam handling 98
L.1. Program steps 98
L.2. Parameter input 100
L.3. Chemical analysis 102
L.4. Program run (example model A) 104

M. Acronyms and formulae 110

N. References 111

O.1. List of Figures 115
O.2. List of Tables 116

A. Abstract

The proto-stellar phase of a low-mass star like the Sun lasts only for a short time of about $10^4 – 10^5$ years, but in this phase crucial steps in stellar evolution and the assignments for circumstellar discs take place. The mass of such protoplanetary discs in the range of ~ 0.01 $M_{Star,}$ typical for those stars, is sufficient to form a planetary system. This mass is essentially represented by H_2 and He, the origins of chemical reactions. Protoplanetary discs (PPD) are characterized by strong vertical and radial temperature and density gradients, various radiation fields at diversified disc locations. This implies rich and manifold disc chemistry both in the gas phase and on the surfaces. Based on the radially decreasing temperature, disc chemistry can be roughly divided in inner disc chemistry up to ~ 20 AU and chemistry in the outer disc regions beyond ~20 AU. This thesis presents chemical models of a protoplanetary T Tauri star disc with special attention to carbon containing reactions and species.

To reach necessary transparency it was the aim of the thesis to reduce drastically the number of elements, species and therefore reactions and to introduce target-oriented species and reactions to form a chemical network. The subsequent reactions offer a comprehensible chain to basic chemicals out of C, H, O and N.

The construction of the desired chemical network materialises in so called ‘reaction trees’ (RT), in which abundant and reactive molecules / atoms like H_3^+ and He^+ start and establish a chemical reaction sequence. This artificial network can support speculations, how such models could develop further in a protoplanetary disc reality and describe the chemical pathways there as easily as possible. Following many proven and tested chemical networks, final versions of minimised test models were used in the thesis for comparisons and discussions.

The implementation of the selected chemical networks within the calculation program ‘ProDiMo’ starts with the definition of the reference network as benchmarking for each of the models. In this thesis the version DIANA-SMALL (part of the DIANA project; q.v.: section M) was chosen as the reference model. The assessment of the various main formation and destruction reactions found 36 essential reactions commonly used in all models including the reference model and 28 other reactions shared among the thesis models only.

To appraise the advantages and disadvantages of the designed thesis models in comparison with the reference model, following features were scrutinised:

1. The concentration diagrams $\varepsilon_i = n_i / n_H$ visualised as log ε_i for the examples HCO^+ and HCN
2. Heating and cooling processes for all models;
3. Temperature distribution of two thesis models with and without condensates/ices compared with the reference model;
4. The resultant line fluxes of the species involved like: ^{12}CO, ^{13}CO, HCN, OI, CH^+, HCO^+ and N_2H^+;
5. The dominant carbon resource for thesis models compared to the reference model.

As a result of the comparisons and further considerations it is possible to create new, corrected RTs and to form functional, even more minimised chemical networks : first the 36+28 commonly used reactions in the models, secondly the 71 gas-phase reactions used in the thesis models and thirdly the 71 + 23 condensate/ice reactions. Further considerations will select the absolutely necessary reactions required to meet the conditions of the disc calculated with the ProDiMo correctly; alternatively to find a way to rearrange the code for appropriate calculations to an even further minimised model.

These test runs could be the starting point of further assessments for the thesis aims: to verify with a small number of selected reaction sequences the design of a functional network. Subsequent reactions could produce molecules which would function as building blocks for relevant organic substances like sugars, amino acids, nucleotides and the like, thus creating all the basic chemicals out of C, H, N, O, whose observation in reality has already started.

A. Zusammenfassung

Die protostellare Phase eines Sterns mit 1-2 Sonnenmassen dauert nur etwa 10^4-10^5 Jahre, aber in dieser Zeit werden entscheidende Zuordnungen für die Sternentwicklung und die der umgebenden Scheibe getroffen. Die Masse einer solchen protoplanetaren Scheibe mit etwa ~ 0,01 M_{Star} reicht aus, um ein Planetensystem zu bilden und wird im Wesentlichen von den Elementen Wasserstoff und Helium repräsentiert, die auch die Ausgangselemente für die chemischen Reaktionen darstellen. Protoplanetare Scheiben (PPD) sind gekennzeichnet durch starke vertikale und radiale Temperatur-und Dichtegradienten sowie von verschiedenartigen Strahlungsfeldern in den unterschiedlichen Scheibenebenen, was eine ergiebige, mannigfaltige Scheibenchemie sowohl in der Gasphase als auch auf Festkörpern hervorruft. Die chemischen Reaktionen in der Scheibe können aufgrund der radial abnehmenden Temperatur in eine innere Region bis etwa 20 AU und eine äußere außerhalb dieses Radius aufgeteilt werden. In dieser Arbeit wird das chemische Modell einer PPD um einen T Tauri Stern gezeigt mit einer speziellen Ausrichtung auf Reaktionen sowie Moleküle und Ionen, die Kohlenstoff enthalten.

Um eine ausreichende Klarheit der Aussage zu erhalten, war es das Ziel dieser Arbeit, sowohl die Anzahl der Elemente als auch der Moleküle / Ionen (Spezies) und somit die Fülle der Reaktionen drastisch zu beschränken, die ein chemisches Netzwerk schaffen, mit dem durch nachfolgende Reaktionen eine nachvollziehbare Reaktionskette zu Basischemikalien bestehend aus C, H, O, und N dargestellt werden kann. Die Konstruktion des gewünschten Netzwerkes verwirklichte sich in “Baumdiagrammen“ (RT), zu denen reaktive Moleküle/Ionen wie H_3^+ und He^+ den Anfang eines Reaktionsablaufs bildeten. Dieses künstliche chemische Netzwerk könnte Spekulationen anregen, wie sich solch ein Model in der Realität einer PPD weiterentwickeln und in möglichst einfacher Weise beschreiben ließe. Nach vielen erprobten chemischen Netzwerken wurden endgültige Varianten der Test-Modelle für diese Arbeit in Vergleichen und Diskussionen verwendet.

Die Durchführung der Berechnung mit den gewählten Modellen im Kalkulationsprogramm „ProDiMo“ beginnt mit der Definition eines Referenznetzwerks als Leistungsvergleich. In dieser Arbeit wurde die Variante DIANA_SMALL (Teil des DIANA Projektes ; siehe Kapitel ‚M’) als Referenzmodell gewählt. Durch die Bewertung der verschiedenen Hauptaufbau– und Abbaureaktionen wurden 36 Reaktionen gefunden, die von allen Modellen und auch vom Referenzmodell gleichermaßen genutzt wurden, sowie 28 andere, die nur in den Modellen der Arbeit Verwendung fanden.

Zur eingehenden Prüfung der Vor- und Nachteile der entworfenen Modelle der Arbeit im Vergleich mit dem Referenzmodell wurden einige Kenndaten untersucht:

1. Konzentrationsdiagramme $\varepsilon_i = n_i / n_H$ visualisiert als log ε_i mit den Beispielen HCO^+ und HCN;
2. Heiz- und Kühlprozesse aller Modelle;
3. der Vergleich der Temperaturverteilung zweier Modelle mit und ohne Kondensate/Eise mit dem Referenzmodell;

4. die Linien-Flussdichten der beteiligten Spezies wie: ^{12}CO, ^{13}CO, HCN, OI, CH^+, HCO^+ und N_2H^+;
5. das bevorzugte Speichermedium für Kohlenstoff der Modelle der Arbeit verglichen mit dem Referenzmodell.

Das Ergebnis der Vergleiche und weitere Überlegungen eröffnet die Möglichkeit neue, korrigierte RTs zu entwerfen, sowie funktionelle, weiter minimierte chemische Netzwerke zu erstellen: erstens mit den 36+28 Reaktionen, die gemeinsam in den Modellen benutzt werden, zweitens die 71 Gasphasen Reaktionen und drittens mit den 71+23 Reaktionen, die auch die Reaktionen mit Kondensaten in den Modellen der Arbeit einbeziehen. Durch weitere Überlegungen können die absolut notwendigen Reaktionen herausgefunden werden, die zur Kalkulation mit dem Programm ProDiMo zur korrekten Behandlung der Scheibengegebenheiten benötigt werden oder eine Programmierung gefunden wird, die eine entsprechende Kalkulation mit einem weiter minimierten Modell gestattet.
Solche Testkalkulationen können der Anfang weiterer Beurteilungen der Arbeitsziele sein: mit einer kleinen Anzahl ausgewählter Reaktionsfolgen die Erstellung eines funktionierenden chemischen Netzwerks zu schaffen. Folgereaktionen stellen Moleküle her, die als Baueinheiten für maßgebliche organische Substanzen wie Zucker, Aminosäuren, Nukleotiden und dergleichen dienen, die also alle die Grundchemikalien aus C, H, O, und N herstellen, dessen Beobachtungen in den PPDs bereits begonnen haben.

B. Introduction:

The proto-stellar phase of a low-mass star like the Sun lasts only for a short time of about 10^4 -10^5 years, but this phase is crucial for the evolution of the star. The mass of such protoplanetary disc is essentially represented by H_2 and He, the origin of chemical reactions and typical for those stars in the range of ~ 0.01 M_{Star}; this mass is sufficient to form a planetary system. Furthermore, protoplanetary discs are characterized by strong vertical and radial temperature and density gradients, various radiation fields at diversified disc locations. This implies a rich and manifold disc chemistry, photochemistry, molecular-ion reactions, neutral-neutral reactions, gas-grain surface interactions, and grain surface reactions. A summary of relevant reactions is provided in Annex B.0. Based on the radially decreasing temperature, disc chemistry can be roughly divided in inner disc chemistry up to ~ 20 AU and chemistry in the outer disc regions beyond ~20 AU.
A schematic diagram of a protoplanetary disc with its physical and chemical structure is given in Fig.B.1. below and a picture of a typical disc by a Hubble telescope observation is shown on the frontispiece page.

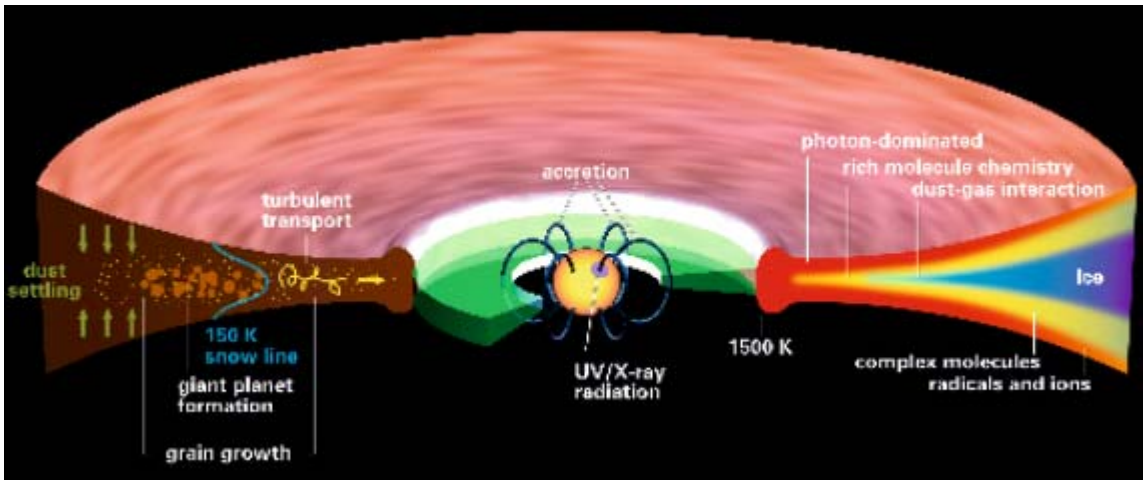

Fig. B.1.: Schematic diagram of a protoplanetary disc with its physical and chemical structure of a ~ 1-5 Myr. old PPD around a Sun like T Tauri star. Explanations in the diagram (courtesy of Henning & Semenov 2013)

In this thesis chemical models of a protoplanetary T Tauri star disc are presented with special attention to carbon containing reactions and species. The evaluation of chemical reactions in protoplanetary discs (PPD) has a long tradition:
1. One model for gas-phase chemistry in interstellar clouds was reported in the early eighties; it was denominated as basic model and library of chemical reactions and chemistry among C, N, and O compounds (Prasad & Huntress 1980). It illustrated principal chemical reactions involved in C-H, C-C, O-H, C-O, N-H and C-N chemistry as well as the coupling between O-H, C-O, C-H, N-H, and C-N. In fact there were all conceivable reactions present, regardless of their observability at that time.
2. The ion chemistry of interstellar clouds was compiled; the conclusion was that most of the molecules in space are formed by gas-phase processes and dominated by ion-molecule reactions. The described network diversifies with the starting species CH_3^+ and has its origin in cosmic ray ionised molecular hydrogen (H_2) and helium (He) (Smith 1992).
3. The same route was already described by Herbst and Klemperer (1973); both identified key-processes, and gathered about 50 reactions for C, H, He, N, O, S and metals in

accordance with kinetic and thermodynamic aspects. At the same time these reactions were studied in some laboratories in order to provide comparative data for observations.
4. The chemistry of small translucent molecular clouds was evaluated; it described nitrogen chemical networks with 21 nitrogen species. The network starts with the reaction N_2 and He^+:

$$N_2 + He^+ \rightarrow N^+ + N + He$$

and has a central exchange point with $HNCH^+$ e.g.:

$$N + CH_3^+ \rightarrow HNCH^+ + H$$

The molecules HCN and HNC play prominent roles: their abundances appear high enough to affect the hydrocarbon chemistry of the network (Turner 1997).
5. In astrophysical environments lacking dust, molecules can only be formed through gas-phase chemistry; the sum of reactions e.g.:

$$X+Y \leftrightarrow XY + \boldsymbol{h\nu}$$

can be separated either to $\{ X+ e^- \rightarrow X^- + \boldsymbol{h\nu}$ followed by $X^- + Y \rightarrow XY + e^- \}$

in dust free medium or, on the contrary with dust to:

$$X + dust \rightarrow X\text{-}dust \; ; \; X\text{-}dust + Y \rightarrow XY + dust + IR\ radiation$$

(Stancil 1998).

6. Some new H and H_2 reactions with small hydrocarbon ions, which contribute to benzene synthesis in dense interstellar clouds, describe certain initial sequences of ion-neutral reactions leading to hydrocarbon products in the ISM (McEwan 1999).
7. Reappraisals of chemical reaction chain proposals took place as soon as detection accuracy and observability increased. Since then more complex organic molecules have been discovered in PPD; several interesting complex molecules were detected lately. A good example is amino-acetonitril [NH_2CH_2CN], discovered in a hot core of a star-forming region with a fractional abundance of $\sim 10^{-9}$ (Blagojevich 2003). This molecule can be transformed to glycine, the simplest amino-acid. However, the required homochirality, one of the prerequisites of life as we know it, is still an unsolved problem.
Several other routes to the formation of glycine (and other simple amino acids) under interstellar conditions have already been proposed via Strecker synthesis (e.g.: Danger 2011):

$$RCHO + NH_3 \rightarrow [RCH{=}NH]^* + HCN \rightarrow [RCHNH_2CN]^* + H_2O$$

$$\rightarrow RCHNH_2COOH \qquad []^* \text{ means activated mode}$$

8. Quite recently the primary data of chemical reaction sequences have been updated on the basis of observational facts and complemented by heterogeneous chemistry which takes place on grain surfaces. This chemistry has become an important, if not dominant route of molecule formation.
All the rate coefficients relevant for the chemical networks and their temperature dependences have to be known in detail to set up chemical models that illustrate the product

channels and their subsequent branching reactions. The overview of chemical reactions and their classification is collected in the Annex B.0. (Schlemmer 2015).

Of special interest and directly in the focus of this thesis is the chemistry of PPDs around T-Tauri objects. These discs will somewhere along their way become solar-type planetary systems and / or coagulate into comets or meteorites, carrying the occurred chemistry.

Opposite to chemical models in ISM, clouds, solar nebula and the like, PPD models result from diversity of extensive chemical kinetics, which are based on myriads of reactions. This requires intensive computer-aided simulation models. Special attention has to be paid to thermal gas balances, various heating and cooling processes, photoelectric heating of gas, dust heating and cooling mechanisms, heating by PAHs, gas-grain collisions, line cooling of atoms and so forth. All things considered it is a difficult and demanding effort.

Solving the thermal balance and chemical equations in a dynamic equilibrium has been applied to PPDs in a manageable program, named ProDiMo, developed by Woitke et al. (2009). ProDiMo is the basic program used for the present thesis.

In a PPD assuming a Sun-like star, H_2 is the most abundant molecule, representing together with helium almost its total mass. H_2 is formed out of hydrogen atoms by recombination on surfaces of dust grains. In this so called midplane / freeze-out layer (see layer C in Fig.B.2.) the chemistry starts with H_2, initiated by cosmic-ray particles, high energy radiation or X-rays and H_2 ionized as well as helium to H_2^+ and He^+. H_2^+ reacts further with the next H_2 molecule:

$$H_2^+ + H_2 \rightarrow H_3^+ + H$$

which is very exothermic ($\Delta H^0 = \sim 1.7$ eV) and fast (rate coefficient $2 \cdot 10^{-9}$ [$cm^3 s^{-1}$])

A reaction between He^+ and H_2 is possible and exothermic but requires high activation energy.

The ionization of most species is caused by H_3^+ and/or He^+, which are the starting reactions for the reaction channels in this thesis. Differences must be considered in the reactions of H_3^+ and He^+ with N_2 :

$$H_3^+ + N_2 \rightarrow N_2H^+ + H_2 \quad \text{but}$$
$$He^+ + N_2 \rightarrow N + N^+ + He$$

This is because of helium's large ionization potential (24.6 eV).

Moreover condensed species on dust grains, in water ice as carrier, reach much higher concentrations and therefore higher collision probabilities to 'meet' the required counter molecule / ion for chemical reaction than in the gas-phase. Diffusion of hydrophilic substances is elevated in sub-cooled melted water ice.

The current perception of chemical processes, which determine the ionisation structure of a PPD with a central star, can be summarised as follows:

In a typical disc, there is a multitude of chemical reactions that steer the fractional ionisation in different parts of the disc. The disc is by common understanding divided into three layers (depicted in Fig. B.2.)

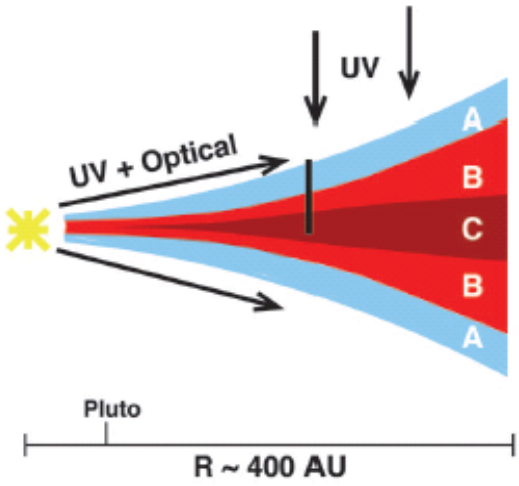

Fig.B.2. : Protoplanetary disc where three chemically distinct zones are indicated (VanDishoeck 2006):
(A) photon-dominated layer
(B) warm molecular layer
(C) midplane freeze-out layer

In the midplane (C) the ionisation is only feasible by cosmic rays and radioactive elements because of shielding effects. The chemistry, which determines the fractional ionisation, is very simple: reduced networks with typically ~ 10 species and a limited number of reactions.
Above the midplane the intermediate layer (B) is located, where the ionisation is performed by X-rays. This layer turns out as the most complex area as far as chemistry is concerned and delivers most of the questions, how a chemical equilibrium might be constructed. Numerous reactions can take place: different types of ion-ion, neutral-ion, radical- and neutral- neutral reactions are feasible and have to be considered. Consequently, more than hundred species with thousands of reactions have to be analysed. In the surface layer (A) UV photons dominate the ionisation; again, a reduced network can be constructed (Semenov et al. 2004).

As elaborated above, intensive computer-aided simulation models were constructed to calculate thermal gas balances, photoelectric gas and dust heating processes as well as cooling mechanisms heating by PAHs, gas-grain collisions and line cooling of atoms.

Looking retrospectively, the first calculation models were developed for chemical composition studies of planets and primitive bodies in the solar system in 1996 (Aikawa et al.). Until 2013, 46 models were reported with different approaches and results (compilation in: Henning and Semonov 2013 ; see Annex B.1. 'calculation models'). Some of the milestone models dealing with different radiations / irradiations and numbers of element and species for chemical networks are mentioned in the following:

1. Meijerink and Glassgold (2007), presented a thermal-chemical model, where stellar X-rays play an important role in heating the upper gas layers of circumstellar discs. Their chemical network contains about 125 reactions and 25 species, however, concentrating on X-ray irradiation on sulphur, neon and carbon.

2. Woods and Willacy (2008) presented chemical models of a T-Tauri stage disc and a minimum mass solar nebula, paying particular attention to the fractionation of carbon-bearing species. The chemical reaction network is based on the UMIST99 gas-phase rate

file, with two additions: firstly, cosmic ray heating and thermal desorption and secondly, treatment of X-ray chemistry. In total the reaction network comprises 475 gas and grain species and more than 8000 gas phase and surface reactions. Approximately three quarters of these reactions involve ^{13}C, which makes the model-calculations complex.

3. Kamp and Dullemond (2004) constructed a model where dust and gas temperatures are generally equal within 10% for A_V >~0.1. The chemical network consists of 47 species which were connected through 266 reactions, including neutral-neutral, ion-molecule, photo-ionization and photo-dissociation reactions. The model accounts for cosmic-ray induced photoreactions and charge- exchange reactions. Neither grain surface reactions nor ice formation are included. It has a limited species and reaction portfolio and concentrates on models for the vertical temperature structure of the disc.

4. Woitke, Kamp and Thi (2009) presented a thermo-chemical model named ProDiMo capable for calculating physical, thermal and chemical structure of PPDs. The benefits of the modelling through ProDiMo lie in fully coupled treatment of 2D dust continuum radiative transfer, gas phase and photochemistry, ice formation, heating and cooling balance and the hydrostatic disc structure.

In particular, the authors use the calculated radiation field as input for the photo-chemistry and as background continuum for the non-local thermodynamic equilibrium modelling of atoms, ions and molecules. Another advantage of the code is the robustness of its kinetic chemistry module which is applicable to densities between 10^2 and 10^{16} [cm^{-3}]. This enables a complete modelling of discs ranging from the dust condensation radius to several hundred AU.

The heating & cooling balance of the gas in the disc depends like the chemical reactions on the local continuous radiation field and the local dust temperature. These are the results of: photo ionization / photo dissociation, radiative pumping, adsorption and desorption from grain to gas, and they depend on each other (ProDiMo short description in: Woitke et al. 2009).

The ProDiMo code is used in this work to calculate the selected element-, species- and reaction portfolios of the thesis models; these results are compared to the reference model (DIANA_SMALL; explained in section D.2.).

The chemical data base for the ProDiMo is the UDfA Database UMIST in the version of 2012 (see details in Annex B.2.-4.), which has been developed over the past 20 years by the continuous compilation of rate coefficients of chemical reactions which may be important in the interstellar medium. However, in these models the role of grain surfaces is not included in the file except the formation rate of H_2 on grain surfaces.

The current problem in astrochemistry is how to integrate the surface chemistry as accurately as possible in the calculation. In surface chemistry, where diffusion processes are involved, the calculations of rate coefficients in hydrophilic or hydrophobic condensates or in cool areas below ~50 K in e.g. microcrystalline ices are very difficult and complicated. A conclusive approach to treat the surface chemistry correctly remains to be found. Therefore, the proposal to ignore the surface chemistry in the first instance, until reliable methods are available, is the declared approach in this thesis.

C. Aims and strategies of the thesis:

The thesis aims to establish new chemical pathways in PPDs by minimising the number of reactions under perpetuation of the calculation assumptions; it follows the established modelling ways by means of the ProDiMo code.

Six elements (H, He, C, O, N, Fe) were selected for this work, although the standard dust composition includes other elements, e.g.: Mg / Si / S / Ca / K / Na / Al…..in form of condensed minerals. It is presumed that the condensed minerals do not take part in the gas phase reactions, especially not at lower temperatures. Chemical pathways ought to be constructed for the gas phase reactions and for the reactions which include condensates / ices. Adsorption and desorption of molecules to and from condensates occurs in a steady state.

The species in the surrounding gas phase can undergo gas/gas reactions as well as reactions on surfaces, where they might have different activation energies, kinetic properties and behaviour. The reactions at solid state or in under-cooled liquids are diffusion related and complex; they are not considered in this thesis, because the calculation is very problematic.

The crucial point of the thesis is not to simply reduce the number elements, species and reactions; the aim is to find a fitting, stable chemical network of reactions which result in molecules / ions as building blocks out of C, H, N, O, producing life-based components, i.e. sugars, amino acids and nucleonic acids.

This chemical network is achieved through the design of reaction trees (RT), where abundant reactive molecules and ions establish chemical reaction sequences. The basis of the design is a bundle of reaction sequences: a primary RT provides one or more produced species as reactants for the next RT; there the species act as the beginning of another sequence. In that manner sequence after sequence is constructed, always reflecting a plausible chemistry with documented rate coefficients and energetic advantages.

The artificial RT systems should lead to a consistent chemical network as it may happen in a PPD reality, aiming to describe chemical pathways as simply as possible.

In the chapter D (‘Detailed chemical models’), the construction starts with the most prominent and abundant species hydrogen and helium, ionised by cosmic rays before they begin to react subsequently and form reaction sequences. The final result should provide insight into the chemistry feasible under the conditions of a standard star.

D. Detailed description of chemical models:

D.1. Stellar Disk properties

In terms of comparability with the selected reference model and calculation program it is important to keep some conditions constant, in particular the parameters of the star, the disk and the dust. Any change in the chemical network has therefore direct effect on its functionality. Tab. D.1.1. comprises the most important stellar and dust parameters (for more details see Section L 'methods' with the file 'parameter.in').

Stellar and disk parameter			
Parameter	Symbol	Value	Dimension
Stellar mass	M*	0.7	M_{Sun}
effective temperature	T_{eff}	4000.0	°K
stellar luminosity	L_{star}	1.0	L_{sun}
excess UV	f_{UV}	0.01	LUV/Lstar
UV powerlaw exponent	pUV	1.0	
X-ray luminosity	Xray lum.	1.0 10+30	erg/s
X-ray emission temp.	Xray Temp..	2.0 10+7	°K
disk mass	Mdisk	0.01	M_{Sun}
dust-to-gas mass ratio	Mdust/Mgas	0.01	
cosmic ray ionisation H2	CRI	1.3 10-17	1/s
strength incident bgr* UV	χ_ISM	1.0	Draine field**
Dust properties:			
dust grain density	ρ_{grain}	2.094	g/cm-3
min. dust part. size	a_{min}	0.05	µm
max.dust part size	a_{max}	3000	µm
dust size distrib.power index	a_{pow}	3.5	
dust settling		2.0	
turbulence α	a_{settle}	1.3 10-3	
max.hollow volume ratio		0.8	
Dust composition:			
MgO+7 FeO+3SiO3		0.60	Vol.fract.
amorphous carbon [Zubko]		0.15	Vol.fract.
vacuum		0.25	Vol.fract.

Tab. D.1.1. : Stellar and disk standard parameter for the model calculations (Woitke 2009; 2015 submitted); more details see Section L 'methods ; parameter.in' .
*) bgr = background radiation
**) Mean interstellar field = Draine field ~ 2 x 10^{-4} erg cm^{-2} s^{-1} sr^{-1}

D.2. Calculation principles

This work uses a radiation thermo-chemical model of PPDs as developed for the DIANA project (Woitke et al. 2009), named 'DIANA-SMALL' (abbr. DM) as benchmarking for the thesis models. Further details of DM follow in section E. All calculations in the DM model utilise the UMIST (University of Manchester Institute of Science and Technology) database for astrochemistry and their 'Rate2012' release.

Other databases for astrochemistry e.g.: KIDA (Kinetic Database for Astrochemistry) and the NIST (National Institute for Science and Technology) chemistry WebBook were occasionally consulted to double-check certain data.

The work involves many steps: back reactions have to be added, positive ions must be neutralized, mainly by electrons and positively charged molecules or the use of dissociative recombination.
To start chemical networks the most abundant species hydrogen and helium H_2 and He are ionised by cosmic rays to form their reactive cations H_2^+ and He^+, before they can react further. The thesis describes these reaction sequences in so called 'reaction trees' (RTs), suitable to design and understand the chosen chains which form relevant organic molecules.
The decisions for the suitable sequences were taken on the basis of chemically reasonable reactions which are kinetically and thermodynamically feasible.
The UMIST 2012 data base was of great help as a guide and as data source for the selected reactions.
For the sake of clarity the system UMIST 2012 is shown for each relevant reaction including the kinetic data and corresponding accuracy. The literature quotation of the source is directly given at that point to avoid confusion with the reference section N for the text. An important note for a numbering dilemma in UMIST 2012 is given below.

Example for documentation:

database	Index	α	β	γ	T_l - T_u (K)	Accuracy	Source
UMIST2012	reaction no.	=rate coeff.	If =0	If=0	valid temp.range	code→annex	Lit.or measurm.

e.g.: Reference: Mitchell, 1990, Phys. Rep., 186, 215.

UMIST2012 =Rate12; Index shows the reaction number; α, ß, γ are the Arrhenius plot factors / exponents; if ß=γ=0 than α= rate coefficient.
UMIST is a permanently replenished data set, but unfortunately the addenda of new reactions change the reaction numbers of each new version; furthermore, the reaction numbers on the UMIST website and UMIST download numbers do not match. In this thesis all reaction numbers in 'database' have been changed to DM numbers, if existing.

The calculation of the rate coefficient utilises the Arrhenius-Kooji formula and the a.m. mentioned factors α, β and γ (e.g.: McElroy 2013):

$$k = \alpha \left(\frac{T}{300}\right)^{\beta} \exp\left(\frac{-\gamma}{T}\right) \quad \mathrm{cm^3 s^{-1}}$$

In cases where a correction of the rate coefficient k seems to be interesting, the appropriate calculations are mentioned in the documentation.

D.3. Reaction sequences ('reaction trees' RT)

The construction of the reaction sequences as "reaction trees" (RT) follows a special pattern seen in the diagram below: the formation reactions "A+B" and "D+E" with their corresponding DM reaction numbers in brackets result in the molecule or ion "C". This "C" reacts further with "F" and "G" and so forth in destruction reactions to different

molecules charged or uncharched as well as ions or atoms. Also in this case the DM reaction number is mentioned.

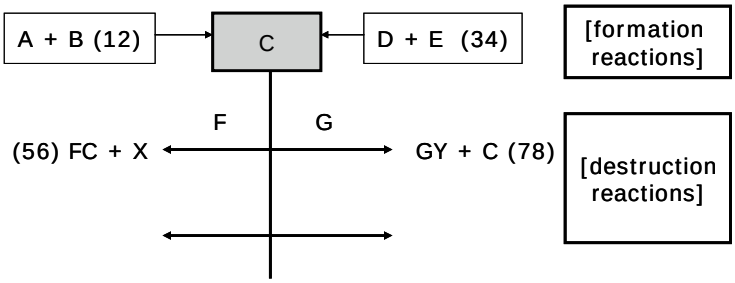

Fig.D.3.1. : Pattern of the RT: formation reactions "A+B" and "D+E" give the molecule or ion "C". Subsequent reaction with "F" and "G" in destruction reactions. All are given with their corresponding DM reaction numbers in brackets.

Reactions of H_3^+:

The starting point / first reaction for number one sequence was the high energy containing trihydrogen cation H_3^+, which is formed out of the most abundant element in universe H / H_2 by energetic radiation and /or cosmic particles (CRP) as well as X-rays by subsequent reactions 733 and 2614.

$$H_2 + CRP \rightarrow H_2^+ + e^- \quad \text{or} \quad \{H_2 + X\text{-}ray \rightarrow H_2^+ + e^-\}$$

leading to different **α**

Database	Index	α	β	γ	T_l - T_u (K)	Accuracy	Source
RATE12	733	1.20e-17	0.00	0.00	10 - 41000	factor 2	Literature Search n.f.

$$H_2^+ + H_2 \rightarrow H_3^+ + H$$

Database	Index	α	β	γ	T_l - T_u (K)	Accuracy	Source
RATE12	2614	2.08e-9	0.00	0.00	10 - 41000	within 25%	Measurement

Reference: Theard, L.P. and Huntress, W.T., J. Chem. Phys., 60, 2840 (1974).

Comparing the rate coefficients of both reactions, the first reaction is unambiguously the decisive step: 10^{-17} vs. 10^{-9}[cm^3 sec^{-1}]. There are more reactions to form H_2^+ but CRPs take effect in any PPD layer. For instance the reaction with He^+ with almost 10^{-14}[cm^3 sec^{-1}]:

$$H_2 + He^+ \rightarrow H_2^+ + He$$

Database	Index	α	β	γ	T_l - T_u (K)	Accuracy	Source
RATE12	459	7.20e-15	0.00	0.00	10 - 300	factor 2	Measurement

Reference: Barlow, 1984, PhD Thesis, University of Colorado.

The molecule H_3^+ was included in the primary "reaction tree" (RT), deriving all most probable reactions of the following models.

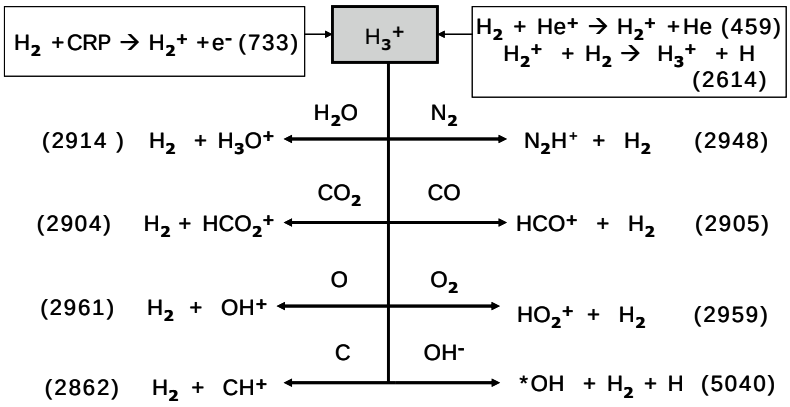

Fig. D.3.2. : Reactions of formation and destruction of H_3^+ for the proposed models.
Numbers in brackets correspond to the DM reaction numbers. *OH is the hydroxyl radical.

Reactions of He^+ :

In the RT for the proposed models similar reactions were performed with the He^+ ion, which is produced via reactions 736 and 10501with rate coefficients of 6.5 10^{-18}[cm^3 sec^{-1}] and 1.3 10^{-17}[cm^3 sec^{-1}] respectively.

$$He + CRP \rightarrow He^+ + e^-$$

Database	Index	α	β	γ	T_l - T_u (K)	Accuracy	Source
RATE12	736	6.50e-18	0.00	0.00	10 - 41000	factor 2	Literature Search

$$He + XPHOT \rightarrow He^+ + e^-$$

Database	Index	α	β	γ	T_l - T_u (K)	Accuracy	Source
ProDiMo	10501	1.30e-17	0.00	0.20	10 - 41000	factor 2	Literature Search
		Scaling by X-ray radiation field					

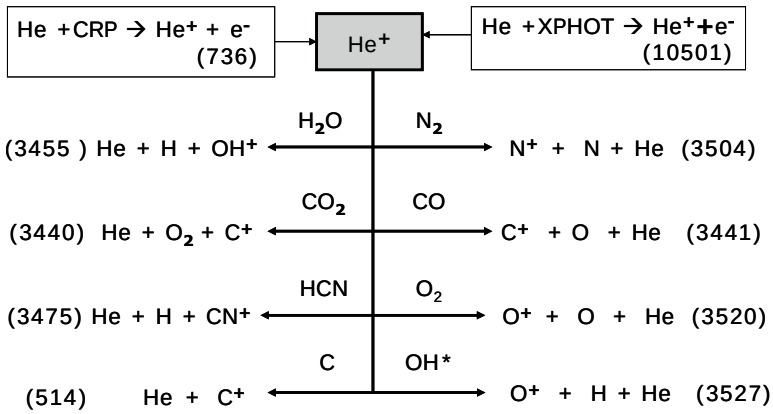

Fig. D.3,3, : Reactions of formation and destruction of He^+ for the proposed models.
Numbers in brackets correspond to the PDM reaction numbers. *OH is the hydroxyl radical.

Reactions of N_2H^+ :

There is one more crucial reaction using the product of nitrogen and the trihydrogen cation to start reaction sequences. The very reactive diazenylium cation N_2H^+ is known from interstellar clouds since 1974. The diazenylium cation was likewise used in a RT proposal.

$$H_3^+ + N_2 \rightarrow N_2H^+ + H_2$$

Database	Index	α	β	γ	T_l - T_u (K)	Accuracy	Source
RATE12	2948	1.80e-9	0.00	0.00	10 - 41000	within 25%	Measurement

Reference: Rakshit, A.B., Int. J. Mass Spectrom. Ion Phys., 41, 185 (1982).

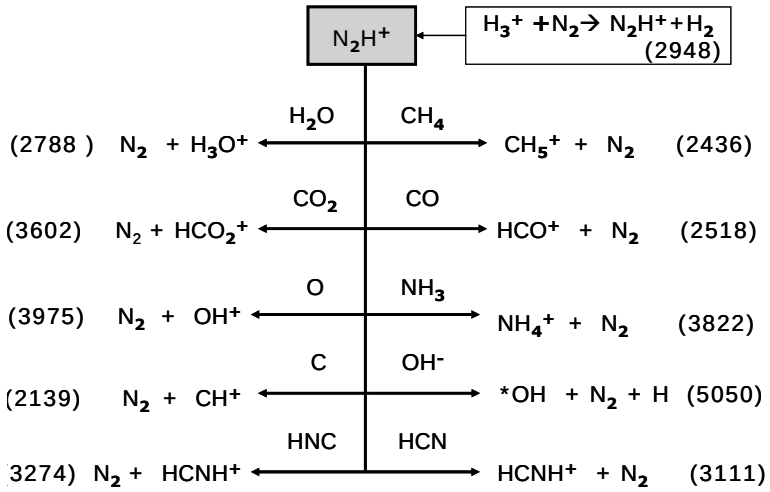

Fig.D.3.4. : Reactions of formation and destruction of N_2H^+ for the proposed models.
Numbers in brackets correspond to the DM reaction numbers. *OH is the hydroxyl radical.

Reactions of CO :

The first attention is paid to the carbon / oxygen reaction chain and the reactions where carbon monoxide or the –CO- group is involved. Several reactions were already shown in the destruction parts of the highly reactive cations (H_3^+ , N_2H^+ and He^+) using carbon monoxide and carbon dioxide.

Carbon monoxide plays a central role in Universe as reaction partner for activated proton (H^+) due to high CO abundance in ISM, dense clouds, PPDs and stellar envelopes .

CO undergoes a lot of important reactions for formation and destruction out of a bulk of diversified molecules.
The most popular reaction for the formation of CO under earth conditions in huge quantities (industrial production) has ΔH^0 of +132 kJ/mol and is therefore omitted from the astrochemical databases.

$$C + H_2O \rightarrow CO + H_2 \qquad \Delta H^0 = +132 \text{ kJ/mol}$$

The reaction 5208 was used instead for the CO synthesis out of the elements, but the rate coefficients are relatively low:

$$C + O_2 \rightarrow CO + O \qquad \Delta H^0 = -394 \text{ kJ/mol}$$

Database	Index	α	β	γ	T_l - T_u (K)	Accuracy	Source
RATE12	5208	5.56e-11 k= 1.6e-10 k= 5.0e-12	0.41	-26.90	10 - 8000 1000 K 10 K	factor 2	Measurement

Reference: Smith, I.W.M., Herbst, E., Chang, Q., 2004, MNRAS, 350, 323.

The reaction 5208 is preferable thermodynamically but not kinetically. The RT also contains the reaction sequence, which is using the C^+ ion first and reacts further with oxygen to CO^+ and closes the loop by ionisation of carbon, outlined in the following short form:

$$C + \gamma \rightarrow C^+ + e^- \qquad \text{or} \qquad C + CRP \rightarrow C^+ + e^-$$

$$C^+ + O_2 \rightarrow CO^+ + O$$

$$CO^+ + C \rightarrow CO + C^+$$

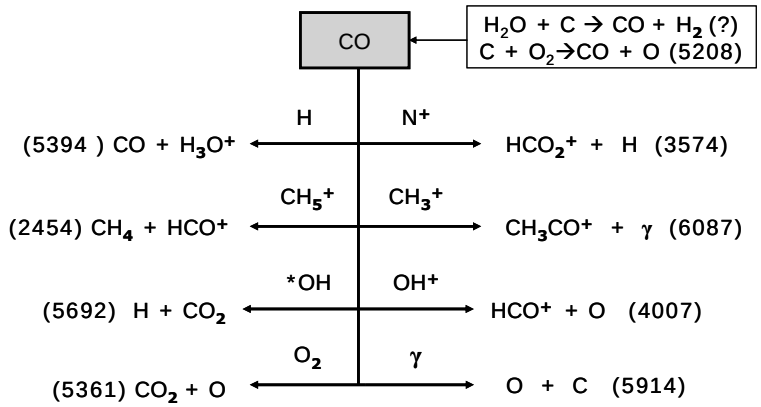

Fig.D.3.5. : Reactions of formation and destruction of CO for the proposed models. Numbers in brackets correspond to the DM reaction numbers. *OH is the hydroxyl radical, γ is a photon, reaction 6087 included in the UMIST2012 regime but not in DM.

The acetyl cation (CH_3CO^+) offers lots of further reactions for complex organic compounds; the chosen formation reaction 6087 has a medium rate coefficient of about 10^{-13} [cm^3 sec^{-1}] and uses the conversion of CH_3^+ .

$$CH_3^+ + CO \rightarrow CH_3CO^+ + \gamma$$

Database	Index	α	β	γ	T_l - T_u (K)	Accuracy	Source
RATE12	6087	1.20e-13 k = 1.0e-12	-1.30	0.00	10 - 300 10 K	factor 2	Measurement

Reference: Herbst, 1985, ApJ, 291, 226.

However, another reaction 2410 has a bit better rate of 10^{-11} [cm^3 sec^{-1}]:

$$CH_4 + CO^+ \rightarrow CH_3CO^+ + H$$

Database	Index	α	β	γ	T_l - T_u (K)	Accuracy	Source
RATE12	2410	5.20e-11	0.00	0.00	10 - 41000	within 25%	Measurement

Reference: Adams, N.G., Smith, D., and Grief, D., Int. J. Mass Spectrom. Ion Phys., 26, 405 (1978).

Below is shown an important, fast down-reaction, that gives high reactive ketene molecules for various reactions with amines, alcohols and other complex organic compounds.

$$CH_3CO^+ + e^- \rightarrow H_2CCO + H$$

Database	Index	α	β	γ	T_l - T_u (K)	Accuracy	Source
RATE12	1201	3.00e-7	-0.50	0.00	10 - 300	factor 2	Literature Search
		k=1.6e-6			10 K		

S.Muller et.al. ,Astron. Astrophys. 535, (2011) Art. No. A103.

Reactions of HCO^+ :

Very important reaction paths in the PPDs are oxygen / carbon containing sequences.
The formylium cation = hydrogenated carbon monoxide cation HCO^+ , which is of pivotal significance in molecular clouds and in PPDs, is produced by the trihydrogen cation (H_3^+) and the diazenylium cation (N_2H^+) with carbon monoxide (CO) in the fast reactions 2905, 2518 respectively. The rate coefficients are around ~10^{-9} [cm^3 sec^{-1}].

$CO + H_3^+$:

Database	Index	α	β	γ	T_l - T_u (K)	Accuracy	Source
RATE12	2905	1.36e-9	-0.14	-3.40	10 - 400	within 25%	Calculation
		k = 2.0e-9			10 K		
		k = 1.9e-9			400 K		

Reference: Kim, J.K., Theard, L.P., and Huntress, W.T., Chem. Phys. Lett., 32, 610 (1975).

$CO + N_2H^+$:

Database	Index	α	β	γ	T_l - T_u (K)	Accuracy	Source
RATE12	2518	8.80e-10	0.00	0.00	10 - 41000	within 25%	Measurement

Reference: Bohme, D.K., Mackay, G.I., and Schiff, H.I., J. Chem. Phys., 73, 4976 (1980); Herbst, E., Bohme, D.K., Payzant, J.D., and Schiff, H.I., Astrophys. J., 201, 603 (1975); Payzant, J.D., Schiff, H.I., and Bohme, D.K., J. Chem. Phys., 63, 149 (1975).

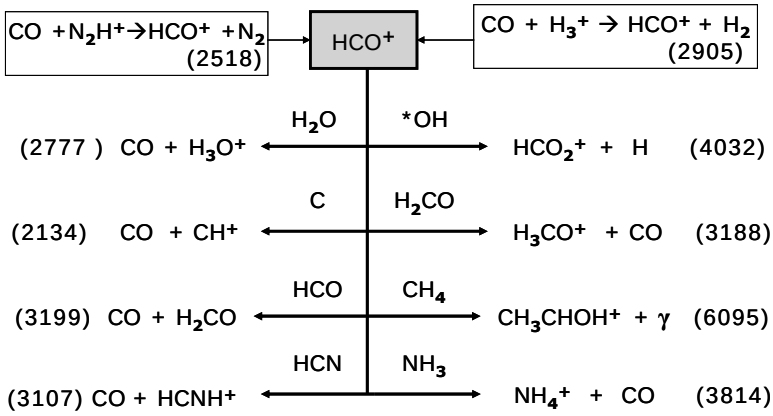

Fig.D.3.6. : Reactions of formation and destruction of HCO^+ for the proposed models. Numbers in brackets correspond to the DM reaction numbers. *OH is the hydroxyl radical**,** **γ** is a photon, reaction 6095 included in the UMIST2012 regime but not in DM.

The reaction of HCO^+ with methane to hydrogenated acetaldehyde (CH_3CHOH^+) has a relatively low rate coefficient. Notwithstanding, it is important for further reactions to complex organic compounds and cyanopolyynes.

$HCO^+ + CH_4$:

Database	Index	α	β	γ	T_l - T_u (K)	Accuracy	Source
RATE12	6095	1.00e-17	0.00	0.00	10 - 300	factor 2	Literature Search

Reference: Herbst & Leung, 1989, ApJS, 69, 271.

Reactions of C^+ :

Carbon and carbohydrates in form of cations are the origin of interesting, very diversified reaction chains. The first focus is on the carbon cation C^+.
Reactions with the hydrogen bearing reactive species will not lead to the carbon cation, only He+ is able to react with carbon, carbon monoxide and carbon dioxide (514, 3441, 3440 resp.) with rate coefficients from ~10^{-9} to ~10^{-16} [cm^3 sec^{-1}] and produces C^+ (see also the He^+ RT):

$He^+ + C$:

	Index	α	β	γ	T_l - T_u (K)	Accuracy	Source
RATE12	514	6.30e-15 k = 4.9e-16	0.75	0.00	10 - 300 10 K	factor 2	Literature Search

Reference: Kimura & Dalgarno, 1993, Chem. Phys. Letts., 211, 454.

$He^+ + CO$:

Database	Index	α	β	γ	T_l - T_u (K)	Accuracy	Source
RATE12	3441	1.60e-9	0.00	0.00	10 - 41000	within 25%	Measurement

Reference: Anicich, V.G., Laudenslager, J.B., Huntress, W.T., an Futrell, J.H., J. Chem. Phys., 67, 4340 (1977); Laudenslager, J.B, Huntress, W.T., and Bowers, M.T., J. Chem. Phys., 61, 4600 (1974).

$He^+ + CO_2$:

Database	Index	α	β	γ	T_l - T_u (K)	Accuracy	Source
RATE12	3440	4.00e-11	0.00	0.00	10 - 41000	within 25%	Measurement

Reference: Anicich, V.G., Laudenslager, J.B., Huntress, W.T., an Futrell, J.H., J. Chem. Phys., 67, 4340 (1977); Laudenslager, J.B, Huntress, W.T., and Bowers, M.T., J. Chem. Phys., 61, 4600 (1974).

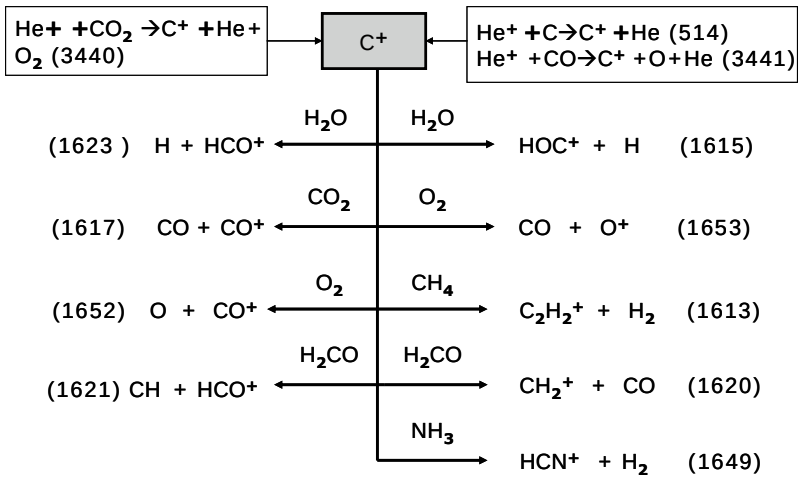

Fig.D.3.7. : Reactions of formation and destruction of C^+ for the proposed models. Numbers in brackets correspond to the PDM reaction numbers. Reaction 1615 is present in the UMIST2012 regime but not in DM.

The RT of C^+ shows interesting reactions, unfortunately the reaction with oxidane (H_2O) leaves only one of two possible end products; DM neglects the HOC^+ product, in spite of its better rate coefficient compared to HCO^+ (~10^{-9} to ~ 10^{-11}[cm^3 sec^{-1}]):

$C^+ + H_2O \rightarrow HOC^+$:

Database	Index	α	β	γ	T_l - T_u (K)	Accuracy	Source
RATE12	1615	2.09e-9	-0.50	0.00	10 - 41000	within 25%	Measurement
		k = 1.1e-8			10 K		
		k = 1.1e-9			1000 K		

Reference: Anicich, V.G., Huntress, W.T., and Futrell, J.H., Chem. Phys.Lett., 40, 233 (1976); Watson, W.D., Anicich, V.G., and Huntress, W.T., Astrophys. J. Lett., 205, L165 (1976).

$C^+ + H_2O \rightarrow HCO^+$:

Database	Index	α	β	γ	T_l - T_u (K)	Accuracy	Source
RATE12	1623	9.00e-10	-0.50	0.00	10 - 41000	within 25%	Measurement
		k = 5.0e-9			10 K		
		k = 4.9e-10			1000 K		

Reference: Anicich, V.G., Huntress, W.T., and Futrell, J.H., Chem. Phys.Lett., 40, 233 (1976); Watson, W.D., Anicich, V.G., and Huntress, W.T., Astrophys. J. Lett., 205, L165 (1976).

Reactions of CH^+ :

All reactions with carbon (C) and the trihydrogen cation (H_3^+), the diazenylium cation (N_2H^+) , the formylium cation (HCO^+) and the hydroperoxyl cation (O_2H^+) produce the methylidyne cation CH+ in the reactions 2862, 2139, 2134 and 2143 respectively. The rate coefficients are all in the same range of about 10^{-9}[cm^3 sec^{-1}].

$H_3^+ + C \rightarrow CH^+ + H_2$:

Database	Index	α	β	γ	T_l - T_u (K)	Accuracy	Source
RATE12	2862	2.00e-9	0.00	0.00	10 - 41000	factor 2	Literature Search

Reference: Prasad & Huntress, 1980, ApJS, 43, 1.

$N_2H^+ + C \rightarrow CH^+ + N_2$:

Database	Index	α	β	γ	T_l - T_u (K)	Accuracy	Source
RATE12	2139	1.10e-9	0.00	0.00	10 - 41000	factor 2	Literature Search

Reference: Prasad & Huntress, 1980, ApJS, 43, 1.

$HCO^+ + C \rightarrow CH^+ + CO$:

Database	Index	α	β	γ	T_l - T_u (K)	Accuracy	Source
RATE12	2134	1.10e-9	0.00	0.00	10 - 41000	factor 2	Literature Search

Reference: Prasad & Huntress, 1980, ApJS, 43, 1.

$O_2H^+ + C \rightarrow CH^+ + O_2$:

Database	Index	α	β	γ	T_l - T_u (K)	Accuracy	Source
RATE12	2143	1.00e-9	0.00	0.00	10 - 41000	factor 2	Literature Search

Reference: Prasad & Huntress, 1980, ApJS, 43, 1.

The methylidyne cation can undergo further reactions, shown in the following RT:

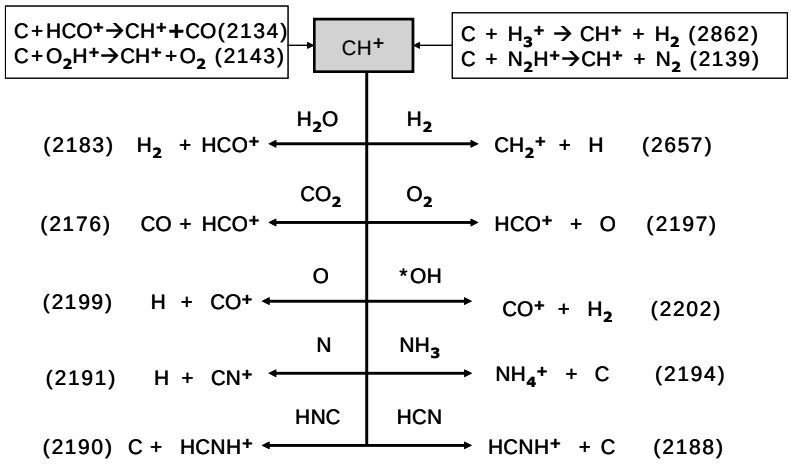

Fig.D.3.8. : Reactions of formation and destruction of CH^+ for the proposed models.
*OH is the hydroxyl radical**,** numbers in brackets correspond to the DM reaction numbers.

Reactions of CH_2^+ :

Hydrogenation of the methylidyne cation delivers the methylene cation CH_2^+ in the reaction 2657 with a rate coefficient in the range of $\sim 10^{-9}$ [cm^3 sec^{-1}].

$CH^+ + H_2 \rightarrow CH_2^+ + H$:

Database	Index	α	β	γ	T_l - T_u (K)	Accuracy	Source
RATE12	2657	1.20e-9	0.00	0.00	10 - 41000	within 25%	Measurement

Reference: McEwan, Scott, Adams et al., 1999, ApJ, 513, 287.

This methylene cation can react as described below:

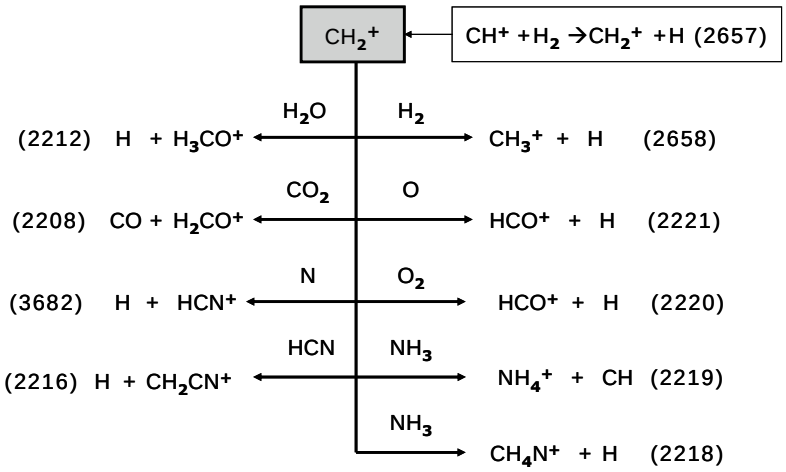

Fig.D.3.9. : Reactions of formation and destruction of CH_2^+ for the proposed models. Numbers in brackets correspond to the DM reaction numbers.

Reactions of CH_3^+ :

Following the route of carbocations, methenium CH_3^+ is formed by hydrogenation of the methylene cation CH_2^+ in the reaction 2658 with a rate coefficient in the range of $\sim 10^{-9}$ [cm^3 sec^{-1}].

$CH_2^+ + H_2 \rightarrow CH_3^+ + H$:

Database	Index	α	β	γ	T_l - T_u (K)	Accuracy	Source
RATE12	2658	1.60e-9	0.00	0.00	10 - 41000	within 25%	Measurement

Reference: Smith, D. and Adams, N.G., Int. J. Mass Spectrom. Ion Phys., 23, 123 (1977); Smith, D. and Adams, N.G., Chem. Phys. Lett., 47, 383 (1977).

Methenium can react in a very diversified way; it delivers above all species with positively charged N-bearing molecule parts such as protonated acetonitrile (CH_3CNH^+).

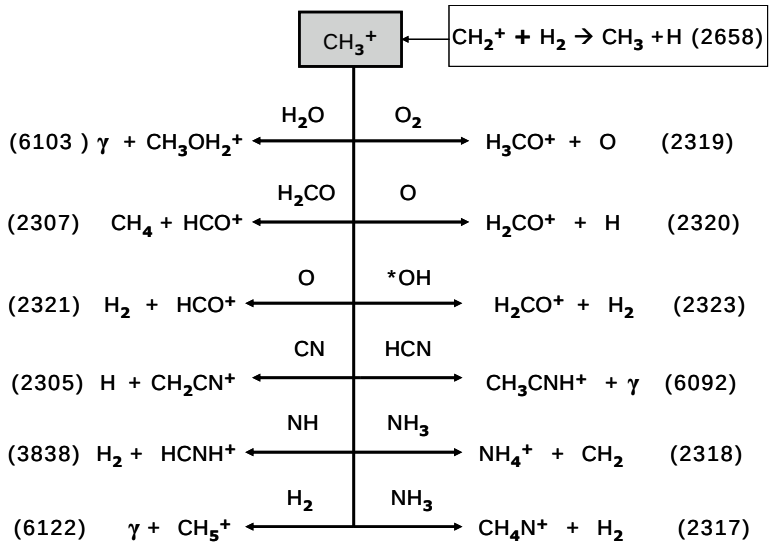

Fig.D.3.10. : Reactions of formation and destruction of CH_3^+ for the proposed models. Numbers in brackets correspond to the DM reaction numbers. **γ** is a photon, *OH is the hydroxyl radical**,** Reaction 6092 is present in the UMIST2012 regime, but not in DM.

Although the protonated acetonitrile CH_3CNH^+ is, like other nitriles, rather important for subsequent reactions (e.g. to: amides, carbonic acids, amidoesters, iminoesters etc.), it is not included in the DM reference model. The very fast reaction has a rate coefficient of about 10^{-8} [cm^3 sec^{-1}]:

Database	Index	α	β	γ	T_l - T_u (K)	Accuracy	Source
RATE12	6092	9.00e-9 k = 5.0e-9	-0.50	0.00	10 - 300 10 K	factor 2	Measurement

Reference: Herbst, 1985, ApJ, 291, 226.

Reactions of CH_5^+ :

Hydrogenation of the methenium cation CH_3^+ delivers the methylene cation methanium or protonated methane (CH_5^+) in the reaction 6122, with a low rate coefficient in the range of 10^{-16} [cm^3 sec^{-1}] :

$CH_3^+ + H_2 \rightarrow CH_5^+ + \gamma$:

Database	Index	α	β	γ	T_l - T_u (K)	Accuracy	Source
RATE12	6122	3.92e-16 k = 1.1e-13 k = 3.7e-16	-2.29	21.30	10 - 300 10 K 300 K	factor 2	Literature Search

Reference: Smith, 1989, ApJ, 347, 282.

On the contrary, methane (CH_4) hydrogenated by H_3^+ offers a much faster possibility:

$H_3^+ + CH_4 \rightarrow CH_5^+ + H_2$:

Database	Index	α	β	γ	T_l - T_u (K)	Accuracy	Source
RATE12	2899	2.40e-9	0.00	0.00	10 - 41000	within 25%	Measurement

Reference: Bohme, D.K., Mackay, G.I., and Schiff, H.I., J. Chem. Phys., 73, 4976 (1980); Herbst, E., Bohme, D.K., Payzant, J.D., and Schiff, H.I., Astrophys. J., 201, 603 (1975); Payzant, J.D., Schiff, H.I., and Bohme, D.K., J. Chem. Phys., 63, 149 (1975).

The structure of CH_5^+ is very complex and different from other molecules, in which the atoms have fixed places. In case of protonated methane, based on quantum effects, the five hydrogen atoms move around the carbon centre in a 'hydrogen scrambling'.

Notwithstanding, CH_5^+ is very reactive and stable below 20K e.g.: in the outer disk.

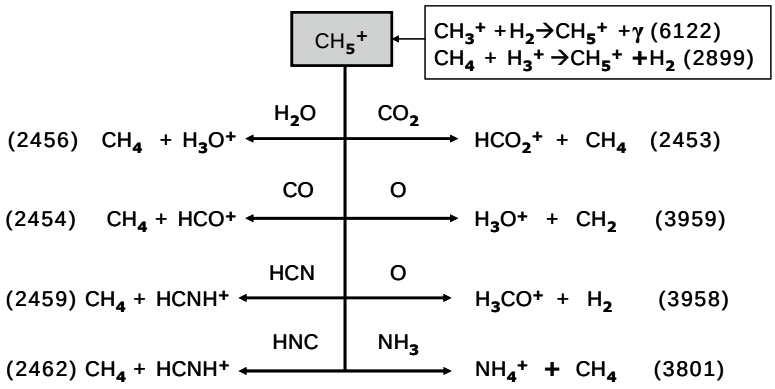

Fig.D.3.11.: Reactions of formation and destruction of CH_5^+ for the proposed models. Numbers in brackets correspond to the DM reaction numbers.

Reactions of HCN :

As with almost all carbon / carbon-hydrogenated cations the reaction with hydrogen cyanide and hydrogen isocyanide results in the same protonated form $HCNH^+$. This high reactive molecule–ion is observable in many gas-phases around stellar objects.

HCN / HNC is found in space with a high abundance ($5\text{-}7\cdot10^{-5}$ rel. to H_2) [J=1→ 0 transition: HCN~ 88.6 and ~86.3 ; HNC~90.66, all in GHz], therefore reactions with HCN and HNC are interesting. They appeared already in previous RTs.

The formation of HCN takes place in reaction (1649) or (3682) to HCN^+ and is followed by neutralization through H (491) :

$C^+ + NH_3 \rightarrow HCN^+ + H_2$

Database	Index	α	β	γ	T_l - T_u (K)	Accuracy	Source
RATE12	1649	1.20e-10 k = 1.1e-10	0.00	-0.50	10 - 41000 10 K	within 25%	Measurement

Reference: Smith, D. and Adams, N.G., Chem. Phys. Lett., 47, 145 (1977).

$CH_2^+ + N \rightarrow HCN^+ + H$

Database	Index	α	β	γ	T_l - T_u (K)	Accuracy	Source
RATE12	3682	2.20e-10	0.00	0.00	10 - 41000	within 25%	Measurement

Reference: Viggiano, A.A, Howarka, F., Albritton, D.L., Fehsenfeld, F.C., Adams, N.G., and Smith, D., Astrophys. J., 236, 492 (1980).

$$HCN^+ + H \rightarrow HCN + H^+$$

Database	Index	α	β	γ	T_l - T_u (K)	Accuracy	Source
RATE12	491	3.70e-11	0.00	0.00	10 - 41000	factor 2	Literature Search

The formation of Isonitril HNC, using the formed HCN, to react further to $HCNH^+$ by reaction 3036:

$$HCN + H_3O^+ \rightarrow HCNH^+ + H_2O$$

Database	Index	α	β	γ	T_l - T_u (K)	Accuracy	Source
RATE12	3036	3.80e-9	-0.50	0.00	10 - 41000	within 25%	Measurement
		k = 4.0e-9			10 K		
		k = 2.1e-9			1000 K		

Reference: V. G. Anicich, *Cometary Comae//Interstellar Clouds*, J. Phys. Chem. Ref. Data, 22, 1469(1993).

Subsequently, the charge equalization fission to hydrogen-isocyanide (1351) follows.

$$HCNH^+ + e^- \rightarrow HNC + H$$

Database	Index	α	β	γ	T_l - T_u (K)	Accuracy	Source
RATE12	1351	9.50e-8	-0.65	0.00	10 - 300	within 25%	Measurement
		k = 8.7e-7			10 K		

Reference: Semaniak, J., Minaev, B.F., Derkatch, A.M., et al., 2001, ApJS, 135, 275.

Both reactants were used in the different RTs. The RT of HCN is given as example

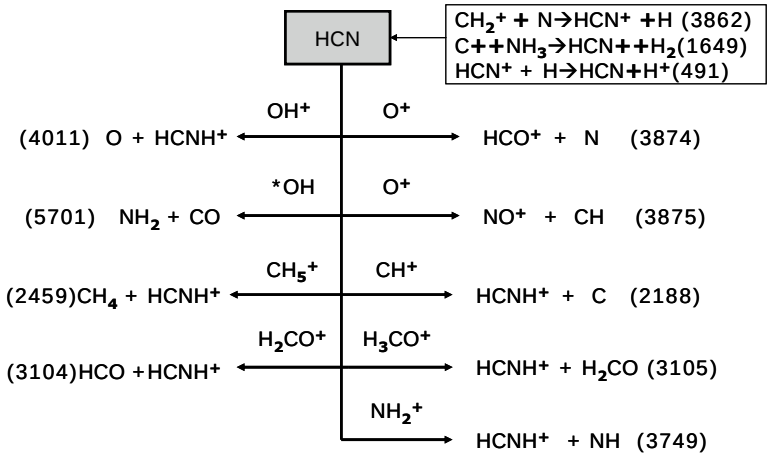

Fig.D.3.12. : Reactions of formation and destruction of HCN for the proposed models.
*OH is the hydroxyl radical. Numbers in brackets correspond to the DM reaction numbers.

The previously mentioned highly reactive hydrogen cyanide and hydrogen isocyanide come out in many reactions in their protonated form $HCNH^+$.

Reactions of CN^+ :

The formation reaction for the chemically related cyan-cation CN^+ uses CH+ and nitrogen (2191) and appears first in the aforementioned RT for CH^+.

$CH^+ + N \rightarrow CN^+ + H$:

Database	Index	α	β	γ	T_l - T_u (K)	Accuracy	Source
RATE12	2191	1.90e-10	0.00	0.00	10 - 41000	within 25%	Measurement

Reference: Viggiano, A.A, Howarka, F., Albritton, D.L., Fehsenfeld, F.C., Adams, N.G., and Smith, D., Astrophys. J., 236, 492 (1980).

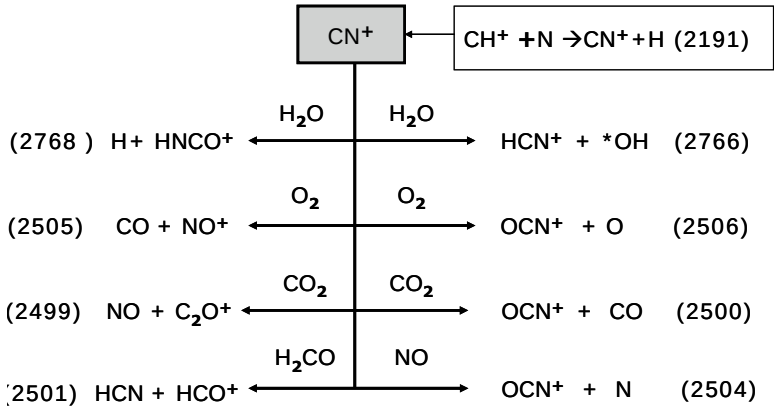

Fig.D.3.13 : Reactions of formation and destruction of CN^+ for the proposed models.
*OH is the hydroxyl radical. Numbers in brackets correspond to the DM reaction numbers.

CN^+ offers different reactions to the same reactants as oxidane and oxygen shown above, as well as reactions to highly reactive molecules such as OCN^+ and C_2O^+; these can for example form the ethenonium cation HC_2O^+ in a fast reaction:

$$C_2O^+ + H_2O \rightarrow HC_2O^+ + H_2$$

Database	Index	α	β	γ	T_l - T_u (K)	Accuracy	Source
RATE12	3125	1.00e-9	-0.50	0.00	10 - 41000	factor 2	Literature Search
		k = 5.5e-9			10 K		
		k = 9.4e-8			1000 K		

Reference: I.Cherneff, arxiv.org/pdf/0907.3621 ; UMIST1999-2012 all the same alpha without reference

It is a very reactive cation and yields to groups of lactones, esters, amides, organic acids; it undergoes dimerization, oligomerisation and other reactions. It could be considered as one of the focal points to life-giving molecules.

Reactions of O^+ :

Several reactions with the oxygen cation O^+ seemed to be important but only a few of them were used in the ProDiMo model calculations. The main formation reactions use He^+ (3520) and C^+ (1653), whilst the last reaction produces CO as well:

$He^+ + O_2 \rightarrow O^+ + O + He$:

Database	Index	α	β	γ	T_l - T_u (K)	Accuracy	Source
RATE12	3520	1.10e-9	0.00	0.00	10 - 41000	within 25%	Measurement

Reference: Adams, N. and Smith, D., Int. J. Mass Spectrom. Ion Phys., 21, 349 (1976) and J. Phys. B, 9, 1439 (1976).

$C^+ + O_2 \rightarrow O^+ + CO$

Database	Index	α	β	γ	T_l - T_u (K)	Accuracy	Source
RATE12	1653	4.54e-10	0.00	0.00	10 - 41000	within 25%	Measurement

Reference: Smith, D. and Adams, N.G., Int. J. Mass Spectrom. Ion Phys., 23, 123 (1977); Smith, D. and Adams, N.G., Chem. Phys. Lett., 47, 383 (1977).

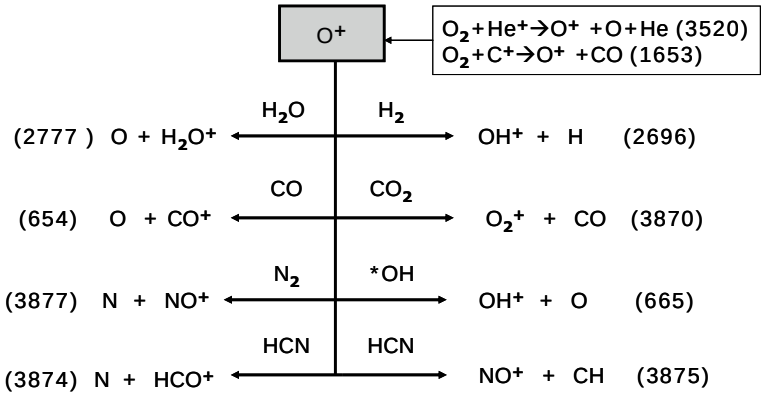

Fig.D.3.14.: Reactions of formation and destruction of O^+ for the proposed models. *OH is the hydroxyl radical**.** Numbers in brackets correspond to the DM reaction numbers.

Reactions of O_2H^+ :

Another highly reactive molecule is the hydro peroxide cation O_2H^+; its main formation reaction (2959) starts with oxygen and trihydrogen cation:

$$H_3^+ + O_2 \rightarrow O_2H^+ + H_2$$

Database	Index	α	β	γ	T_l - T_u (K)	Accuracy	Source
RATE12	2950	9.30e-10	0.00	100.00	10 - 3000	within 25%	Literature Search
		k = 5.5e-9			10 K		
		k = 9.4e-8			1000 K		

Reference: Adams, N.G. and Smith, D., Chem. Phys. Lett, 105, 604 (1984).

The RT of the hydroperoxide cation shows hydrogenation reactions; in all cases oxygen is one of the products.

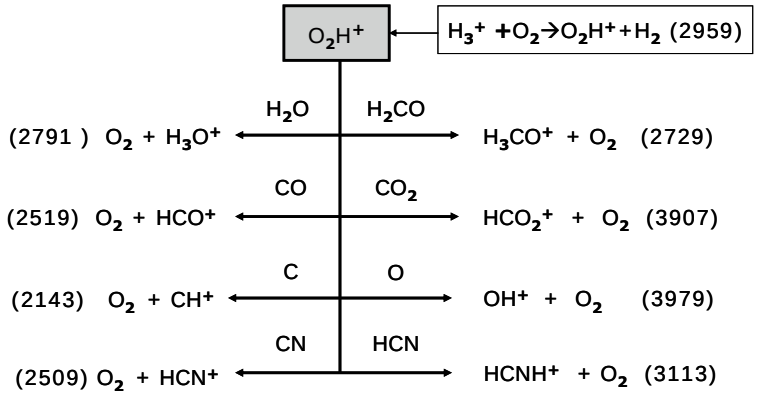

Fig.D.3.15. : Reactions of formation and destruction of O_2H^+ for the proposed models.
*OH is the hydroxyl radical. Numbers in brackets correspond to the DM reaction numbers.

In this RT, the reaction to protonated carbon dioxide HCO_2^+ (3907) [$4_{04} - 3_{03}$ lines observed at 85.53 and 106.91GHz] is important to the models, however, the formation competes with 2904, which takes the direct route from H_3^+ with a higher rate coefficient:

$O_2H^+ + CO_2 \rightarrow HCO_2^+ + O_2$:

Database	Index	α	β	γ	T_l - T_u (K)	Accuracy	Source
RATE12	3907	1.10e-9	0.00	0.00	10 - 41000	within 25%	Measurement

Reference: Lininger, W., Albritton, D.L., Fehsenfeld, F.C., Schmeltekopf, A.L., and Ferguson, E.E., J. Chem. Phys., 62, 3549 (1975).

$H_3^+ + CO_2 \rightarrow HCO_2^+ + H_2$

Database	Index	α	β	γ	T_l - T_u (K)	Accuracy	Source
RATE12	2904	2.00e-9	0.00	0.00	10 - 41000	within 25%	Measurement

Reference: Rakshit, A.B., Int. J. Mass Spectrom. Ion Phys., 41, 185 (1982).

A bunch of reactions followed up to this cation either ionic or bi-radically, forming new molecules / ions. The ionic reactions have rate coefficients of approximately 10^{-9} [cm^3 sec^{-1}].

Reactions of *OH (hydroxyl radical)**:**

Extremely reactive are radicals in circum-stellar envelopes, dense clouds and the like; this also applies to the *OH radical. The selected formation reactions are the only reactions with the negatively charged hydroxyl ion (OH^-), either 5040 or 5050. This ion is formed by oxidane dissociation [$2\ H_2O \rightarrow H_3O^+ + OH^-$]. Both reactions are new in UMIST2012 and surprisingly have the same rate coefficients.

$H_3^+ + OH^- \rightarrow *OH + H_2 + H$

$N_2H^+ + OH^- \rightarrow *OH + N_2 + H$

Database	Index	α	β	γ	T_l - T_u (K)	Accuracy	Source
RATE12	5040	7.51e-8	-0.50	0.00	10 - 41000	Factor 10	Estimate
		k = 4.3e-7			10 K		
		k = 4.1e-8			1000 K		

Reference: Nanase Harada and E.Herbst, A&A J.,685, 1, 272 (2008)

RATE12	5050	7.51e-8	-0.50	0.00	10 - 41000	Factor 10	Estimatet

Reference: Nanase Harada and E.Herbst, A&A J.,685, 1, 272 (2008).

Remark to References: In this article there are 46 reactions with the same rate coefficient, but in the article no OH^- is mentioned. There are $[C_xH_y]^-_{n;m}$ cited only!!

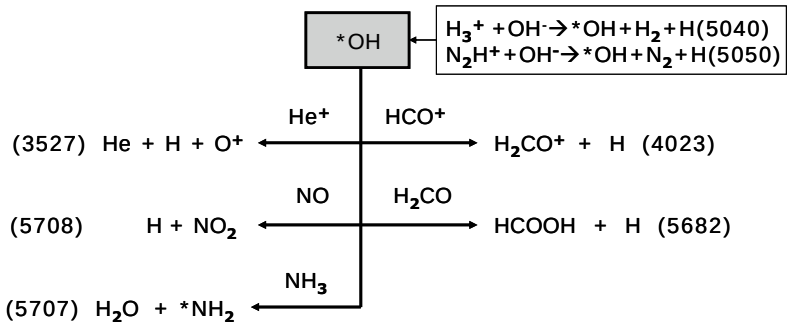

Fig.D.3.16. : Reactions of formation and destruction of *OH radical for the proposed models.
Numbers in brackets correspond to the DM reaction numbers.
Reaction 5682 and the formation reactions are present in the UMIST2012 regime but not in DM.

The *OH radical is a prominent species in the category of highly reactive molecules. It is converting to further reactive molecules in gas-phase reactions with the formylium cation to protonated formaldehyde:

$$*OH + HCO^+ \rightarrow H_2CO^+ + H$$

Database	Index	α	β	γ	T_l - T_u (K)	Accuracy	Source
RATE12	4023	1.00e-9	-0.50	0.00	10 - 41000	factor 2	Literature Search
		k = 5.5e-8			10 K		
		k = 5.5e-10			1000 K		

Subsequently it reacts with protonated formaldehyde to formic acid (HCOOH), which is an oxidation process representing a live-common substance. Both reactions were not included in DM.

$$*OH + H_2CO \rightarrow HCOOH + H$$

Database	Index	α	β	γ	T_l - T_u (K)	Accuracy	Source
RATE12	5682	2.00e-13	0.00	0.00	298 - 298	within 25%	Measurement

Reference: Mallard et al., 1994, NIST Chemical Kinetics Database, NIST, Gaithersburg, MD.

The low rate coefficient of formation and the instability against H_3^+ / CRP makes HCOOH sensitive in subsequent reactions; e.g. the fast decay back to the formylium cation:

$$H_3^+ + HCOOH \rightarrow HCO^+ + H_2O + H_2$$

Database	Index	α	β	γ	T_l - T_u (K)	Accuracy	Source
RATE12	2921	4.30e-9	-0.50	0.00	10 - 41000	within 25%	Measurement
		k = 2.4e-8			10 K		
		k = 2.4e-9			1000 K		

Reference: Mackay, G.I., Hopkinson, A.C., and Bohme, D.K., J. Am. Chem. Soc., 100, 7460 (1978).

However, HCOOH might be frozen out (at ~ 280 K) before it disintegrates; in this case it acidifies the condensates / ices around dusts / grains and supports reactions under acid conditions.

The first phase of the thesis has been accomplished in two steps: the probable RTs have been constructed and the reactions, which can give insight into the preferred chemistry under the conditions of an imaginary celestial body, evaluated.

The second phase of the thesis, described in Section E, shows how a severely reduced chemical network can be managed by the calculation program ProDiMo.

E. Design, implementation and screening of reactions

The implementation of the selected chemical network into the calculation program ProDiMo starts with the definition of the standard network, which is benchmarking tool for each of the DIANA projects (project data in section O 'Acronyms and formulae').
In the purpose of this thesis the version DIANA-SMALL has been chosen as the reference model; in the following named DM. It is necessary for the above mentioned steps to understand the structure of this reference model and its specifications, in order to learn how to construct the thesis models.

E.1. Specifications of DM

The DM construction has the following characteristics:

1. The reference model operates with 12 elements; their abundances, relative to the total hydrogen number density, are collected in Tab.E.1.1.:

Elements & Abundances	
H	1,0000
He	$9.64\ 10^{-2}$
C	$1.38\ 10^{-4}$
N	$7.94\ 10^{-5}$
O	$3.02\ 10^{-4}$
Ne	$8.91\ 10^{-5}$
Na	$2.29\ 10^{-9}$
Mg	$1.07\ 10^{-8}$
Si	$1.74\ 10^{-8}$
S	$1.86\ 10^{-7}$
Ar	$1.20\ 10^{-6}$
Fe	$1.74\ 10^{-9}$

Tab. E.1.1.: Elements and abundances of the reference model **DM**

2. Species input: 90 species, contained in UMIST 2012, are shown in Tab. E.1.2.

UMIST 2012 Species input for Reference Model DM :					
H	CH2+	CO2	HN2+	SO2	Na
H+	CH3	CO2+	NO	SO2+	Na+
H-	CH3+	HCO2+	NO+	HSO2+	Na++
H2	CH4	N	O	S	Mg
H2+	CH4+	N+	O+	S+	Mg+
H3+	CH5+	N++	O++	S++	Mg++
H2exc	CN	NH	OH	Si	Fe
He	CN+	NH+	OH+	Si+	Fe+
He+	HCN	NH2	H2O	Si++	Fe++
C	HCN+	NH2+	H2O+	SiH	Ne
C+	HCNH+	NH3	H3O+	SiH+	Ne+
C++	CO	NH3+	O2	SiH2+	Ne++
CH	CO+	NH4+	O2+	SiO	Ar
CH+	HCO	N2	SO	SiO+	Ar+
CH2	HCO+	N2+	SO+	SiOH+	Ar++

Tab. E.1.2. : 90 UMIST2012 species of the reference model **DM**

3. Additional reaction partners:
Another necessary part of the reactions are energy carriers, electrons to neutralize the cations and surfaces like dust for adsorption / desorption of condensates and dimerisation of atomic hydrogen. They have no concentration limit.

PHOTON
CRP(cosmic ray particles)
CRPHOT(cosmic ray photons)
XPHOT(for X-ray chemistry)
e^- (electron)
dust(defined in Tab.D.1.1.)

4. Condensates / ices species input for the reference model DM:

Condensates / ices input:			
CO#	CH4#	HCN#	SiO#
H2O#	NH3#	N2#	
CO2#	O2#	SO2#	

Tab. E.1.2. : Condensates / ices for the reference model **DM.**

5. There are 81 reactions to be added to the calculation, which are not part of the UMIST2012 chemical data base: 36 include the X-ray chemistry into all models, 16 electron reactions (demanding/producing) and 27 reactions between cations and neutral species, 2 reactions concerning hydrogen formation (a complete list to be found in Annex E Tab.E.1.3.).

Species and reactions of the reference model DM are listed below in Tab.E.1.5.:

Model	**Species** (number)	**UMIST** reactions	**reactions** cond./ices	**Total***	**photo-reactions** dissociations	ionisation	**mult temp.fit** reactions
DM	100	1065	142	1288	42	13	13

Tab. E.1.5. : Overview of the reference model **DM**, the different reactions in number and
*) including the 81 reactions described in E.1.5. and listed in Annex E Tab.E.1.3.

The selection of reactions to meet the aims of the thesis leads to construction of thesis models; the calculations by ProDiMo system evaluate the accuracy of the selected chemical networks. To get a quick overview, the constructed minimised interim models ("Ch.10"-"Ch.28" [Ch.=chemical model]) were calculated in small 15 times 15 grid point matrixes. This measure facilitated short calculation times and immediate results which allowed to alter, if necessary, the reaction sequence either by adding or removing reaction(s). The overview also supplies the answer whether the interim model is able to produce the required species or react further with it. This is the way to establish requested reaction sequences to guarantee for a consistent chemical network and functional images.

Each step is checked by the program ‘chemical analysis’; more explanation follows in the section L ‘methods’.
Below is an example of three network steps showing the development towards a reasonable sequence. The numbers in the diagrams are identifiers of the equivalent reaction numbers of the DM / UMIST2012 regime readout with the ProDiMo program steps ‘chemical analysis’ and ‘text’ ; q.v. section L ‘methods’.
Details of the involved reaction follow below. The illustrations take CO as an example:

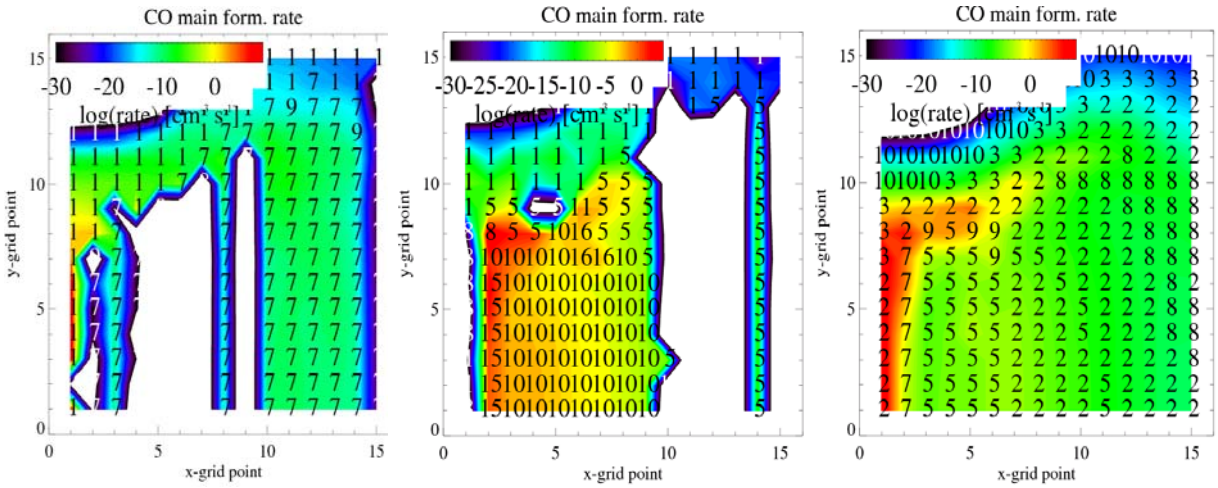

Fig.E.1.4.1.: Development of a chemical network improvement in a 15/15 grid. Formation rates of the example CO using the ProDiMo program part ‘chemical analysis’ for interim models Ch.23 (left), Ch.24 (middle) and Ch.28 (right) [Ch.=chemical model]

The calculation code ProDiMo produces blank spaces in the diagrams of the grid point matrix areas; in case the species in question has a very low concentration / is not produced. Alternatively, a numerical deviation has occurred. These blank spaces are described by the words ‘disturbance’, ‘disturbing’ and ‘distort’.
After screening with the crude 15/15 grid point matrix the outcome was ~360 reactions; these were confirmed in the next stage with a matrix of 30/30 grid point, which brought higher accuracy, but demanded longer calculation time.

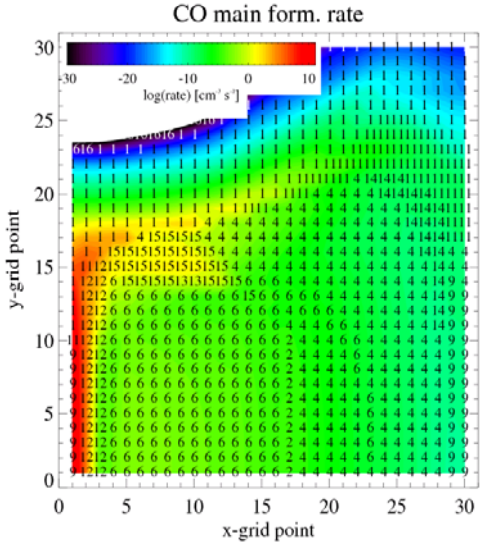

Fig.E.1.4.2. : Development of a chemical network improvement in a 30/30 grid point matrix. Formation rates of CO for interims models “Ch.30”.

At the end of that very time consuming process and designing new interim models "Ch. 29 to 40", 232 reactions remain in model "Ch.40".The 'fine-tuning' step at 40/40 grid point matrix verified the interim 30/30 matrix results and identified the most critical reactions in "Ch. 40". Consequently, the reactions, which would distort the results, were taken out. All this effort was absolutely necessary for a reliable and correct performance of the ProDiMo system.

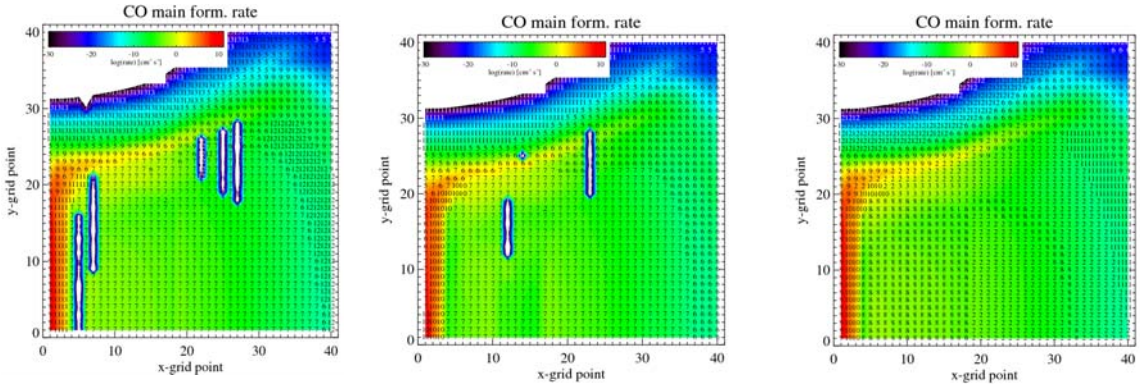

Fig.E.1.4.3.: Network in the 40/40 grid point matrix. Formation rates of CO using the ProDiMo program part 'chemical analysis' for interims models Ch.34 (left), Ch.37 (middle) and Ch.40 right).

Subsequent 40/40 grid point series were started to further optimise and reduce the number of reactions and to find out the most disturbing reactions. The results of the test-models "Ch. 40 to 48" are all listed in Annex E Tab.E.1.4. .

To begin with, the test model "Ch.41" was created out of model "Ch.40" by removing the 10 reactions listed in Tab. E.1.6. :

Test model "Ch.41"

No.	Removed reactions
1258	$H_2CO^+ + e^- \rightarrow CO + 2H$
1357	$HCO^+ + e^- \rightarrow CO + H$
1358	$HCO_2^+ + e^- \rightarrow CO_2 + H$
1359	$HCO_2^+ + e^- \rightarrow CO + O + H$
1360	$HCO_2^+ + e^- \rightarrow CO + OH$
5617	$O + CN \rightarrow CO + N$
5235	$CH_2 + NO \rightarrow HCN + OH$
5327	$CH + O \rightarrow CO + H$
488	$H + CN^+ \rightarrow CN + H^+$
491	$H + HCN^+ \rightarrow HCN + H^+$

Tab. E.1.6.: Test model "Ch.41" created out of model "Ch.40" by removing the above mentioned 10 reactions

The model "Ch.41" caused several interferences in the ProDiMo calculation, which became apparent for example in the main formation / destruction rate diagrams, the log **ε** diagrams of the different molecules e.g.: CO, HCO+, HCN etc.

After several trials to add or remove critical reactions for the performance of the calculation code, the test model "Ch.43New" was created; its basic figures are listed in Tab.E.1.7. below.

Model	Species (number)	UMIST reactions	Total*	photo-reactions dissociations	photo-reactions ionisation	mult temp.fit reactions	thermodynamics of the reactions exothermic	thermodynamics of the reactions endotherm.**
"Ch. 43 New"	68	239	320	13	5	61	187	37

Tab. E.1.7. : Overview of the interim model "Ch.43New" and the different reactions in number.
*) including the 81 reactions listed in Annex E Tab.E.1.3.
**) ΔH_0 = between -10 to -22 eV

The interference-free diagrams of the test-model "Ch.43New" encouraged the next step into 70/70 grid point matrix, which could not be calculated anymore with the own data processor; it was managed by the "university-cluster" data processing (UCDP).

The last satisfying model "Ch.43New" was calculated within 70/70 grid point matrix on UCDP; the diagrams showed interferences, although 40/40 grid point matrix calculations resulted in acceptable diagrams.

An apparent deviation of the interim model "Ch.43New" to the reference model DM was detected in the fluxes of the diazenylium cation N_2H^+, which was 7 orders of magnitude lower (10^{-29} to 10^{-22} [W/m²] resp.).

Following actions were taken to solve this problem:

1. the e^- reaction 1412, which operates in temperature optimum 130 to 1000K, was added to the already included 1411, which works in the range of 10-130K only.

$$N_2H^+ + e^- \rightarrow N_2 + H \quad (1411; 1412)$$

2. reaction 5318, which operates in temperature range10 to 300 K, was added:

$$CH + O_2 \rightarrow CO_2 + H \quad (5318; 5317)$$

5318 is like 5317, which was already in the calculations, but with different temperature range (300 to 3000K).

3. the reactions 5617 / 5618 have the similar variation of temperature ranges (10-295 / 295-4500K)

$$O + CN \rightarrow CO + N \quad (5617; 5618\ )$$

4. since too many e^- were left, reactions for more e^- uptake were added:

$$H_3^+ + e^- \rightarrow 3\,H \quad (1286)$$
$$H_2^+ + e^- \rightarrow 2\,H \quad (1247)$$

5. The reactions 5617 and 5618 were deleted at the end, despite the fact that they solved problems in the run of the 40/40 grid points matrix.

Even though the reference model DM contains hydride (H^-) as a species, the negative ions (H^-, OH^-, O^-) were removed in the thesis models under the assumption that these ions prevent the correct performance of the code in minimised networks. Furthermore their reactions were considered to be less important for the performance of the thesis networks, especially when minimisation is the declared aim. It was supposed that the broader elements, species and reaction portfolio of DM can sidestep these interferences.
Further evaluations concerning negative ions are worthwhile, with special attention to OH^- as product of the water dissociation equilibrium [$2\ H_2O \rightarrow H_3O^+ + OH^-$].
Ten more reactions were removed as well, to create a test-model "Ch.47". Reaction by reaction was returned to Ch.47 after each new run of calculation, until the performance promised a better result. Two reaction groups were identified; first group: reaction is disturbing, when added. Second group: reaction is disturbing, when deleted.

1. first group when added:

1258	$H_2CO^+ + e^- \rightarrow CO + H + H$
5327	$CH + O \rightarrow CO + H$
5235	$CH_2 + NO \rightarrow HCN + OH$
1413	$N_2H^+ + e^- \rightarrow N + NH$
5618	$O + CN \rightarrow CO + N$
5053	$OH^- + NO^+ \rightarrow OH + NO$
2454	$CH_5^+ + CO \rightarrow HCO^+ + CH_4$

2. second group when taken out:

1357	$HCO^+ + e^- \rightarrow CO + H$
1358	$HCO_2^+ + e\text{-} \rightarrow CO_2 + H$
1359	$HCO_2^+ + e\text{-} \rightarrow CO + O + H$
1360	$HCO_2^+ + e\text{-} \rightarrow CO + OH$

There are electron-related reactions which are disturbing when present (1258 and 1413) and those when they are missing (2nd group). In 5 of 7 reactions CO and NO is involved. Surprising and interesting are the 3 reactions with HCO_2^+, where dissociative neutralisation discharges CO/CO_2 by cutting different covalent bindings in the molecules.

In case of the fast reaction 1413, having a rate coefficient of 1.92 10^{-8} [$cm^3\ sec^{-1}$] the species NH is formed

$N_2H^+ + e^- \rightarrow N + NH$

Database	Index	α	β	γ	T_l - T_u (K)	Accuracy	Source
RATE12	1413	1.92e-8	-0.84	0.00	151 - 1000	within 25%	Measurement

Reference: Geppert, W.D., Thomas, R., Semaniak, J., et al., 2004, ApJ, 609, 459.

although there are faster destruction reactions with 2.55 10^{-7}[$cm^3\ sec^{-1}$] like:

$N_2H^+ + e^- \rightarrow N_2 + H$

Database	Index	α	β	γ	T_l - T_u (K)	Accuracy	Source
RATE12	1411	2.55e-7	-0.84	0.00	151 - 1000	within 25%	Measurement

Reference: Geppert, W.D., Thomas, R., Semaniak, J., et al., 2004, ApJ, 609, 459.

the reaction 1413 is more disturbing but NH can react further in a destruction of more diazenylium by reaction 3837:

$NH + N_2H^+ \rightarrow NH_2^+ + N_2$

Database	Index	α	β	γ	T_l - T_u (K)	Accuracy	Source
RATE12	3837	6.40e-10	-0.50	0.00	10 - 41000	factor 2	Literature Search

Reference: Prasad & Huntress, 1980, ApJS, 43, 1.

The electron consuming reactions of the 2nd group are all very fast, in the range of ~10^{-7}[cm^3 sec^{-1}] and might be stabilizing the electron access.
However, the detected line fluxes of the diazenylium cation N_2H^+ became only marginally better; they were still 7 orders of magnitude lower in the test model "Ch.47". A minimised model could apparently not bypass the loss of the diazenylium cation. Admittedly, this ion is a problem in many chemical network models in a gas phase.
Cross-checks with the test-model "Ch.48" confirmed the necessity of the presence of the 2nd group reactions 1357, 1358, 1359 and 1360.
The test-model "Ch.47" is the ultimate model which enables the development of the theoretical PPD models for pure gas-phase reactions as well as reactions with condensates/ices, dust / grains; these will be presented in the next section F.

F. Development of the models A – E :

F.1. The principles of all models:

All thesis models **A – E** have following characteristics in common:

1. Element input: 6 elements, abundances seen in Tab.F.1.

Elements & Abundances:	
H	1,0000
He	$9.64\ 10^{-2}$
C	$1.38\ 10^{-4}$
N	$7.94\ 10^{-5}$
O	$3.02\ 10^{-4}$
Fe	$1.74\ 10^{-9}$

Tab. F.1.: Elements and abundances of the thesis models **A** – **E**

2. Species input: 68 species contained in UMIST 2012 shown in Tab. F.2.

UMIST 2012 Species input for Models A - E:					
He	OH	H3+	N++	NO	CH4N+
He+	OH+	HCO	NH+	NO+	CH3OH2+
C	CH	HCO+	NH2	H2CO	C2H2+
C+	CH+	H2O	NH2+	Fe++	HNCO+
C++	CH2	H2O+	NH3	HNC	OCN+
O	CH2+	H3O+	NH3+	O2H+	C2O+
O+	CH3+	H	N2	HCO2+	NO2
O++	CH4	H+	HN2+	HCNH+	NH
Fe	CH5+	H2	CN	NH4+	
Fe+	O2	CO2	CN+	H3CO+	
CO	O2+	N	HCN	H2CO+	
CO+	H2+	N+	HCN+	CH2CN+	

Tab. F.2. : 68 UMIST2012 species of the thesis models **A** – **E** .

3. Additional reaction partners:

Another necessary part of the reactions are energy carriers, electrons to neutralize the cations and surfaces like dust for adsorption / desorption of condensates and dimerisation of atomic hydrogen. They have no concentration limit.

PHOTON
CRP (cosmic ray particles)
CRPHOT(cosmic ray photons)
XPHOT (for X-ray chemistry)
e^- (electron)
dust (defined in Tab.D.1.1.)

4. Condensates / ices species input for the thesis models **C**, **D**, **E** (and "F")

Condensates / ices input:			
CO#	HCN#	CH#	NO#
H2O#	N2#	CH2#	H2CO#
CO2#	C#	HCO#	HNC#
CH4#	O#	N#	NO2#
NH3#	Fe#	NH2#	NH#
O2#	OH#	CN#	

Tab. F.3. : Condensates / ices for the thesis models **C – E** (and "F")

5. There are 81 reactions to be added to the calculations, which are not part of the UMIST2012 chemical data base; 36 include the X-ray chemistry into all thesis models, 16 electron reactions (demanding/producing) and 27 reactions between cations and neutral species, 2 reactions concerning hydrogen formation (a complete list to be found in Annex E Tab.E.1.3.).

6. The results of the thesis models, their comparison to one another and to the reference model DM are presented in the sections G. and H.

F.2. Construction of the thesis models

The final version of the test model "Ch.47" was used as the basis for the thesis models. The variations with and without condensates / ices are listed below:

Model	**Species** (number)	**UMIST** reactions	**reactions** cond./ices	**Total***	**photo-reactions** dissociations	ionisation	**mult temp.fit** reactions
A	68	232		313	13	4	2
B	68	914		995	34	8	11
C	91	232	94	407	13	4	2
D	91	914	94	1008	34	8	11
E	91	232	94	407	13	4	2
"F"	91	238	94	413	13	4	2
for comp. **DM**	100	1065	142	1288	42	13	13

Tab. F.2.1. : Overview of the thesis models **A** – **E** ("F") and the different reactions in number .
*) including the 81 reactions described in G.1.5. and listed in Annex E Tab.E.1.3.
For comparison reasons reference model **DM** is added.

Model **A** was the first thesis model, identical to the test model "Ch.47", calculated in the 70/70 grid point matrix by the UCDP. It operated with good performance without irregularities in the main formation / destruction rate diagrams [radius vs. height] and in the log **ε** diagrams for the different molecule concentrations, e.g.: CO, HCO^+, HCN.

Model **B** was constructed in the next step aiming to a more direct comparison with the DM; the same species were used as in model A, but all reactions of these species, available in the UMIST 2012 chemical data base, were included. This model delivered correct presentations of all relevant diagrams: no irregularities were found in the main formation / destruction rate diagrams or in the log **ε** diagrams of the various molecules.

Although Model B, compared with DM and its 1065 UMIST 2012 reactions and 100 species, contained 2/3 of the species and 50% elements of DM, only 14% fewer reactions were the outcome. This gives the impression of an effective choice of species.

At lower temperatures in the outer regions of the PPD, most of the neutral species freeze out of the gaseous phase into condensates first and then ices. To include these condensates into the ProDiMo calculation of the thesis models, model **C** was created by adding 23 condensed species to model A. The number of species and of reactions increased, whereas the UMIST 2012 reactions remained constant at 232. Thesis model C gave clear, undisturbed diagrams. Annex F Tab.F.4 show the additional 94 reactions concerning condensates/ices.

Model C included more and other condensates / ices than DM; genuine comparison between the two models was therefore not appropriate. On the other hand, to create a special "New DM" for this purpose could not be justified, because DM condensate species are used as reference for many other ProDiMo calculations in PPDs.

Model **D** was developed from C in the same manner as model B from A: the same species were used as in model C, but all reactions of these species, available in the UMIST 2012 chemical data base, were included. The model D performed during the calculation on the UCPD as satisfactorily as model B did. No irregularities were found in the main formation / destruction rate diagrams or in the log **ε** diagrams for the different molecules.

The number of reactions and the presence of condensates / ices of the model D is something near to the reference DM, it has the same number of species but a lot more condensates / ices (factor 2.3), contains 85% of reactions, however, many of those are different from the reactions in DM. The reason for the different reactions is that model D contains half of the DM elements.

A problem occurred with the obvious differences in the line fluxes of the diazenylium cation of the models A, B and C, against DM. In models A and C fluxes were found to be 7 orders of magnitude lower (10^{-29} instead of 10^{-22} [W/m²]); in model B already 1000 times better (10^{-25} [W/m²]) and in model D with 5.5 10^{-22} [W/m²] even slightly better than in the reference model DM (see section H.5 for details).

The attempt was to increase the abundance of a metal element in the calculation program input data, in this case Fe by a factor of 100 compared to the other models including DM.

Fe abundance for Model **E**: $1.74 \cdot 10^{-7}$

Model C was taken to analyse the influence of the relative concentration **ε** (Fe^0) as the calculated example to change the Fe abundance and process with the UCPD the model **E**.

However, only very little differences between models C and E were found by comparing the main formation / destruction rate diagrams and log **ε** diagrams of the various molecules. The objective of this action was not fulfilled; the line flux of the diazenylium cation N_2H^+ was expected to increase, but on the contrary, a slight decrease was found:

Model **C** : $7.38 \cdot 10^{-29}$ [W/m²]
E : $4.48 \cdot 10^{-29}$ [W/m²]

After that the following six reactions with Fe^0 were added, because it was supposed, that insufficient Fe^+ producing reactions were present in the reaction portfolio:

221	$C_2H_2^+ + Fe \rightarrow Fe^+ + C_2H_2$
272	$CH_3^+ + Fe \rightarrow Fe^+ + CH_3$
500	$HCO^+ + Fe \rightarrow Fe^+ + HCO$
566	$N_2^+ + Fe \rightarrow Fe^+ + N_2$
593	$NH_3^+ + Fe \rightarrow Fe^+ + NH_3$
2910	$H_3^+ + Fe \rightarrow Fe^+ + H_2 + H$

The rate coefficients of the reactions were all in the range of 1.9 to 4.9 10^{-9} [cm^3 sec^{-1}].

The addition of the six a.m. reactions created the model **"F"**, however, this measure failed completely. In the log **ε** diagram for CO lots of irregularities appeared and the line flux was again marginally decreased ($3.96 \cdot 10^{-29}$ [W/m²]).

This way of consolidation the diazenylium concentrations and line fluxes was abandoned. A 'deterrent example ("F")' of the log **ε** diagrams for CO is shown in Fig. F.3.1.-4. below:

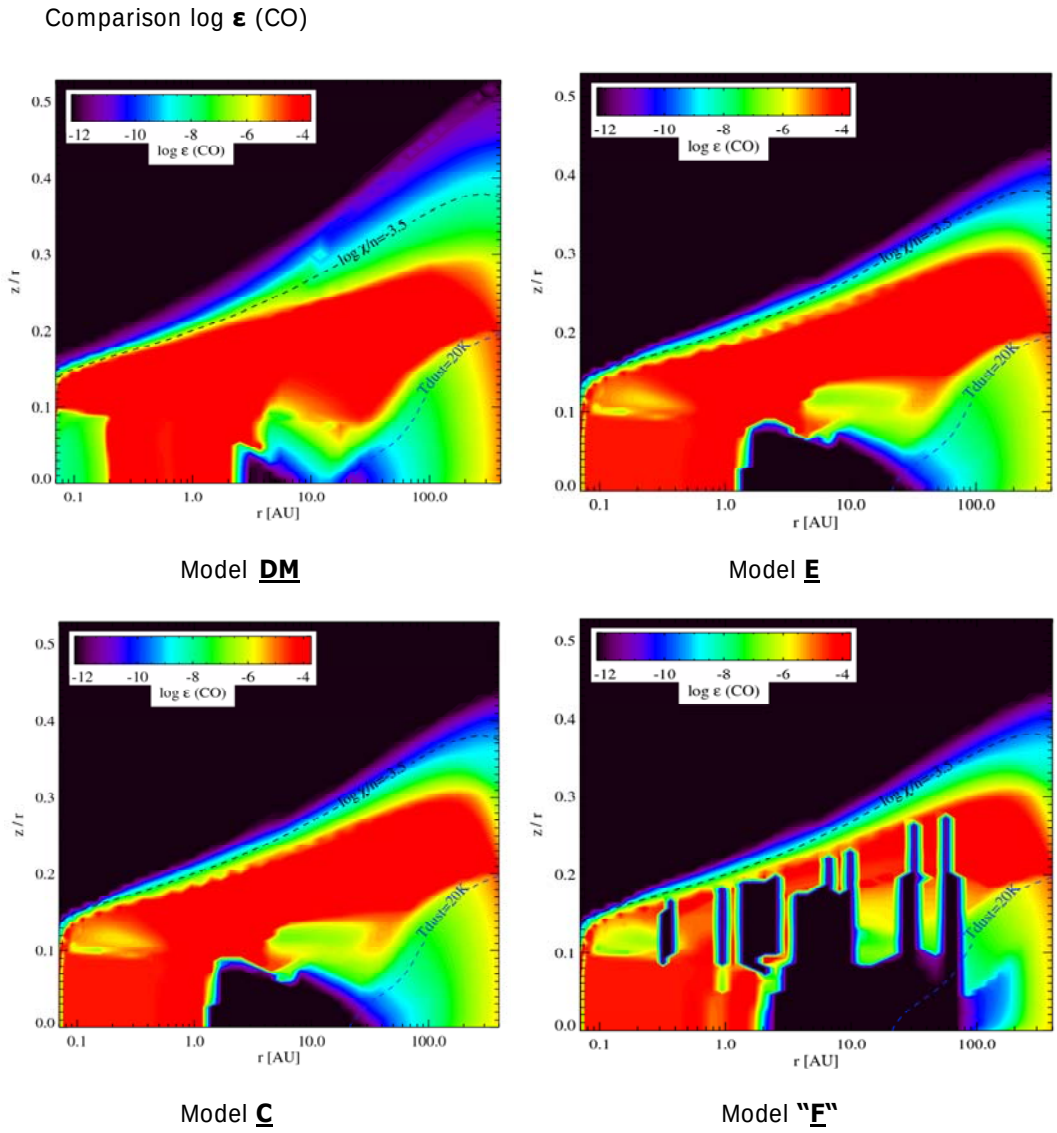

Fig. F.3.1.-4. : log **ε** (CO) of the models **DM** as reference, **C** normal **ε** (Fe^0) of 1.74 10^{-9}, **E** with **ε** (Fe^0) 1.74 10^{-7} and **"F"** with **ε** (Fe^0) 1.74 10^{-7} after addition of 6 iron related reactions.

It became evident, that iron/metal concentrations influence the change of the diazenylium cation line flux only marginally. Obviously, there are other, more effective influences coming from different reaction portfolios as in DM or in the thesis model D. This conclusion could be verified in deeper investigation, using consistent ProDiMo calculation procedure with varying example reactions.

G. Chemical reactions in reference and thesis models

G.1. Identification of important reactions in the models

The grid point diagrams calculated in ProDiMo program identify the 1st main or 2nd main formation rates and destruction rates. The 1st main formation / destruction rates comprise the major share of the below described areas I and II, whereas the 2nd main rates cover the minor share which can contain different reactions to the main rates but not necessarily. Fig.G.2.1. show the partition of the areas.

The areas I and II are roughly oriented on the diversified energy intake in PPDs and correlate with three layer types A, B and C in the Fig.B.2. The **area I** (axis of abscissa 0-70 vs. axis of ordinate 0-20) combines the midplane and the neighbouring parts of the warm molecular layer (layer B and C of Fig.B.2.); **area II** (axis of abscissa 0-70 vs. axis of ordinate 20-60) includes the photo dominated area and the upper part of the warm molecular layer (layer A and B of Fig.B.2.).

G.2. Evaluation of the most important species reactions in the models

In order to compare the thesis models A-E with the reference model DM, the most important species, which are essential for the construction of the RTs, were identified.
Ions: HCO^+, CN^+, HCN^+, H_3O^+, $C_2H_2^+$, NO^+, H_3^+, N_2H^+, molecules: CO, HCN, CN, CO_2, H_2O, NO and hydrogen.

The reactions of the species were evaluated in the following procedure:

1. The 70/70 grid diagram for each species was divided into the area I and II (see Fig.G.2.1.)
2. Three reactions, which cover a large region in the diagram, were chosen for each species in the areas I and II by their identification number.
3. These numbers were translated by the program ‘chemical analysis’ in the ‘txt.’ part of the chemical analysis program into the respective DM reaction numbers (details in section L 1. ‘program steps’).
4. The reactions of all species are listed under their DM reaction numbers in Annex G as Tab.G.2.4.
5. An example is given below for the procedure using the species ‘CO’ in model **C** in Fig. G.2.2-3.

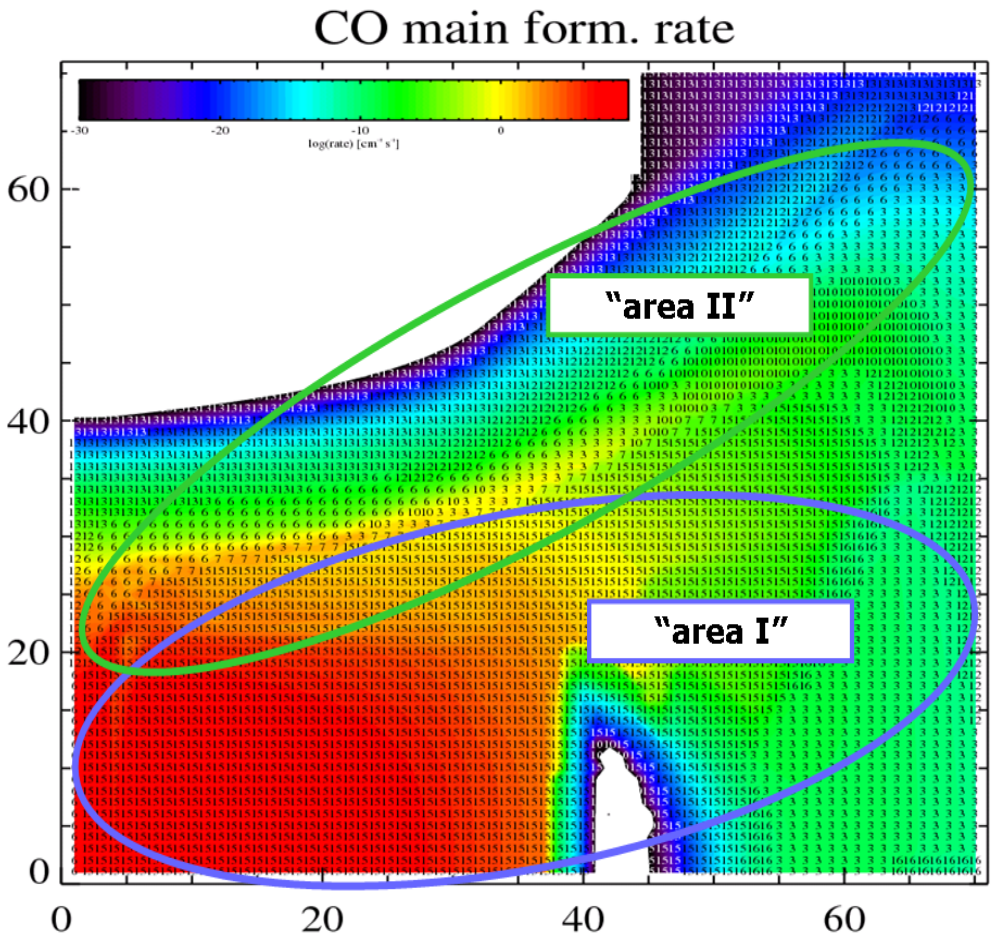

Fig. G.2.1.: Definition of the areas I and II (definition in the text), ready for analysis of the appropriate formation / destruction rates and their resp. reactions; here: the example CO in model **C** for 'main formation rate'.

Model C			
species	area	grid no.*	reaction no. and type in DM
Main formation reactions			
CO	I	15	11293 DT: CO# + dust --> CO + dust
	I	3	1357 DR: HCO+ + e- --> CO + H
	II	13	6093 RA: C + O --> CO + PHOTON
Main destruction reactions			
CO	I	11	11292 IC: CO + dust --> CO# + dust
	I	4	2905 IN: H3+ + CO --> HCO+ + H2
	II	8	5914 PH: CO + PHOTON --> O + C

Model C			
species	area	grid no.*	reaction no. and type in DM
2nd main formation reactions			
CO	I	8	2777 IN: H2O + HCO+ --> CO + H3O+
	I	11	5393 NN: H + CO2 --> CO + OH
	II	6	1653 IN: C+ + O2 --> CO + O+
2nd main destruction reactions			
CO	I		same as main destruction reactions
	II	9	10529 XP: CO + XPHOT --> C++ + O + e-

Tab. G.2.2.-3.: Main and second main reactions of CO formation and destruction for model **C**.
*) link to 'chemanalyse.txt files – q.v. section L.2

G.3. Compilation of model reactions

According to the selection criteria described in the identification part H.2., the reactions were first sorted by the species type and /or species group (such as CO group contain e.g.: CO, CO^+, CO#). All these reactions are crucial for the RT sequences, but not necessarily the most frequent and important formation / destruction reactions in the group of species (q.v. Tab.G.3.1.-9.). Additional reactions, which are common to all thesis models plus the reference model, are also identified and listed separately in Tab.G.3.10. and Tab.G.3.11.

G.3.1. Sorting by species or by species group

Tab.G.3.1.-9. list the species reactions in the reference model DM, restricted to the thesis elements and the reactions of thesis models A-E. This table includes the added reactions of ProDiMo and reactions for condensates/ices, which are different from reference and thesis models. The arrangement form follows the most important pathways constituents in order to find similarities or differences.
Remarkably, the minimised models A, C and E show important reactions which are not recognised as such in the comprehensive models B and D, although they belong to their chemical networks. In models B and D other reactions seem to be more important.

Reactions present in A, C and E, but not registered in models B & D as important reactions:

1617 $C^+ + CO_2 \rightarrow CO^+ + CO$
2134 $C + HCO^+ \rightarrow CO + CH^+$
2664 $H_2 + CO^+ \rightarrow HCO^+ + H$
3440 $He^+ + CO_2 \rightarrow O_2 + C^+ + He$
3619 $C_2H_2^+ + N \rightarrow HCN + CH^+$
3875 $O^+ + HCN \rightarrow NO^+ + CH$
5617 $O + CN \rightarrow CO + N$

It is obvious, that most of the reactions are about the CO formation / destruction, whereas models B & D contain other important reactions for this purpose. The above reactions must be kept for even more minimised models to guarantee an operating chemical network.Tab.G.3.1.-9. shows individual tables of the species groups, separately discussed.

Reactions of CO ; CO+ , CO#					beyond the double line CO is the product										
reaction no.	educt 1		educt 2		product 1		2		3	**DM**	**A**	**B**	**C**	**D**	**E**
2518	CO	+	HN2+	-->	HCO+	+	N2			**o**	**o**	**o**	**o**	**o**	**o**
5914	CO	+	PHOTON	-->	O	+	C			**x**		**x**	**x**		**x**
10529	CO	+	XPHOT	-->	C++	+	O	+	2e-	**o**	**o**	**o**	**o**	**o**	**o**
10531	CO	+	XPHOT	-->	C	+	O++	+	2e-			**x**			
11169	CO	+	XPHOT	-->	C	+	O++	+	2e-	**x**					
11292	CO	+	dust	-->	CO#	+	dust			**x**			**x**	**x**	**x**
2515	CO	+	HCO2+	-->	CO2	+	HCO+				**x**	**x**			
11293	CO#	+	dust	-->	CO	+	dust			**x**			**x**	**x**	**x**
11295	CO#	+	PHOTON	-->	CO					**x**					
2454	CH5+	+	CO	-->	HCO+	+	CH4							**x**	
2613	H2+	+	CO	-->	HCO+	+	H			**x**		**x**		**x**	
2737	H2O+	+	CO	-->	HCO+	+	OH							**x**	
2905	H3+	+	CO	-->	HCO+	+	H2			**o**	**o**	**o**	**o**	**o**	**o**
3574	N+	+	CO	-->	NO+	+	C			**o**	**o**	**o**	**o**	**o**	**o**
5692	OH	+	CO	-->	CO2	+	H			**o**	**o**	**o**	**o**	**o**	**o**
489	H	+	CO+	-->	CO	+	H+			**x**		**x**			
2664	H2	+	CO+	-->	HCO+	+	H				**x**		**x**		**x**
877	CO2	+	CRPHOT	-->	CO	+	O			**o**	**o**	**o**	**o**	**o**	**o**
1357	HCO+	+	e-	-->	CO	+	H			**o**	**o**	**o**	**o**	**o**	**o**
1653	C+	+	O2	-->	CO	+	O+				**x**		**x**		**x**
2134	C	+	HCO+	-->	CO	+	CH+				**x**		**x**		**x**
2777	H2O	+	HCO+	-->	CO	+	H3O+			**o**	**o**	**o**	**o**	**o**	**o**
3814	NH3	+	HCO+	-->	CO	+	NH4+			**x**					
5244	CH2	+	O	-->	CO	+	H	+	H			**x**			
5393	H	+	CO2	-->	CO	+	OH				**x**		**x**	**x**	**x**
5617	O	+	CN	-->	CO	+	N				**x**		**x**		**x**
5913	CO2	+	PHOTON	-->	CO	+	O			**x**		**x**		**x**	
6093	C	+	O	-->	CO	+	PHOTON					**x**	**x**	**x**	**x**
1617	C+	+	CO2	-->	CO+	+	CO				**x**		**x**		**x**
1652	C+	+	O2	-->	CO+	+	O								
5957	HCO+	+	PHOTON	-->	CO+	+	H					**x**			
6072	C+	+	O	-->	CO+	+	PHOTON				**x**				
5354	CN	+	O2	-->	NO	+	CO				**x**	**x**			

Tab.G.3.1.: Formation and destruction reactions of CO, CO^+ and CO# (condensates/ices) in all models; beyond the double line CO is the product. Markings: reactions of the resp. models (**x**); reactions included in all models (**o**). Reaction numbers > 10.000 are not from UMIST, but from DM.

Reactions of HCO+					beyond the double line HCO+ is the product										
reaction no.	educt 1		educt 2		product 1		2		3	**DM**	**A**	**B**	**C**	**D**	**E**
1357	HCO+	+	e-	-->	CO	+	H			**o**	**o**	**o**	**o**	**o**	**o**
5957	HCO+	+	PHOTON	-->	CO+	+	H					**x**			
2134	C	+	HCO+	-->	CO	+	CH+				**x**		**x**		**x**
2777	H2O	+	HCO+	-->	CO	+	H3O+			**o**	**o**	**o**	**o**	**o**	**o**
3814	NH3	+	HCO+	-->	CO	+	NH4+			**x**					
4032	OH	+	HCO+	-->	HCO2+	+	H			**x**		**x**		**x**	
64	CH	+	O	-->	HCO+	+	e-				**x**	**x**			**x**
1623	C+	+	H2O	-->	HCO+	+	H			**x**	**x**	**x**	**x**	**x**	
2183	CH+	+	H2O	-->	HCO+	+	H2			**x**					
2221	CH2+	+	O	-->	HCO+	+	H					**x**		**x**	
2321	CH3+	+	O	-->	HCO+	+	H2				**x**		**x**		
2454	CH5+	+	CO	-->	HCO+	+	CH4							**x**	
2518	CO	+	HN2+	-->	HCO+	+	N2			**o**	**o**	**o**	**o**	**o**	**o**
2613	H2+	+	CO	-->	HCO+	+	H			**x**		**x**		**x**	
2664	H2	+	CO+	-->	HCO+	+	H				**x**		**x**		**x**
2737	H2O+	+	CO	-->	HCO+	+	OH							**x**	
2905	H3+	+	CO	-->	HCO+	+	H2			**o**	**o**	**o**	**o**	**o**	**o**
3919	O	+	C2H2+	-->	HCO+	+	CH					**x**	**x**	**x**	**x**
2515	CO	+	HCO2+	-->	CO2	+	HCO+				**x**	**x**			

Tab.G.3.2.: Formation and destruction reactions of HCO^+ and in all models; beyond the double line HCO^+ is the product. Markings: reactions of the resp. models (**x**); reactions included in all models (**o**).

In the CO, CO^+ and CO# group eight reactions commonly used by all models were ascertained corresponding to the selection criteria described in G.2. Combined with the next group of HCO^+ reactions, which are C-O related as well, twelve reactions have been used by all models. It is logically consistent that models with condensates/ ices (C,D,E) contain the same reactions; noticeably, the minimised models A, C, E also have their specific reactions (1617, 1653, 2134, 2321, 2664, 5617), because certain reactions are more important in small network models. The reference model DM has a special approach,

because in DM more elements are involved leading to different pathways for an operating chemical network.

There are reactions conjointly used in the comprehensive models DM, B and D (2613, 5913, 489[DM, B only], 4032), regardless of whether the model has condensates/ices or not.

Reactions of CO2 ; CO2#					beyond the double line CO2 is the product										
reaction no.	educt 1		educt 2		product 1		2		3	**DM**	**A**	**B**	**C**	**D**	**E**
877	CO2	+	CRPHOT	-->	CO	+	O			**o**	**o**	**o**	**o**	**o**	**o**
5913	CO2	+	PHOTON	-->	CO	+	O			**x**		**x**		**x**	
11300	CO2	+	dust	-->	CO2#	+	dust			**x**			**x**	**x**	**x**
1617	C+	+	CO2	-->	CO+	+	CO				**x**		**x**		**x**
2499	CN+	+	CO2	-->	C2O+	+	NO				**x**	**x**	**x**		
2612	H2+	+	CO2	-->	HCO2+	+	H					**x**		**x**	
2904	H3+	+	CO2	-->	HCO2+	+	H2				**x**	**x**	**x**	**x**	**x**
3440	He+	+	CO2	-->	O2	+	C+	+	He		**x**		**x**		**x**
3602	HN2+	+	CO2	-->	HCO2+	+	N2				**x**			**x**	
3714	NH+	+	CO2	-->	NO+	+	HCO					**x**		**x**	
4006	OH+	+	CO2	-->	HCO2+	+	O					**x**		**x**	
5393	H	+	CO2	-->	CO	+	OH				**x**		**x**	**x**	**x**
2515	CO	+	HCO2+	-->	CO2	+	HCO+				**x**	**x**			
2778	H2O	+	HCO2+	-->	CO2	+	H3O+					**x**			
5317	CH	+	O2	-->	CO2	+	H			**o**	**o**	**o**	**o**	**o**	**o**
5636	O	+	HCO	-->	CO2	+	H			**o**	**o**	**o**	**o**	**o**	**o**
5692	OH	+	CO	-->	CO2	+	H			**o**	**o**	**o**	**o**	**o**	**o**
11301	CO2#	+	dust	-->	CO2	+	dust			**x**			**x**	**x**	**x**
11303	CO2#	+	PHOTON	-->	CO2					**x**				**x**	**x**

Tab.G.3.3.: Formation and destruction reactions of CO_2, and CO_2# (condensates/ices) in all models; beyond the double line CO_2 is the product. Markings: reactions of the resp. models (**x**); reactions included in all models (**o**).

Reactions of HCO2+					beyond the double line HCO2+ is the product										
reaction no.	educt 1		educt 2		product 1		2		3	**DM**	**A**	**B**	**C**	**D**	**E**
2515	CO	+	HCO2+	-->	CO2	+	HCO+				**x**	**x**			
2778	H2O	+	HCO2+	-->	CO2	+	H3O+					**x**			
2612	H2+	+	CO2	-->	HCO2+	+	H					**x**		**x**	
2904	H3+	+	CO2	-->	HCO2+	+	H2				**x**	**x**	**x**	**x**	**x**
3602	HN2+	+	CO2	-->	HCO2+	+	N2				**x**			**x**	
4006	OH+	+	CO2	-->	HCO2+	+	O					**x**		**x**	
4032	OH	+	HCO+	-->	HCO2+	+	H			**x**		**x**		**x**	

Tab.G.3.4.: Formation and destruction reactions of HCO_2^+ in all models; beyond the double line HCO_2^+ is the product. Markings: reactions of the resp. models (**x**).

Six reactions of the CO_2 group are contained in the CO and HCO^+ group (877, 1617, 2515, 5393, 5692, 5913). Two new reactions of CO_2# on dust (11300, 11301) in models DM, C, D, and E appear often in the CO and dust groups.

If the CO_2 group is combined with the next group of HCO_2^+ reactions, another C-O related group, it becomes clear that CO_2 is either educt or product in most reactions. Only reaction 4032 uses the OH radical with a very fast rate coefficient and is preferred by the comprehensive models DM, B and D, seen already in the Tab.G.3.2.

Counting now all C-O related reactions, double counting eliminated, all thesis models and the reference model use more or less the same number of C-O reactions (20 to 22), regardless of whether they have condensates/ ices or not.

Reactions of HCN ; HCN+ , HCN#					beyond the double line HCN is the product										
reaction no.	educt 1		educt 2		product 1		2		3	**DM**	**A**	**B**	**C**	**D**	**E**
906	HCN	+	CRPHOT	-->	CN	+	H			**x**		**x**		**x**	
3111	HCN	+	HN2+	-->	HCNH+	+	N2					**x**		**x**	
5955	HCN	+	PHOTON	-->	CN	+	H			**o**	**o**	**o**	**o**	**o**	**o**
11312	HCN	+	dust	-->	HCN#	+	dust			**x**			**x**	**x**	**x**
389	H+	+	HCN	-->	HCN+	+	H			**x**	**x**		**x**	**x**	**x**
3036	H3O+	+	HCN	-->	HCNH+	+	H2O			**o**	**o**	**o**	**o**	**o**	**o**
3475	He+	+	HCN	-->	CN+	+	He	+	H	**o**	**o**	**o**	**o**	**o**	**o**
3875	O+	+	HCN	-->	NO+	+	CH			**x**	**x**		**x**		**x**
4011	OH+	+	HCN	-->	HCNH+	+	O					**x**			
5401	H	+	HCN	-->	CN	+	H2			**o**	**o**	**o**	**o**	**o**	**o**
481	H2O	+	HCN+	-->	HCN	+	H2O+					**x**			
491	H	+	HCN+	-->	HCN	+	H+			**o**	**o**	**o**	**o**	**o**	**x**
2680	H2	+	HCN+	-->	HCNH+	+	H			**o**	**o**	**o**	**o**	**o**	**o**
2776	H2O	+	HCN+	-->	CN	+	H3O+			**x**		**x**		**x**	
1348	HCN+	+	e-	-->	CN	+	H			**x**		**x**		**x**	
1350	HCNH+	+	e-	-->	HCN	+	H					**x**		**x**	**x**
3619	N	+	C2H2+	-->	HCN	+	CH+				**x**		**x**		**x**
3812	NH3	+	HCNH+	-->	HCN	+	NH4+			**x**	**x**	**x**		**x**	
5235	CH2	+	NO	-->	HCN	+	OH			**x**	**x**		**x**		**x**
5369	H2	+	CN	-->	HCN	+	H			**o**	**o**	**o**	**o**	**o**	**o**
5405	H	+	HNC	-->	HCN	+	H				**x**	**x**	**x**	**x**	**x**
5484	N	+	CH2	-->	HCN	+	H				**x**		**x**		
5497	N	+	HCO	-->	HCN	+	O				**x**				
5533	NH3	+	CN	-->	HCN	+	NH2			**x**		**x**		**x**	
11313	HCN#	+	dust	-->	HCN	+	dust			**x**			**x**	**x**	**x**
495	HCN+	+	NO	-->	HCN	+	NO+								
1647	C+	+	NH2	-->	HCN+	+	H			**x**		**x**			
1649	C+	+	NH3	-->	HCN+	+	H2					**x**		**x**	
2663	H2	+	CN+	-->	HCN+	+	H			**o**	**o**	**o**	**o**	**o**	**o**
2766	H2O	+	CN+	-->	HCN+	+	OH			**x**		**x**		**x**	
2901	H3+	+	CN	-->	HCN+	+	H2							**x**	
3571	N+	+	CH4	-->	HCN+	+	H2	+	H			**x**			
3682	N	+	CH2+	-->	HCN+	+	H			**o**	**o**	**o**	**o**	**o**	**o**

Tab.G.3.5. : Formation and destruction reactions of HCN, HCN^+ and HCN# (condensates/ices) in all models;beyond the double line HCN or HCN^+ is the product. Markings: reactions of the resp. models (**x**); reactions included in all models (**o**).

Reactions of CN ; CN+					beyond the double line CN is the product										
reaction no.	educt 1		educt 2		product 1		2		3	**DM**	**A**	**B**	**C**	**D**	**E**
5354	CN	+	O2	-->	NO	+	CO				**x**	**x**			
5910	CN	+	PHOTON	-->	N	+	C			**x**	**x**		**x**	**x**	**x**
10526	CN	+	XPHOT	-->	C++	+	N	+	2e-			**x**			
10528	CN	+	XPHOT	-->	C	+	N++	+	2e-			**x**			
11164	CN	+	XPHOT	-->	C++	+	N	+	2e-	**x**					
2305	CH3+	+	CN	-->	CH2CN+	+	H				**x**				
2901	H3+	+	CN	-->	HCN+	+	H2							**x**	
5369	H2	+	CN	-->	HCN	+	H			**o**	**o**	**o**	**o**	**o**	**o**
5491	N	+	CN	-->	N2	+	C					**x**		**x**	
5533	NH3	+	CN	-->	HCN	+	NH2			**x**		**x**		**x**	
5617	O	+	CN	-->	CO	+	N				**x**		**x**		**x**
5619	O	+	CN	-->	NO	+	C							**x**	
2499	CN+	+	CO2	-->	C2O+	+	NO				**x**	**x**	**x**		
2506	CN+	+	O2	-->	OCN+	+	O					**x**			
2663	H2	+	CN+	-->	HCN+	+	H			**o**	**o**	**o**	**o**	**o**	**o**
2766	H2O	+	CN+	-->	HCN+	+	OH			**x**		**x**		**x**	
2768	H2O	+	CN+	-->	HNCO+	+	H						**x**	**x**	**x**
488	H	+	CN+	-->	CN	+	H+			**o**	**o**	**o**	**o**	**o**	**o**
682	O	+	CN+	-->	CN	+	O+					**x**		**x**	
906	HCN	+	CRPHOT	-->	CN	+	H			**x**		**x**		**x**	
1230	CH4N+	+	e-	-->	CN	+	H2	+	H2			**x**	**x**	**x**	**x**
1348	HCN+	+	e-	-->	CN	+	H			**x**		**x**		**x**	
1349	HCNH+	+	e-	-->	CN	+	H	+	H	**x**					
2776	H2O	+	HCN+	-->	CN	+	H3O+			**x**		**x**		**x**	
5202	C	+	NH	-->	CN	+	H			**x**					
5204	C	+	NO	-->	CN	+	O					**x**		**x**	
5311	CH	+	N	-->	CN	+	H				**x**		**x**	**x**	**x**
5401	H	+	HCN	-->	CN	+	H2			**o**	**o**	**o**	**o**	**o**	**o**
5955	HCN	+	PHOTON	-->	CN	+	H			**o**	**o**	**o**	**o**	**o**	**o**
5971	HNC	+	PHOTON	-->	CN	+	H				**x**				
6091	C	+	N	-->	CN	+	PHOTON					**x**		**x**	
1650	C+	+	NH	-->	CN+	+	H			**o**	**o**	**o**	**o**	**o**	**o**
2191	CH+	+	N	-->	CN+	+	H			**o**	**o**	**o**	**o**	**o**	**o**
3475	He+	+	HCN	-->	CN+	+	He	+	H	**o**	**o**	**o**	**o**	**o**	**o**
3491	He+	+	HNC	-->	CN+	+	He	+	H			**x**		**x**	
6071	C+	+	N	-->	CN+	+	PHOTON			**o**	**o**	**o**	**o**	**o**	**o**

Tab.G.3.6. : Formation and destruction reactions of CN and CN^+ in all models; beyond the double line CN or CN^+ is the product. Markings: reactions of the resp. models (**x**); reactions included in all models (**o**).

In the HCN, HCN+ and HCN# group nine reactions commonly used by all models were ascertained corresponding to the selection criteria described in G.2. Combined with the next group of CN, CN+ reactions, which are C-N related as well, thirteen reactions have been used by all models. Counting all C-N related reactions, double counting eliminated, it turned out that model B has 38, D has 37, DM, A and C 28/27 respectively. Model E has 24 reactions only; is that due to the highest Fe concentration? The small models A, C, E have no specific reactions like in the C-O group, but there are reactions conjointly used for the comprehensive models DM, B and D (906, 1348, 2766, 2776, 3875, 5533).
The conclusion is firstly that C-N based reactions have a higher share of commonly used reactions, secondly more reactions in total on the entire chemical network than the C-O related reactions.

Reactions of C2H2+					beyond the double line C2H2+ is the product										
reaction no.	educt 1		educt 2		product 1		2		3	DM	A	B	C	D	E
1005	C2H2+	+	e-	-->	CH	+	CH				x	x	x	x	x
3619	N	+	C2H2+	-->	HCN	+	CH+				x		x		x
3837	NH	+	C2H2+	-->	CH2CN+	+	H				x	x	x	x	x
3919	O	+	C2H2+	-->	HCO+	+	CH					x	x	x	x
1613	C+	+	CH4	-->	C2H2+	+	H2				x	x	x	x	x
2170	CH+	+	CH4	-->	C2H2+	+	H2	+	H			x		x	
2473	CH	+	CH3+	-->	C2H2+	+	H2				x	x	x	x	x

Tab.G.3.7.: Formation and destruction reactions of $C_2H_2^+$ and in all models; beyond the double line $C_2H_2^+$ is the product. Marking for: reactions of the resp. models (**x**); reactions included in all models (**o**).

Although it is missing in the DM reference model, the species of $C_2H_2^+$ is included in the RTs, because of its importance for chemical reactions in the gas-phase of PPDs. Some most likely additive reactions can be started with $C_2H_2^+$ or C_2H_2, using CO, H2O, halogens, NH_3 or amines, aldehydes and even trimerisation to benzene or oligomerisation to higher unsaturated hydrocarbons, cyclic (up to the already observed fullerenes) or linear ones; moreover using H_2 to form ethene, followed by lots of additive reactions. There is definitely a large bunch of possibilities.

Reactions of "dust"															
reaction no.	educt 1		educt 2		product 1		2		3	DM	A	B	C	D	E
11292	CO	+	dust	-->	CO#	+	dust			x			x	x	x
11293	CO#	+	dust	-->	CO	+	dust			x			x	x	x
11296	H2O	+	dust	-->	H2O#	+	dust			x			x	x	x
11297	H2O#	+	dust	-->	H2O	+	dust			x			x	x	x
11300	CO2	+	dust	-->	CO2#	+	dust			x			x	x	x
11301	CO2#	+	dust	-->	CO2	+	dust			x			x	x	x
11312	HCN	+	dust	-->	HCN#	+	dust			x			x	x	x
11313	HCN#	+	dust	-->	HCN	+	dust			x			x	x	x
10247/10274	2 H	+	dust	-->	H2	+	dust			o	o	o	o	o	o

Tab.G.3.8.: Formation and destruction reactions of dust in all models. Marking for: reactions of the resp. models (**x**); reactions included in all models (**o**). The dimerisation of H on dust has a different number in DM as in the thesis models.

The reactions with condensates / ices occurred in the calculation system with dust as partner. They are not as numerous as expected for 23 ices in the thesis models (compared to 10 ices in DM). Especially the CH_4# and NH_3# with relatively high abundances are missing. The reason might be that in cold regions dust/grains act as condensation nuclei and van der Waals forces hold the molecules / atoms in the first instance at/on the surface. The integrated column densities of CH_4 in the gas phase were determined at 20K to $\sim 10^{14}$ [cm^{-2}], bound on solids to $\sim 10^{18}$ [cm^{-2}], whereas for the CO molecule both values were $\sim 10^{18}$ [cm^{-2}] (Reboussin 2015).

Further reactions at solid state or undercooled liquids are diffusion related and complex; their calculation is very problematic.

Concerning ice / dust reactions, no differences were found between the models with condensates / ices (DM, C, D and E), although there were more condensate / ice species programmed for models C, D and E than for the reference model (23 vs.10 ; see Tab.E.1.2. vs. Tab.F.3.). All reactions involve CO#, CO2#, HCN# and H2O#; just 9 reactions including back-reactions.

Reactions of e-					beyond the double line e- is released										
reaction no.	educt 1		educt 2		product 1		2		3	**DM**	**A**	**B**	**C**	**D**	**E**
1005	C2H2+	+	e-	-->	CH	+	CH				**x**	**x**	**x**	**x**	**x**
1230	CH4N+	+	e-	-->	CN	+	H2	+	H2			**x**	**x**	**x**	**x**
1285	H3+	+	e-	-->	H2	+	H					**x**	**x**	**x**	**x**
1286	H3+	+	e-	-->	H	+	H	+	H				**x**		**x**
1295	H3CO+	+	e-	-->	CH	+	H2O				**x**				
1301	H3O+	+	e-	-->	H2O	+	H			**o**	**o**	**o**	**o**	**o**	**o**
1304	H3O+	+	e-	-->	OH	+	H	+	H	**o**	**o**	**o**	**o**	**o**	**o**
1348	HCN+	+	e-	-->	CN	+	H			**x**		**x**		**x**	**x**
1349	HCNH+	+	e-	-->	CN	+	H	+	H	**x**					
1350	HCNH+	+	e-	-->	HCN	+	H					**x**		**x**	**x**
1357	HCO+	+	e-	-->	CO	+	H			**o**	**o**	**o**	**o**	**o**	**o**
1411	HN2+	+	e-	-->	N2	+	H			**o**	**o**	**o**	**o**	**o**	**o**
1427	NH4+	+	e-	-->	NH3	+	H			**x**		**x**	**x**	**x**	**x**
1428	NO+	+	e-	-->	O	+	N			**o**	**o**	**o**	**o**	**o**	**o**
6182	H+	+	e-	-->	H	+	PHOTON			**o**	**o**	**o**	**o**	**o**	**o**
64	CH	+	O	-->	HCO+	+	e-				**x**	**x**			**x**
943	NO	+	CRPHOT	-->	NO+	+	e-					**x**		**x**	
5934	H2O	+	PHOTON	-->	H2O+	+	e-					**x**		**x**	
6001	NO	+	PHOTON	-->	NO+	+	e-				**x**	**x**	**x**	**x**	**x**
10526	CN	+	XPHOT	-->	C++	+	N	+	2e-			**x**			
10528	CN	+	XPHOT	-->	C	+	N++	+	2e-			**x**			
10529	CO	+	XPHOT	-->	C++	+	O	+	2e-		**x**	**x**	**x**	**x**	**x**
10531	CO	+	XPHOT	-->	C	+	O++	+	2e-			**x**			
11164	CN	+	XPHOT	-->	C++	+	N	+	2e-	**x**					
11167	CO	+	XPHOT	-->	C++	+	O	+	2e-	**x**					
11169	CO	+	XPHOT	-->	C	+	O++	+	2e-	**x**					

Tab.G.3.9.: Formation and destruction reactions of e^- in all models; beyond the double line e^- is produced. Markings: reactions of the resp. models (**x**); reactions included in all models (**o**).

The calculation system ProDiMo contains 81 reactions which are mainly X-ray chemistry related (q.v. Tab.E.1.3.). The most frequent e^- reactions for X-ray chemistry are reacting in area II of the PPD, shown in Tab.G.3.9. under no.10526 – 11169; they supply $2e^-$ each and are used to destroy CN and CO, which is not important for the RTs reactions. The special problem of the amount of free e^- and the diazenylium cation in reactions 1411 and 1413 is dealt with in section E.

G. 3.2. Reactions present in all models

Assessment of the important main formation and destructions reactions found 36 reactions commonly used in all models including the standard model. These reactions can be acknowledged as essential for the stability of the entire chemical network (q.v. Tab.G.3.10.).

Reaction No.							
404	H+	+	NO	-->	NO+	+	H
488	H	+	CN+	-->	CN	+	H+
491	H	+	HCN+	-->	HCN	+	H+
493	H	+	O+	-->	O	+	H+
621	NO+	+	Fe	-->	Fe+	+	NO
877	CO2	+	CRPHOT	-->	CO	+	O
1301	H3O+	+	e-	-->	H2O	+	H
1304	H3O+	+	e-	-->	OH	+	2H
1411	HN2+	+	e-	-->	N2	+	H
1428	NO+	+	e-	-->	O	+	N
1650	C+	+	NH	-->	CN+	+	H
2191	CH+	+	N	-->	CN+	+	H
2518	CO	+	HN2+	-->	HCO+	+	N2
2614	H2+	+	H2	-->	H3+	+	H
2621	H2+	+	N2	-->	HN2+	+	H
2663	H2	+	CN+	-->	HCN+	+	H
2672	H2	+	H2O+	-->	H3O+	+	H
2680	H2	+	HCN+	-->	HCNH+	+	H
2777	H2O	+	HCO+	-->	CO	+	H3O+
2905	H3+	+	CO	-->	HCO+	+	H2
2914	H3+	+	H2O	-->	H3O+	+	H2
2948	H3+	+	N2	-->	HN2+	+	H2
3036	H3O+	+	HCN	-->	HCNH+	+	H2O
3475	He+	+	HCN	-->	CN+	+	He + H
3574	N+	+	CO	-->	NO+	+	C
3682	N	+	CH2+	-->	HCN+	+	H
3694	N	+	NH2+	-->	HN2+	+	H
5317	CH	+	O2	-->	CO2	+	H
5369	H2	+	CN	-->	HCN	+	H
5401	H	+	HCN	-->	CN	+	H2
5636	O	+	HCO	-->	CO2	+	H
5692	OH	+	CO	-->	CO2	+	H
5955	HCN	+	PHOTON	-->	CN	+	H
6141	H	+	OH	-->	H2O	+	PHOTON
6182	H+	+	e-	-->	H	+	PHOTON
10247/10274	2 H	+	dust	-->	H2	+	dust

Tab.G.3.10. : Commonly used reactions in all thesis models **A**-**E** and the reference model **DM** seen as essential reactions. The dimerisation of H on dust has a different number in DM as in the thesis models.

Tab.G.3.11. lists 28 other reactions, which are important for the thesis models but are not present in the reference model. Some of the reactions deal with C_2H_2 / $C_2H_2^+$, which are not in the reference model; others contain identical species as in DM, namely HCN, CN, NO and their equivalent cations, but in different reaction paths.

Reaction No.									
389	H+	+	HCN	-->	HCN+	+	H		
407	H+	+	O	-->	O+	+	H		
1005	C2H2+	+	e-	-->	CH	+	CH		
1357	HCO+	+	e-	-->	CO	+	H		
1613	C+	+	CH4	-->	C2H2+	+	H2		
1617	C+	+	CO2	-->	CO+	+	CO		
1653	C+	+	O2	-->	CO	+	O+		
2134	C	+	HCO+	-->	CO	+	CH+		
2473	CH	+	CH3+	-->	C2H2+	+	H2		
2698	H2	+	O2H+	-->	O2	+	H3+		
2904	H3+	+	CO2	-->	HCO2+	+	H2		
2961	H3+	+	O	-->	OH+	+	H2		
3440	He+	+	CO2	-->	O2	+	C+	+	He
3619	N	+	C2H2+	-->	HCN	+	CH+		
3837	NH	+	C2H2+	-->	CH2CN+	+	H		
5235	CH2	+	NO	-->	HCN	+	OH		
5311	CH	+	N	-->	CN	+	H		
5393	H	+	CO2	-->	CO	+	OH		
5399	H	+	H2O	-->	OH	+	H2		
5405	H	+	HNC	-->	HCN	+	H		
5514	N	+	OH	-->	NO	+	H		
5617	O	+	CN	-->	CO	+	N		
5910	CN	+	PHOTON	-->	N	+	C		
5935	H2O	+	PHOTON	-->	OH	+	H		
6001	NO	+	PHOTON	-->	NO+	+	e-		
6002	NO	+	PHOTON	-->	O	+	N		
6071	C+	+	N	-->	CN+	+	PHOTON		
10529	CO	+	XPHOT	-->	C++	+	O	+	2 e-

Tab.G.3.11. : Important reactions used in the thesis models **A** – **E** .

During the interpretation process of the 36 essential reactions in Tab.G.3.10, it became clear in which area (I or II) the reactions appear and whether they are 1st main or 2nd main rates (explained in G.1.). The diagrams show that the same reactions take place in the more photon-dominated layer in one model; in another model they appear closer to the warm molecular layer. No trend or pattern could be found for this phenomenon. However, in a few cases, the reactions 1411, 2191, 2518, 3475, 5317 and 6141 use all four variation possibilities: area I and II, main and 2nd main rate.

The 28 reactions in Tab.G.3.11 also show the variation in which area they appear and/or whether they represent the main or the 2nd main rates. Although many variations were found for reactions 2134, 2473, 2904, 5235, 5393, 5405, 6001 and 6002, no definite pattern was observed, The explanation could be that the above mentioned reactions have the same validity; due to a small change, e.g. of energy intake, one reaction is replaced by another reaction (~50:50 chance).

Besides the above observations, it is noticeable that reactions with photons occurred strictly in area I and $C_2H_2^+$ destruction reactions in the colder area II.

3.3. Verification of the RT reactions

The comparison between the proposed reactions in the RTs (see section D) and the identified reactions out of the essential reactions in G.3.2 offers the possibility to create new, corrected RTs. Supposed the combination of reactions occurred in reality, the reaction products could be the source for subsequent reaction sequences. The following

RTs are marked with the reactions, which are principal components of the thesis models A and C (with and without condensates/ices respectively).

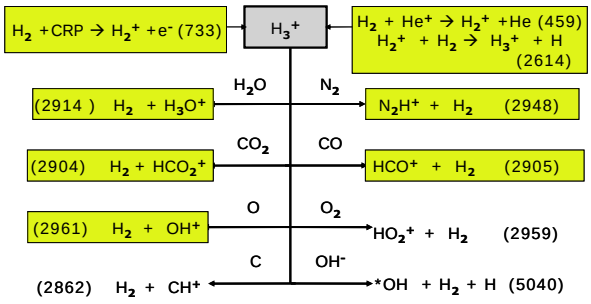

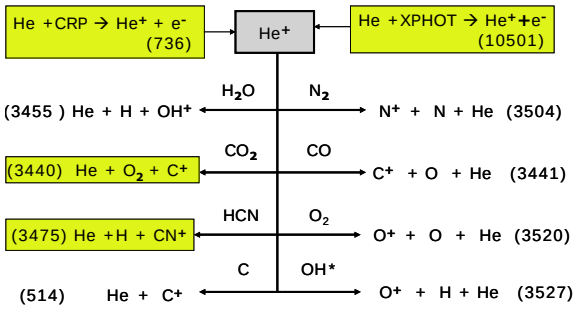

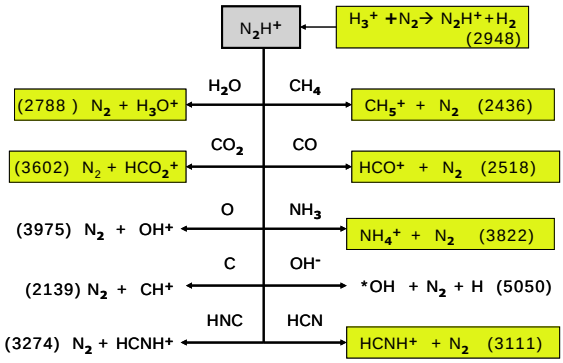

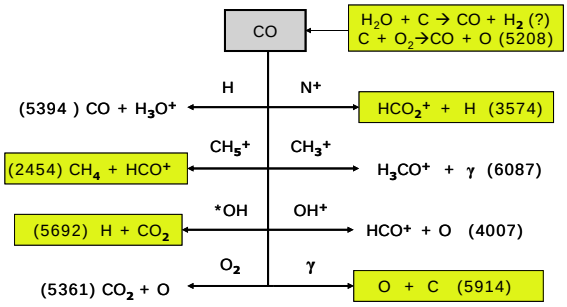

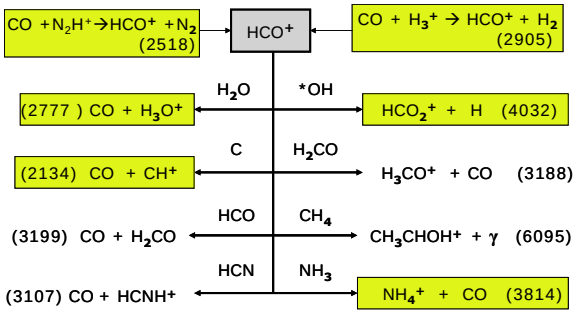

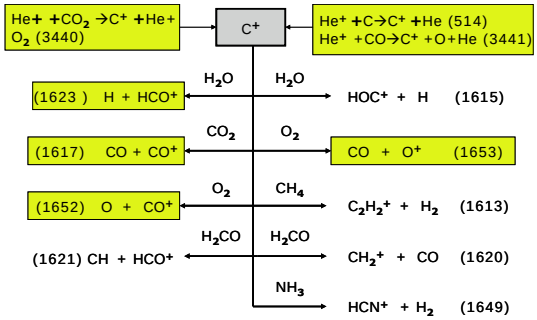

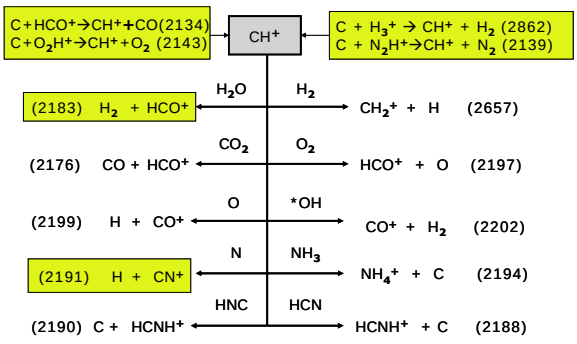

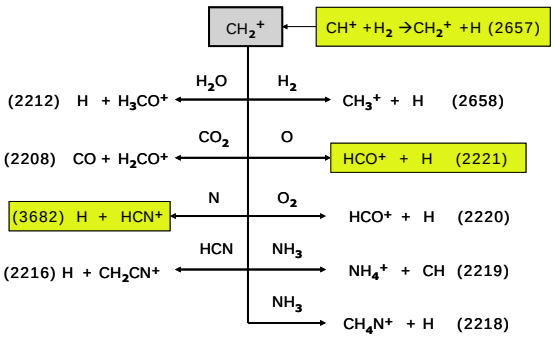

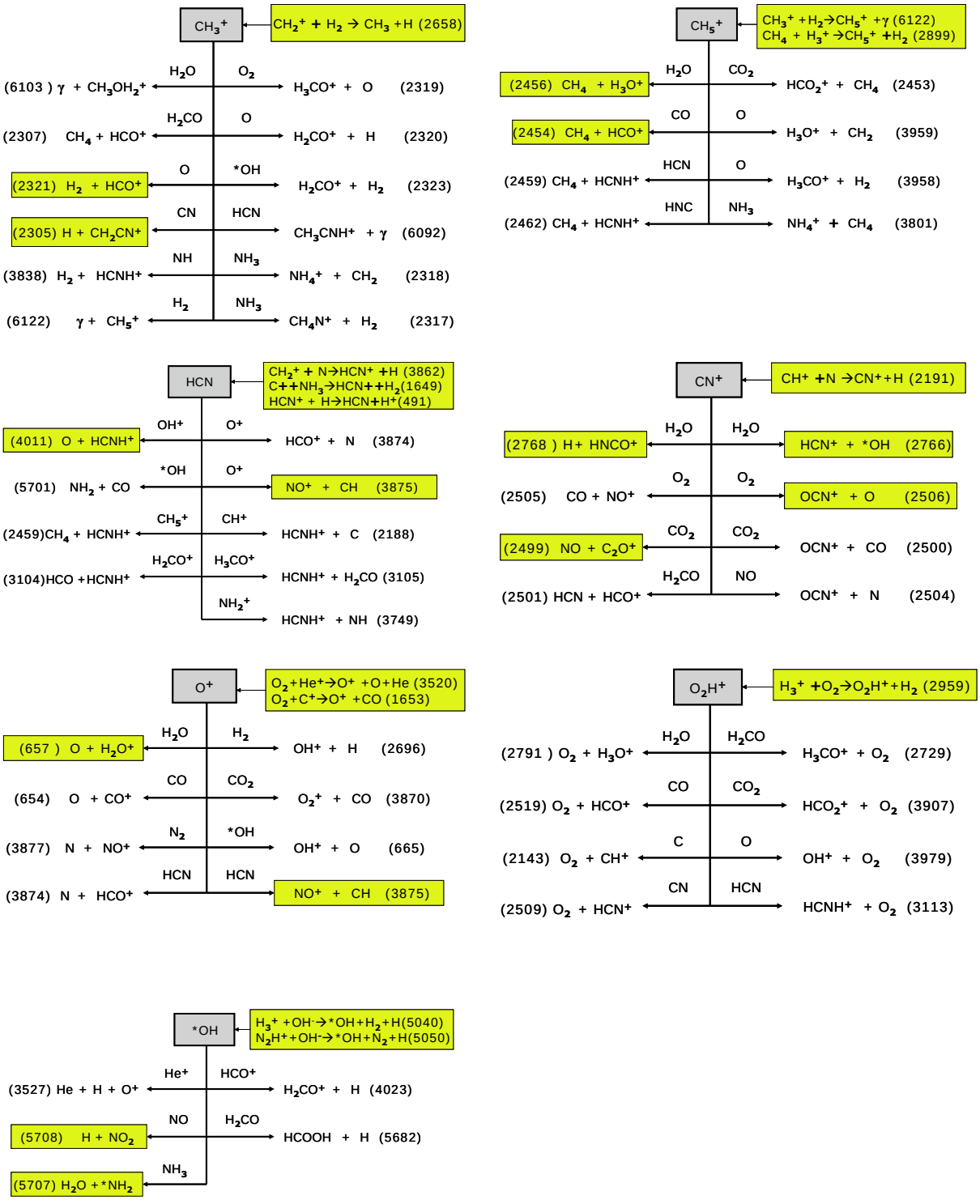

Fig. G.12. : RTs with the most important reactions the thesis models **A** and **C** . The formation reactions are both most important and very probable reactions according to section D. (all marked yellow)

The Fig. G.12. shows 71 reactions which are verifying the initial RTs and their proposed reaction sequences used in the thesis models **A** and **C**. The marked reactions are the result of successful calculations by the ProDiMo programme and identification of main and 2nd main rates as described in section G.2. For the formation reactions of the ions / molecules, which were the sources of the RTs, the most appropriate reactions of the models portfolio were selected as described in section D.2.

The confirmed reactions could be the beginning of considerations about further reactions to relevant molecules or ions which, on their part, can start subsequent reactions. Or, on the other hand, can be the reaction portfolio towards even more minimised models of organic reactions in a PPD.

3.4. Test calculation using the most important reactions

Following the analysis of Fig.G.12, the next and ultimate step will investigate the functionality of minimised chemical networks by simple 40/ 40 grid points tests: firstly with 36+28 reactions commonly used in the thesis models, secondly with either 71 reactions (gas phase, model **A**) or 94 reactions (gas + condensates/ices, model **C**). Further considerations will select the absolutely necessary reactions required to meet the conditions of the disc calculated with the ProDiMo correctly; alternatively to find a way to rearrange the code for appropriate calculations to an even further minimised model.

The results will demonstrate whether it is possible to create even more minimised models with reasonable results in terms of irregularities found in the main formation / destruction rate diagrams and in the log **ε** diagrams for the different molecules and ions.

H. Comparison of models and discussion

H.1. General remarks

To stabilize the entire chemical network it is necessary to include all appropriate reactions for formation and destruction. The standard properties of a (proto) star (q.v. Tab. D.1.1) should be maintained, because variations would influence the results of the chosen chemical network. In the foregoing sections all these aspects were considered and the results were described in models **A - E .**

For the readout of appropriate pictures and graphs ProDiMo offers two different routes: one is using the 'chemical analysis programme' to show the main and 2nd main formation / destruction rates. The other route utilises the programme 'out.ps', which produces a data collection of all pictures, diagrams and graphs. Section L. (" Methods") describes in detail how the programme steps 'chemical analysis programme' and the 'out.ps' data are handled and the results analysed and visualised.

H.2. Comparing the concentration features of the models

The diagrams and figures were read out from the 'out.ps' part of the ProDiMo calculation results and all the obtained pictures were interpreted. The concentrations relative to hydrogen are expressed as $\log \varepsilon_i = n_i / n_{(H)}$. As examples for this evaluation CO, HCO^+ and HCN are described in the following, because these species are important and generally used for assessments of PPDs chemistry.

1. CO (in Fig. H.2.1.)

There is an obvious difference of the CO abundance between the reference model DM and all thesis models: within the pure gas field of the disc at distance 0.03 to 0.2 AU and relative height of 0.0 to 0.1 [z/r], CO is less abundant in DM; this is, by the way, even more noticeable for CO_2 on exactly the same spot.

The thesis models C and E have larger condensation regions at about 1 – 40 AU// 0 – 0.08 z/r than the reference model DM; 60% less reactions allow more space for condensation (only 40 CO reactions compared to 147 in DM). The model D has 142 CO reactions and consequently a similar condensation region as DM.

H.2.1. Example log ε (CO)

Comparison log ε (CO) for models DM , A , B , C, D and E

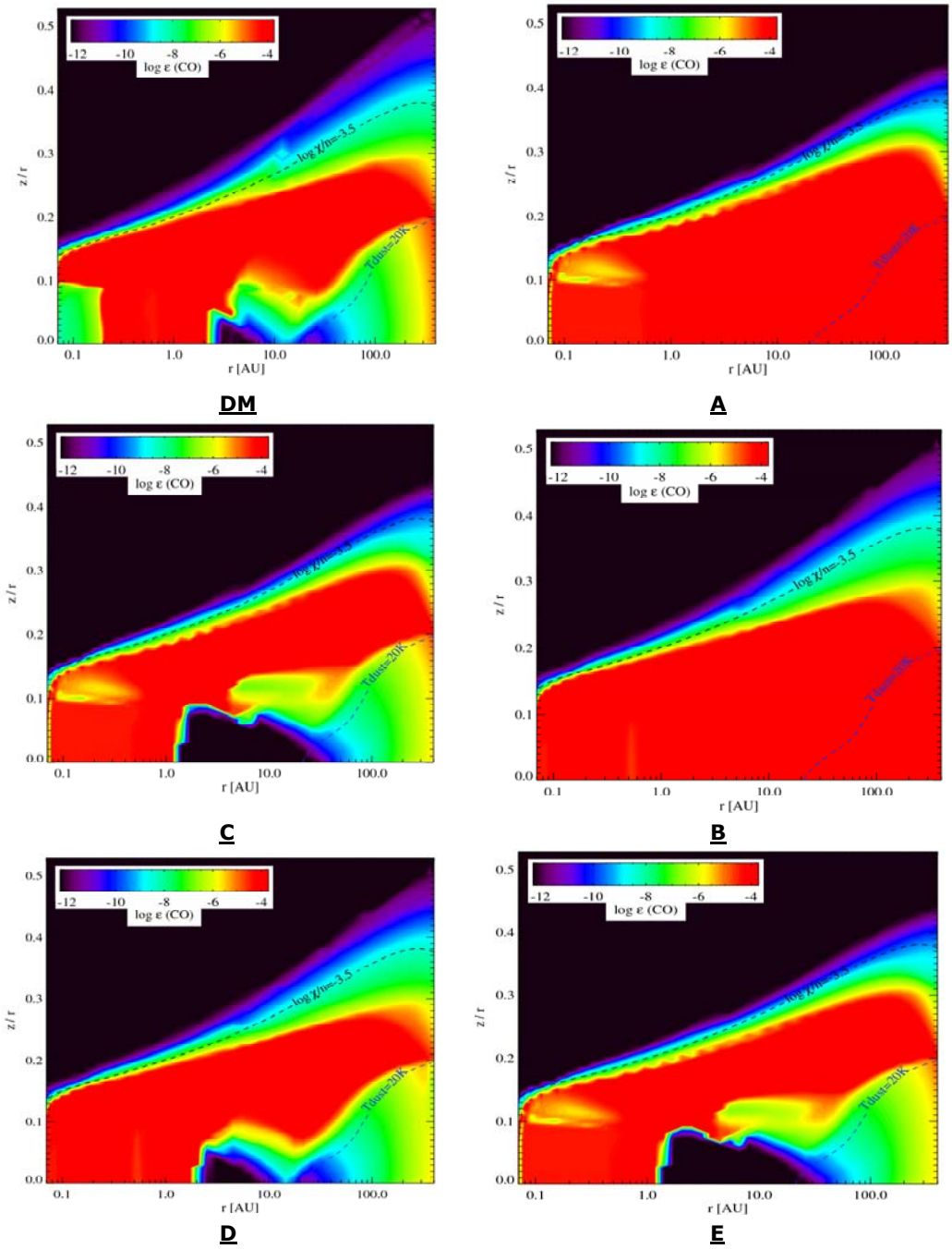

Fig. H.2.1.: Comparison log ε (CO) for models **DM** , **A** , **B** (all reactions of species of A) , **C** (similar to A, but with condensates/ices), **D** (like B but with condensates /ices) and **E** (like C but with 100 fold Fe^0)

2. HCO^+ (in Fig. H.2.2.)

Compared to CO, HCO^+ is less abundant in areas I & II of all models. In the PPD outer regions, at 10 to 100 AU, HCO^+ concentrations of about 10^{-10} [cm^{-3}] are recognised. Close to the midplane (z/r 0.1), concentration is below 10^{-12} [cm^{-3}]: in model DM up to 140 AU, in models A and B up to 100 AU. Models C, D and E show concentrations of about 10^{-10} [cm^{-3}] in outer regions close to the midplane (z/r 0.1 // 10 to 100 AU).

Comparing models DM and B there is no correlation between the number of reactions and the resulting concentrations of HCO^+. The models C and D show similarity, regardless of

the number of reactions. Both vary from DM, probably because of the different reaction portfolio. Therefore the reactions variety seems to be more significant than the sum of reactions. These phenomena should be verified in further investigations.

H.2.2. Example log **ε (**HCO^+)

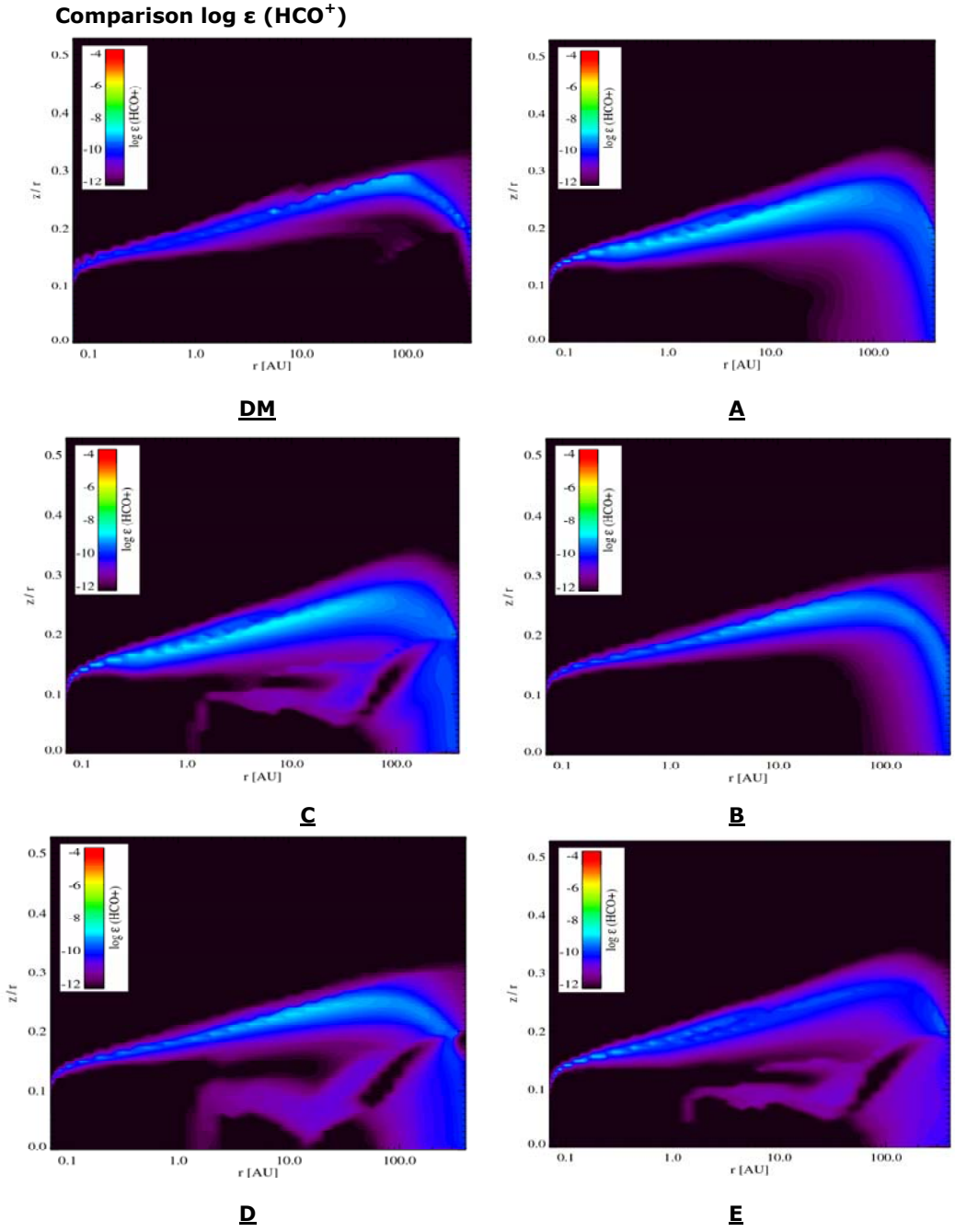

Fig.H.2.2.: Comparison log ε (HCO^+) for models **DM** , **A** , **B** (all reactions of species of A) , **C** (similar to A, but with condensates/ices), **D** (like B but with condensates /ices) and **E** (like C but with 100 fold Fe^0).

3. HCN (in Fig.H.2.3.)

There is a remarkable difference between HCN and HCO^+. Generally, higher HCN concentrations of 10^{-5} – 10^{-6} [cm^{-3}] were found in a dedicated region:

0 – 0.5 AU/ 0 - 0.12 z/r, much more pronounced in the thesis models than in the reference model DM. The thesis models A, C and E, with a smaller reaction portfolio, have bigger region with high concentrations than B and D. It seems in this case that fast reactions are missing to destroy HCN. It is the same region 0 -0.2 AU / 0- 0.1 z/r, where CO and CO_2 have minimum concentration in model DM and for instance H_2O and CH_4 have maximum. This phenomenon is one of the fundamental differences between the reference model DM and the thesis models. Perhaps it is the bigger element portfolio of DM, which is responsible for the difference; not the number of reactions as such. This presumption could be followed up in further test models.

H.2.3. Example log **ε** (HCN)

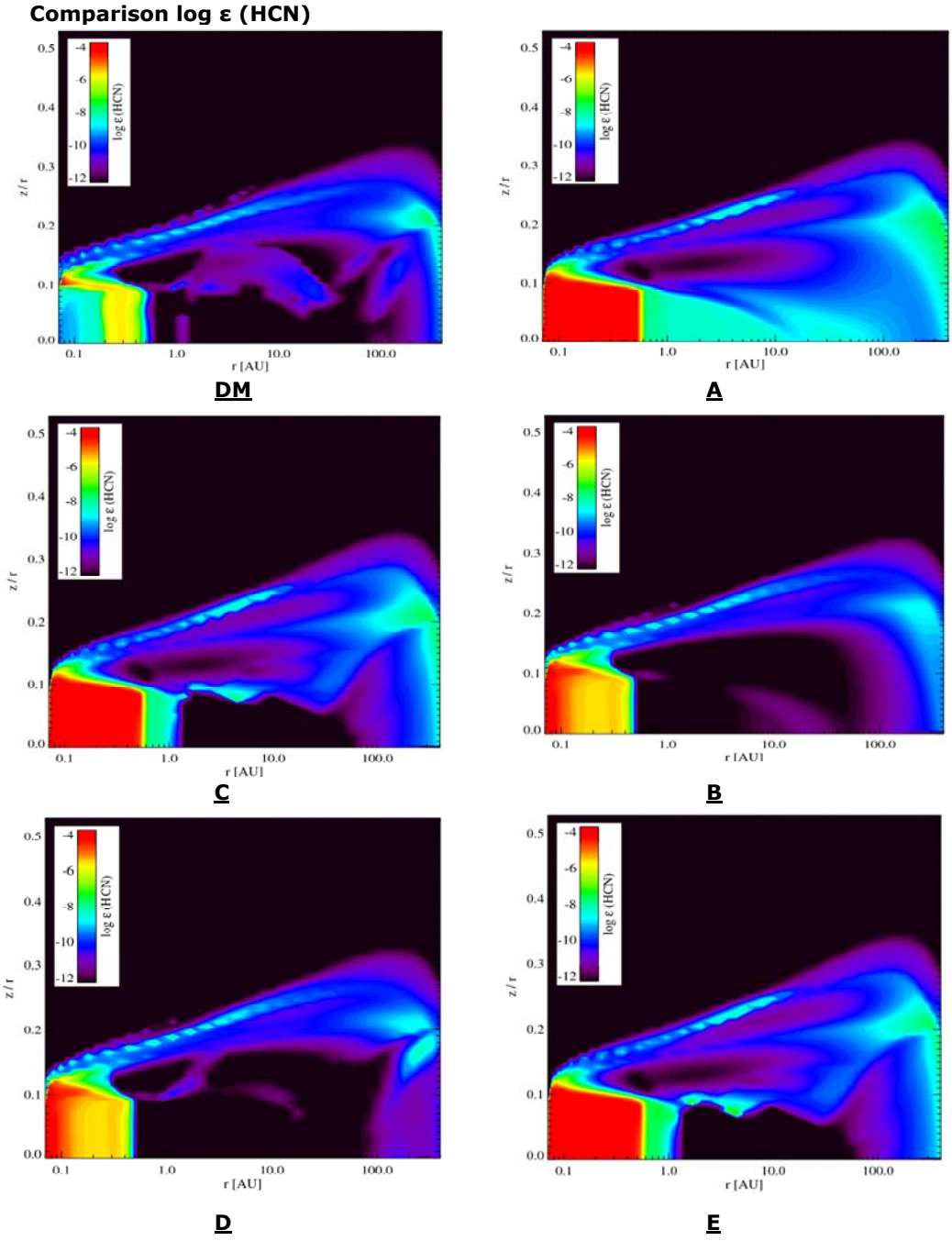

Fig. H.2.3.: Comparison log ε (HCN) for models **DM** , **A** , **B** (all reactions of species of A) , **C** (similar to A, but with condensates/ices), **D** (like B but with condensates /ices) and **E** (like C but with 100 fold Fe^0).

H.3. Thermal balance of the models

This section deals with the most important heating and cooling processes, which reflect the presence and abundances of molecules and or condensates/ices in the various PPD layers. The fundamental question to solve is: will heating and cooling processes alter, if chemical networks are minimised?
The colour coded visualisation makes it easy to compare (q.v. Fig.H.3.1.). The thesis models A and C (232 UMIST 2012 reactions, with and without condensates / ices) are compared to the reference model DM. In the figures the central midplane area of the disk is delineated below A_v~10. Due to thermal accommodation the values of T_{gas} and T_{dust} are equal; they are set at the same value in the ProDiMo standard. UV photons are disregarded in that area, CR-ionisation is the only heating process.
The literature (Bergin 2006; Woitke 2009; Semenov 2013) reports, that at z/r ~0.13 a dividing line exists between the shadow of the inner rim and the direct radiation of the hot surface of the star; this line separates the directly illuminated layers from the shielded and cold midplane regions.
Between A_v~10 and z/r ~0.13 an intermediate warm molecular layer exists, heated by H_2 formation on dust surfaces; in the case of DM by the PAH photo-effect heating. This PAH heating is seen in the models A and C as well, although it is not in their species inventory. Being a standard heating process of the ProDiMo programme, PAH heating is always part of the systemic two-level calculations (Woitke 2009).
In the upper rim of the warm molecular layer CO rotational-vibrational cooling occurs, counterbalancing the increasing UV heating. Above that zone, UV radiation becomes too strong and CO is photo-dissociated.
The hot surface layer is primarily heated by collisional de-excitation of vibrationally excited $H_{2exc.}$ in inner disc regions and by PAH heating in outer disc regions. The H_2 molecules are formed on grain surfaces, excited by UV-fluorescence; they undergo de-exciting collisions, whereby the heat is removed by line cooling mechanisms e.g.: OI, OIII, FeI, FeII etc. lines. These cooling mechanisms are part of the DM model. In models A and C, where $H_{2exc.}$ is missing, this effect is compensated by other mechanisms: carbon photo-ionisation , absorption on dust/grain and formation of H_2 on dust. As described above, the PAH heating occuring in the thesis models is part of the systemic standard calculation. For all models the top (photon-dominated) layer z/r ~0.2 – 0.5 is heated exclusively by X-ray Coulomb heating. The resulting high temperatures are counterbalanced by OIII line cooling, followed by Ly-alpha cooling beyond the OIII area. Infra-red H_2O rotational and rotational-vibrational background heating exists in all models as well. The corresponding cooling mechanisms are more dominant and widespread in the models A and C than in DM.
The influence of condensates is smaller than expected, proven by the similar pictures in model A and C; notwithstanding, the picture for the model C looks more complex than for model A (H_2-line cooling, more cooling by accommodation on grains).
The question at the beginning of this section ‘will heating and cooling processes alter, if chemical networks are minimised’, can be answered as follows: in principle not, but in the thesis models, where H_{2exc} is missing, this effect is compensated by other mechanisms: carbon photo-ionisation , absorption on dust/grain and formation of H_2 on dust. In general, there is a tendency towards lower complexity in case of the thesis models.

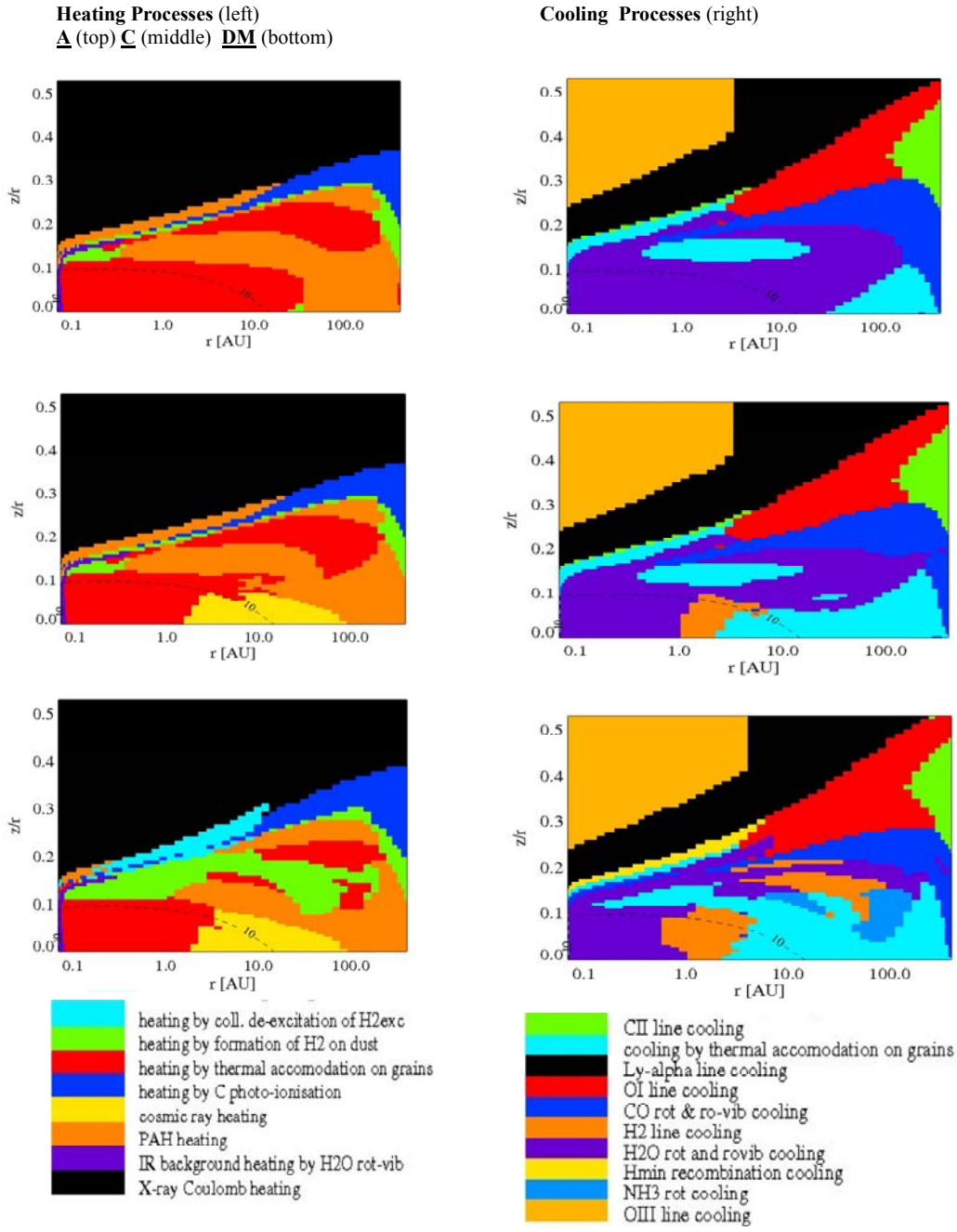

Fig.H.3.1.: Heating processes (left) ./. Cooling Processes (right). **DM** (top), **A** (middle) and **C** (bottom)

H.4. Temperature distribution

The pictures in Fig. H.4.1 illustrate the gas and dust structure in the reference model DM, the thesis model A (without) and model C (incl. condensates/ices). The striking characteristic is the similarity of the hot surface layer above z/r~0.13 in all models.

log T gas (top) ; **log T** gas / T dust (bottom)

Models **A** (left) **DM** (middle) **C** (right)

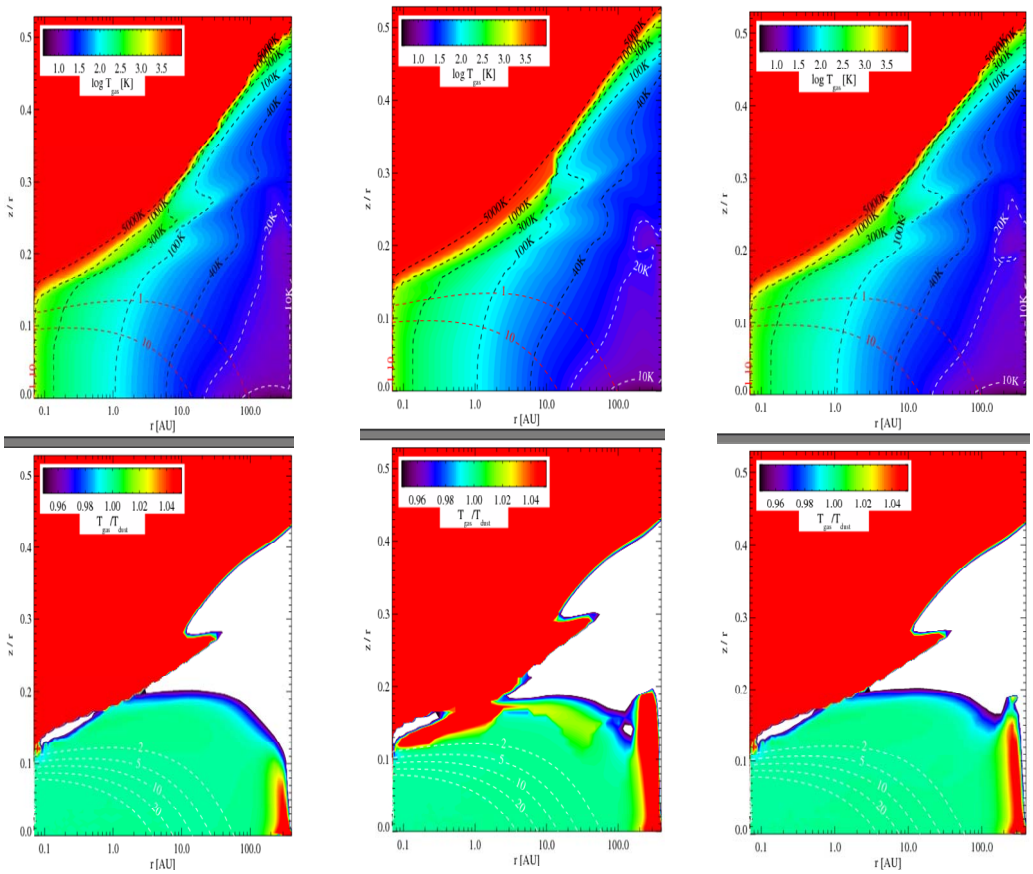

Fig. H.4.1 : log T_{gas} (top) ; T_{gas} / T_{dust} (bottom) of the models **A** (left), **DM**(middle) and **C**(right)

For T_{gas} the border line of 5000K shows a disc form related gradient in a z/r from 0.15 to 0.5 // 0.1 to 100 AU, followed by a thin area of 1000K. A rapid cooling takes place towards the midplane beginning in all models below z/r ~0.1.
The available log T values in the Fig. H.4.1. were analysed by means of the colour coded pictures. Two different regions were chosen for the comparison: z/r 0.1 // 1 AU and z/r 0.2 // 20 AU; one in the cold midplane and the other in the warm molecular layer:
1. z/r 0.1 // 1 AU: model A, C and DM have T_{gas}, ~120K each.
2. z/r 0.2 // 20 AU: model A and C have T_{gas}, ~60K each, the reference model has T_{gas}, ~70K. According to the colouration of T_{gas} / T_{dust} images (bottom row in Fig. H.4.1.), the factor can be determined at 1.04 in regions above 300 /350K.
The conclusion is that the models are almost identical, with small differences in the elevated midplane, where the UV radiation influence is growing. These regions become optically thin, T_{gas} increases and is uncoupled from T_{dust}.

H.5. Comparison of line fluxes

The important perception arising from the chemistry modelling around a star in the PPD, are the resultant line fluxes of the involved species. A group of substantial species was selected and analysed by ProDiMo (q.v. M. 4. 'Programming'); the results are collected in the table Tab. H.5.1.

Model			**DM**	**A**	**B**	**C**	**D**	**E**
Species	ident	Wavelength / Flux [µm] / [Jy]	line fluxes [W/m^2]x 10^{-20}					
CO	J=36-35	72,84/ 0.963	0.30	0.032	0.18	0.032	0.18	0.032
	J=2-1	1300,4/ 0.046	10.4	9.73	10.3	9.46	9.85	9.63
	v=1-0 J=35-36	5040/ 0.293	192	3.26	71.6	3.25	71.6	3.25
^{13}CO	J=2-1	1360,2/ 0.04	3.46	4.55	4.50	3.40	2.84	3.47
HCN	J=3-2	1127,5/ 0.0654	4.35	6.37	3.29	5.98	3.20	5.82
HCO^+	J=3-2	1120,5/ 0.0625	0.50	2.70	2.40	3.30	2.57	1.25
N_2H^+	J=3-2	1072,6/ 0.073	0.0102	6.7x 10^{-7}	1,11x 10^{-3}	7.38x 10^{-7}	0.0594	4.48x 10^{-7}
o-H_2O	4_{23}-3_{12}	78,74/ 0.971	70.0	7.59	71.6	6.79	63.5	7.04
O I	$3p_1$-$3p_2$	63,18/ 0.941	3120	2300	2580	2310	2590	2400
CH^+	J=5-4	72,14/ 0.961	0.68	0.154	0.131	0.154	0.131	0.152

Tab. H.5.1. : Line fluxes, fluxes at selected wavelength of some atoms and molecules observable in PPDs

The discrepancies and conformities among the thesis models and between the thesis models and the reference model are described below:

1. The problem of the diazenylium cation N_2H^+ has been dealt with before in section G. In the a.m. table the following differences are seen: compared to DM the values of models A, C and E are far below the DM and D model values. Model D contains condensates/ices and has 85% of the reactions number in DM, although not the identical ones; it is even higher in line flux compared to DM. Maybe the reaction selection in D was more structured than in DM? (This could be checked by more test models.) Remarkably, the model B, with all possible reactions of model A, has approx. 1000 times higher line flux than model A. Compared to DM, model B has a lower line flux than DM; this may be caused by the absence of condensates in B. In model E, the Fe concentration is increased by factor of 100, shows nevertheless only marginal increase of the line flux. This confirms the assumption that iron/metal does not prevent the decay of the diazenylium cation. Solid phases in the form of condensates / ices (10 species in DM and 23 species in model D) may better stabilize this cation.
2. The line fluxes of CO (observed at 72.84µm, in an attenuated case also at 5040µm) and o-H_2O in the models DM, B and D, which have higher number of reactions, are very similar. The models with a smaller reaction portfolio (A, C and E) show also similar line fluxes, but significantly lower.

3. The species HCO^+ is more rapidly transformed in DM than in all other models; due to the much bigger reaction portfolio with regard to HCO^+. It seems that the [Fe] has slight influence on the flux when comparing models A-D with model E.
4. For the species CH^+ a lower flux is visible in all thesis models: the reaction selection was perhaps not so suitable, compared to the reference model. The reaction selection could be improved in future attempts.

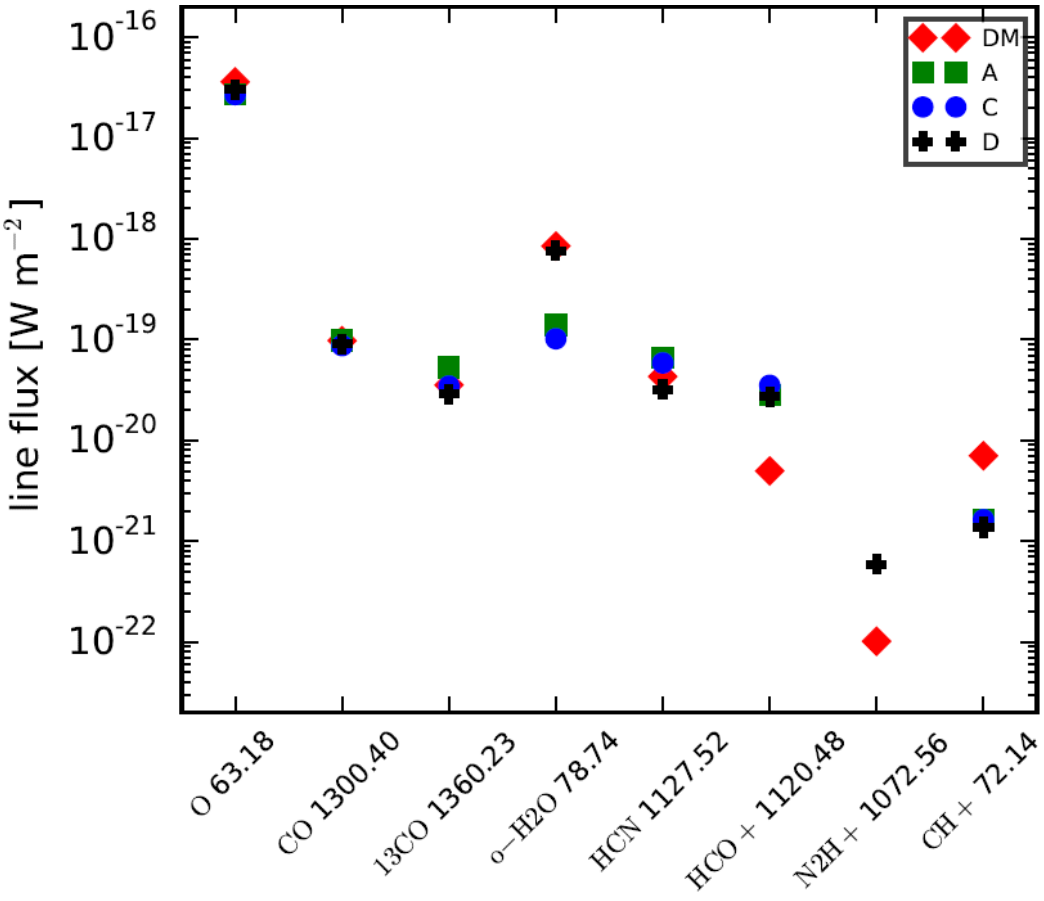

Fig. H.5.2.: Line fluxes [W/m²] for some species and wavelength; O^I: 63.18 µm, CO: 1300.4 µm ^{13}CO: 1360.23 µm, o-H_2O: 78.74, HCN: 1127.52 µm, HCO^+: 1120.48 µm, N_2H^+: 1072.56 µm, CH^+: 72.14 µm.
Colour-code for the standard model **DM** and the thesis models **A**, **C** and **D**.
N_2H^+ for the models **A** and **C** are not shown (because of being 10^{-29}[W/m²]); CH^+ for model **C** is hidden by **A**.

H.6. Chemical composition of the gas in the designed PPDs

H.6.1. Gas compositions

The gas compositions in four picture tables, Fig.H.6.1.1. to Fig.H.6.1.4., depict the concentrations of the species in $\varepsilon = n_i / n_H$ relation: **i** is the species and H is total hydrogen density. The logarithmic scales are colour coded; however, there is a different scaling in upper and 2nd row compared to 3rd and bottom row.

The chemical gas composition is commented as follows:
Comparing relevant species, which contribute mostly to the reactions between hydrogen, oxygen and carbon, there were not many visible differences found, bearing in mind the big differences in number of reactions (model A: 232; DM: 1288). The similar appearance of DM and C is indisputable, because both have condensates/ices, although different ones.
In the reference model DM, between 0-0.2AU/0.0.1 z/r, the [CO_2] is below 10^{-12} [cm^{-3}], whereas in models A, B, C, CO_2 is less abundant in the same area of 10^{-6} to 10^{-7} [cm^{-3}]. HCO^+ appears in a 10^{-9} [cm^{-3}] in region above the midplane in all models except the minimised model C, with condensates/ices. This may be generated by the higher concentration of H_3^+ in that area (only in model C, not very much in DM).

H.6.2. Chemical condensate / ice composition

The reference model DM and the thesis model C show the chemical composition of the condensates/ices in two picture tables, Fig.H.6.2.1. to Fig.H.6.2.2. The concentrations are depicted in the same manner like the gas compositions: log $\boldsymbol{\varepsilon_i} = n_i / n_{(H)}$ relation, with an uniform colour code.
The chemical ice composition is commented below:

The condensate / ice formation is ruled by the distance to the star, by the height above the midplane, by the density of the species and the dust as 'seed' particle. Two obvious differences were found in the comparison of the two models with condensates/ices (the species marked with X#), the reference model DM and thesis model C:

1. N_2# in model C is far below 10^{-12} [cm^{-3}], although it exists as species, but does not appear in any main and 2nd main reaction.
2. CH_4# does not appear in model C in high concentration like in DM, i.e. above 10-30AU. CH_4# is produced in thesis models only by two reactions (2454, 2456).
3. NH_3# is present in model C, but in much smaller region (1-4 AU/0-0.1 z/r), compared to reference model DM in the region 0.7-100 AU/ 0-0.17 z/r. The reason might be that NH_3 is used up in other important gas phase reactions.
4. Other condensates/ices like CO#, H_2O#, CO_2#, HCN# behave in similar way: if important reactions are using up species in main or 2nd main gas phase reactions of minimised models, these depleted species are not available for the ice formation.

Chemical Gas Composition **DM**

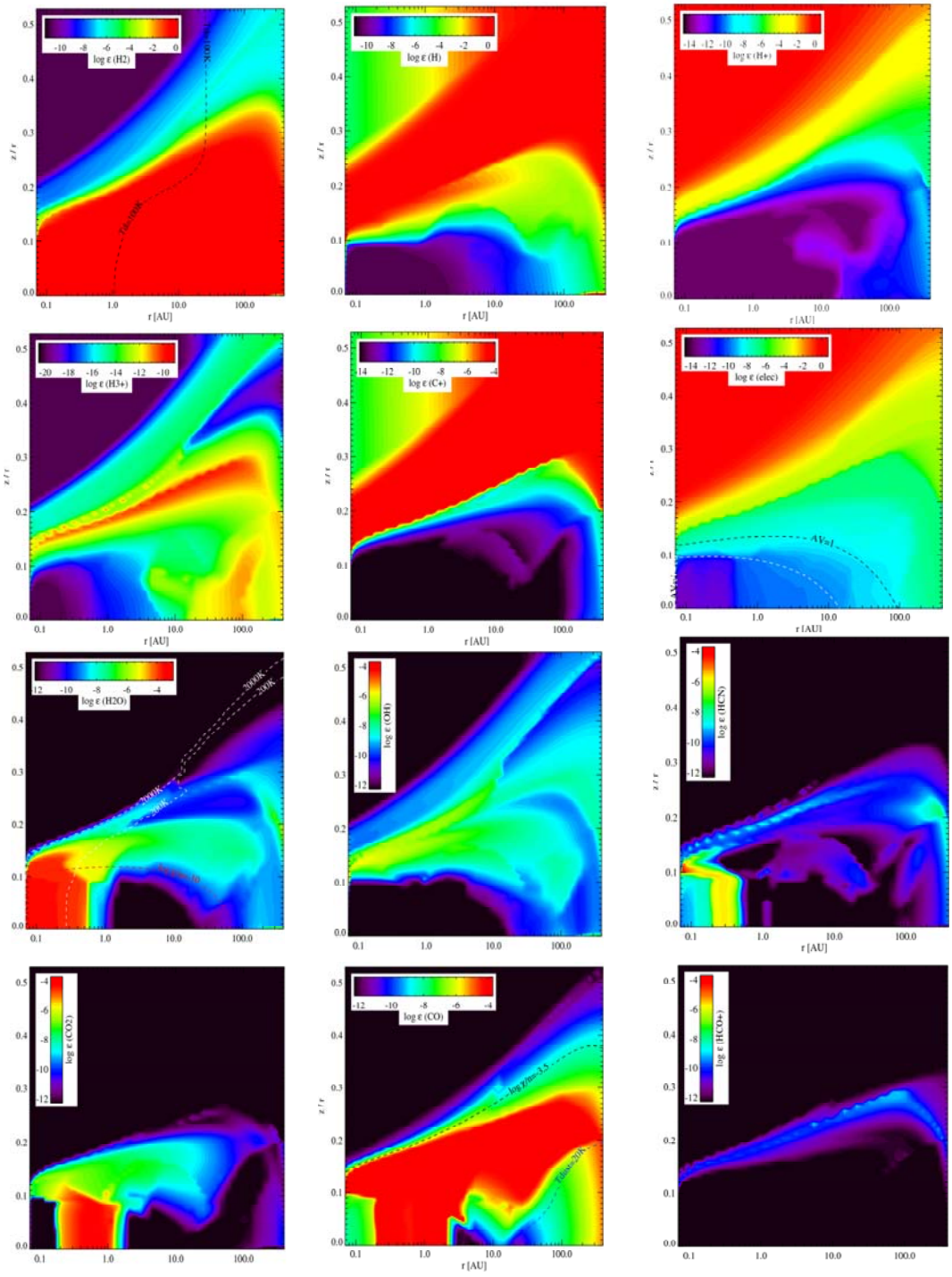

Fig.H.6.1.1.: Chemical composition of the gas in the reference ProDiMo model **DM**. The concentrations shown in log εi = ni / n(H) n_i / n_H relation, where i is the species and H is total hydrogen density.
Upper row: H_2, H, H^+; 2nd row: H_3^+, C^+, free e^-; 3rd row: H_2O, *OH, HCN; bottom row: CO_2, CO, HCO^+.
Note the different scaling in upper and 2nd row compared to 3rd and bottom row.

Chemical Composition Gas **A**

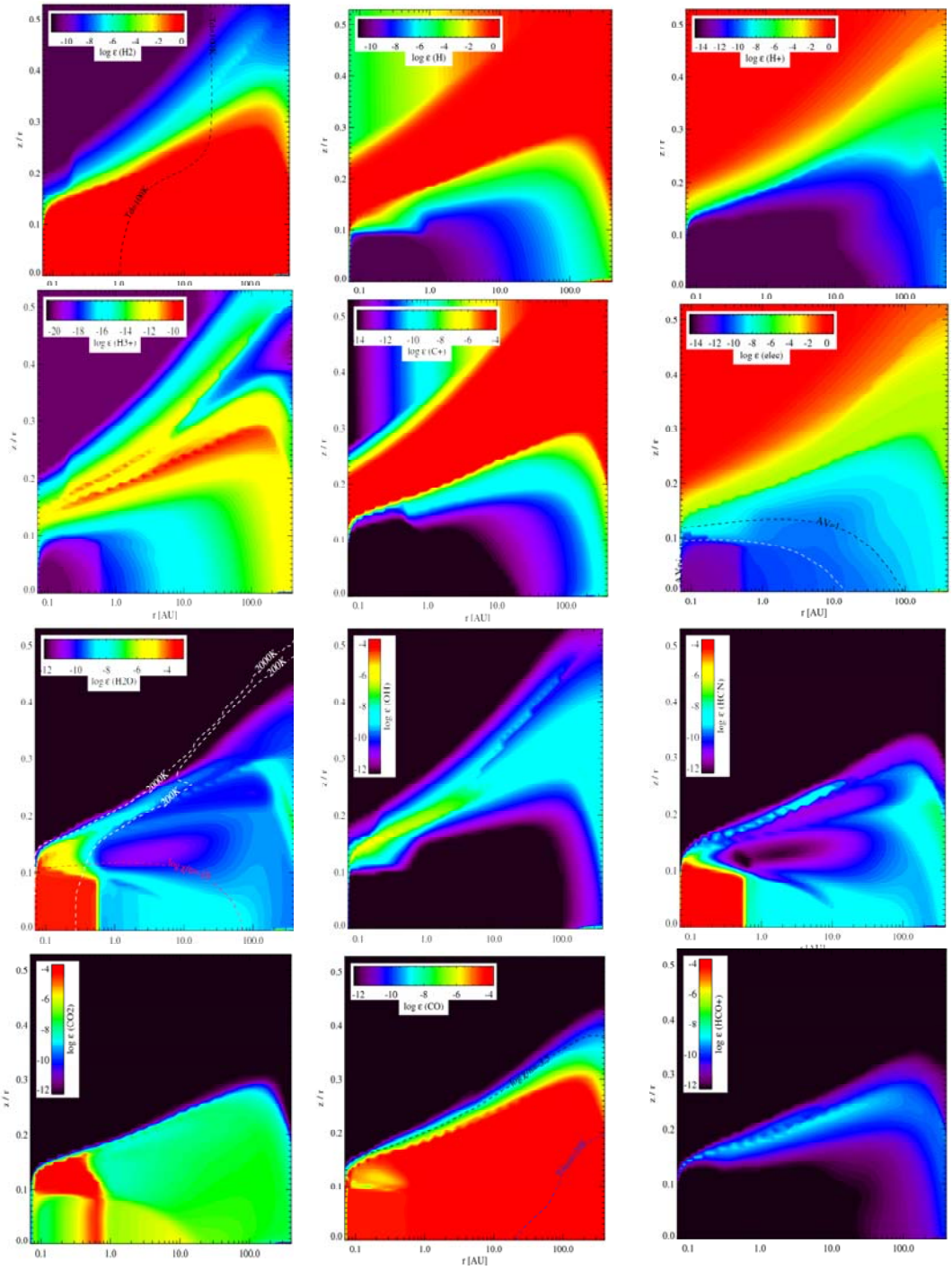

Fig.H.6.1.2.: Chemical composition of the gas in the model **A**. The concentrations shown in log εi = ni / n(H) relation where i is the species and H is total hydrogen density.
Upper row: H_2, H, H^+; 2nd row: H_3^+, C^+, free e^-; 3rd row: H_2O, *OH, HCN; bottom row: CO_2, CO, HCO^+.
Note the different scaling in upper and 2nd row compared to 3rd and bottom row.

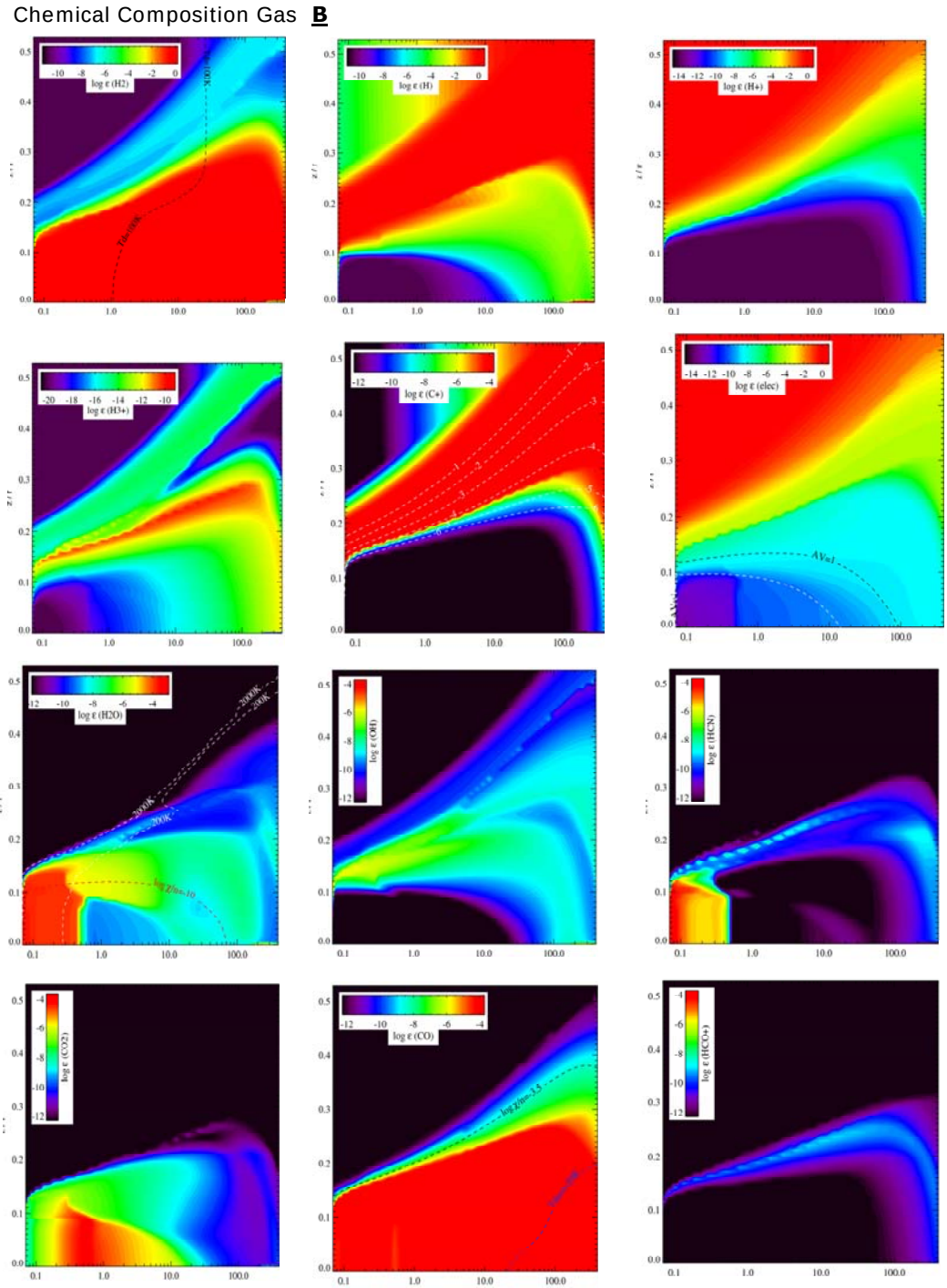

Fig.H.6.1.3.: Chemical composition of the gas in the model **B**. The concentrations shown in log εi = ni / n(H) relation where i is the species and H is total hydrogen density.
Upper row: H_2, H, H^+; 2nd row: H_3^+, C^+, free e^-; 3rd row: H_2O, *OH, HCN; bottom row: CO_2, CO, HCO^+.
Note the different scaling in upper and 2nd row compared to 3rd and bottom row.

Chemical Composition Gas **C**

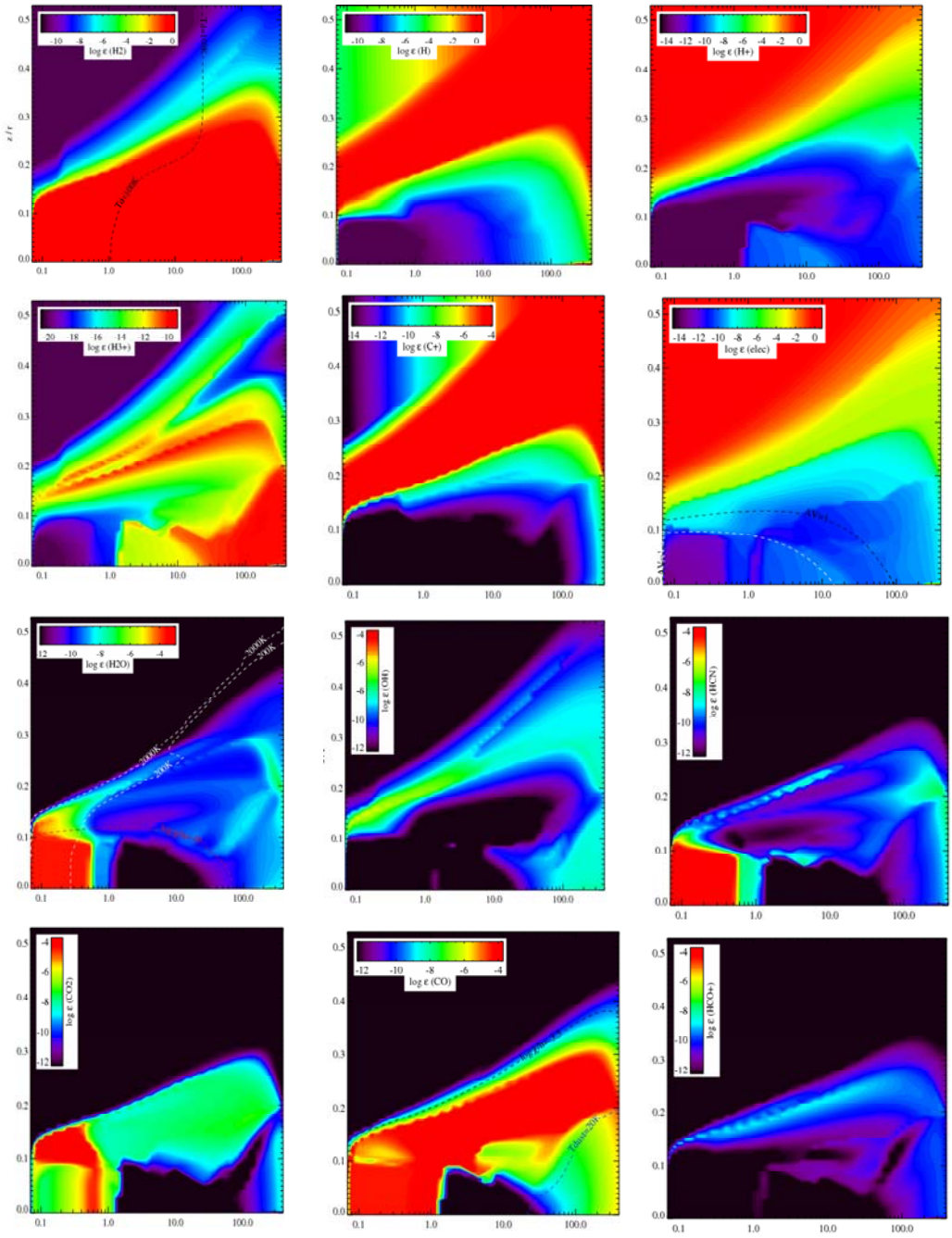

Fig.H.6.1.4.: Chemical composition of the gas in model **C**. The concentrations shown in log εi = ni/ n(H)relation where is the species and H is total hydrogen density.
Upper row: H_2, H, H^+; 2nd row: H_3^+, C^+, free e^-; 3rd row: H_2O, *OH, HCN; bottom row: CO_2, CO, HCO^+.
Note the different scaling in upper and 2nd row compared to 3rd and bottom row.

Chemical Ice Composition **DM**

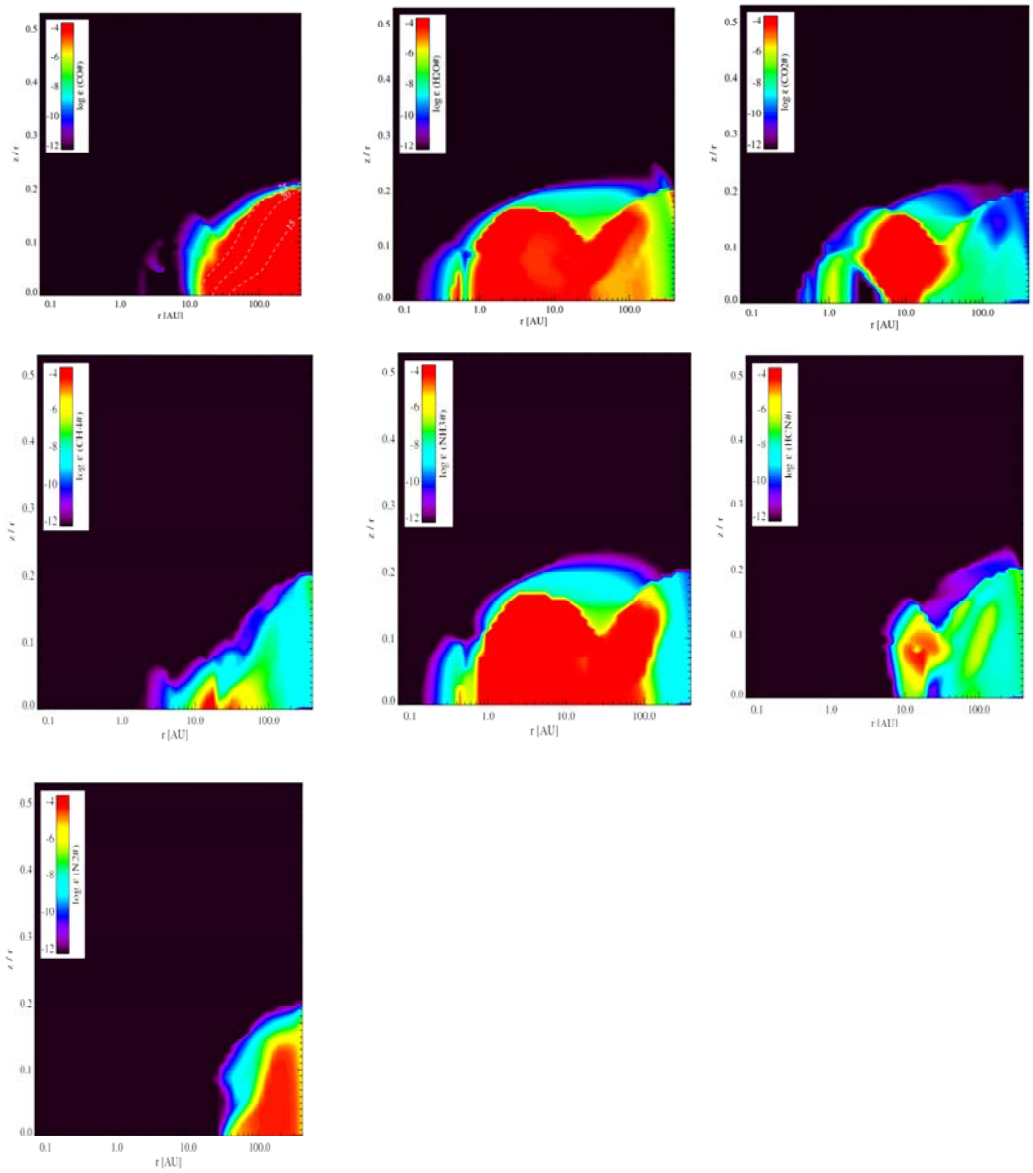

Fig.H.6.2.1.: Chemical composition of condensates/ ices in the reference model **DM**. The concentrations shown in log εi = ni / n(H) relation where i is the species and H is total hydrogen density.
Upper row: #CO, #H_2O,#CO_2; 2nd row: CH_4, #NH_3^+, #HCN; bottom row: #N_2, .

Chemical Ice Composition **C**

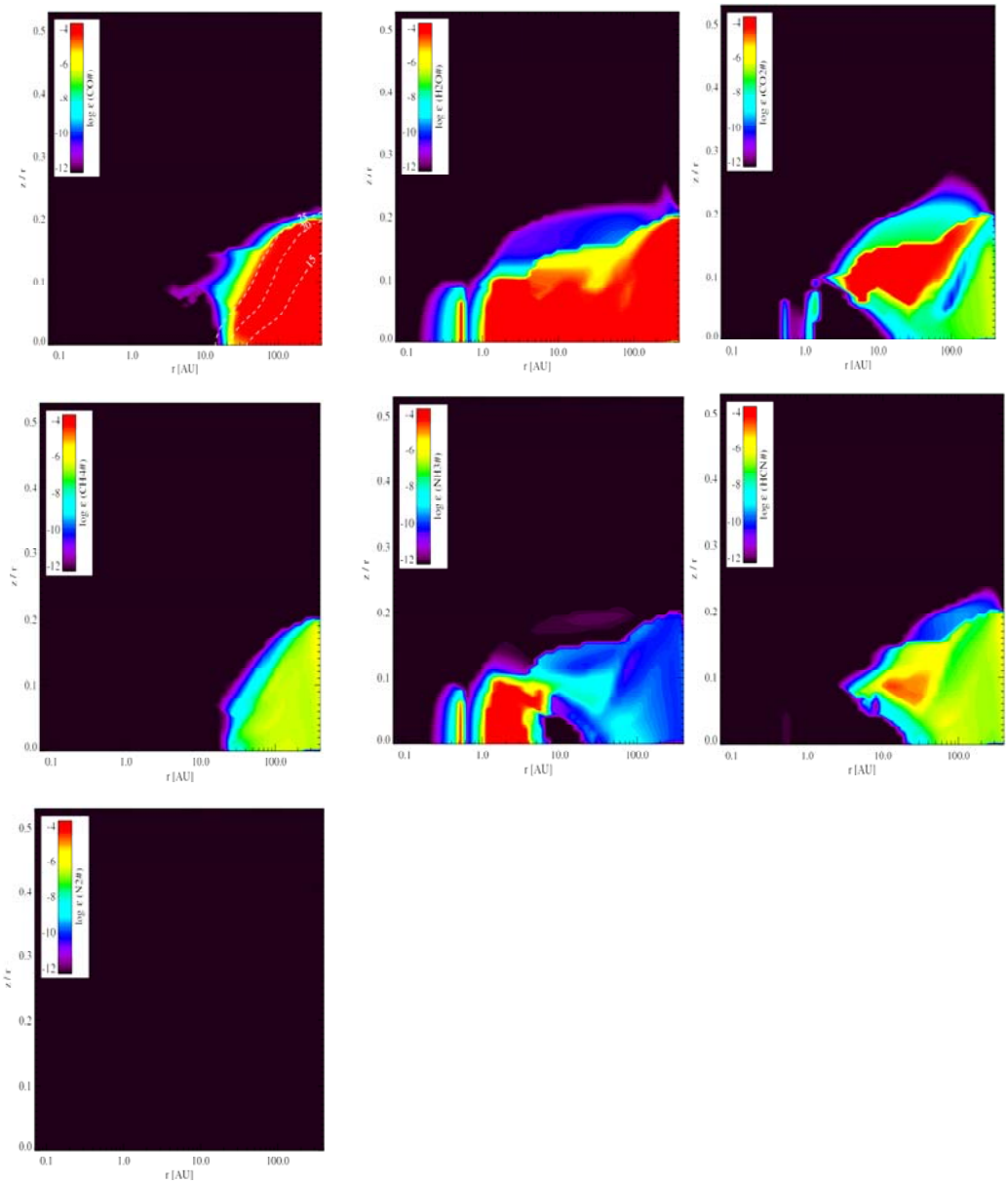

Fig.H.6.2.2.: Chemical composition of condensates / ices in the model **C**. The concentrations shown in log εi = ni / n(H) relation where i is the species and H is total hydrogen density. Upper row: #CO, #H_2O,#CO_2; 2nd row: #CH_4, #NH_3, #HCN; bottom row: #N_2.

H.6.3. Carbon distribution in the midplane

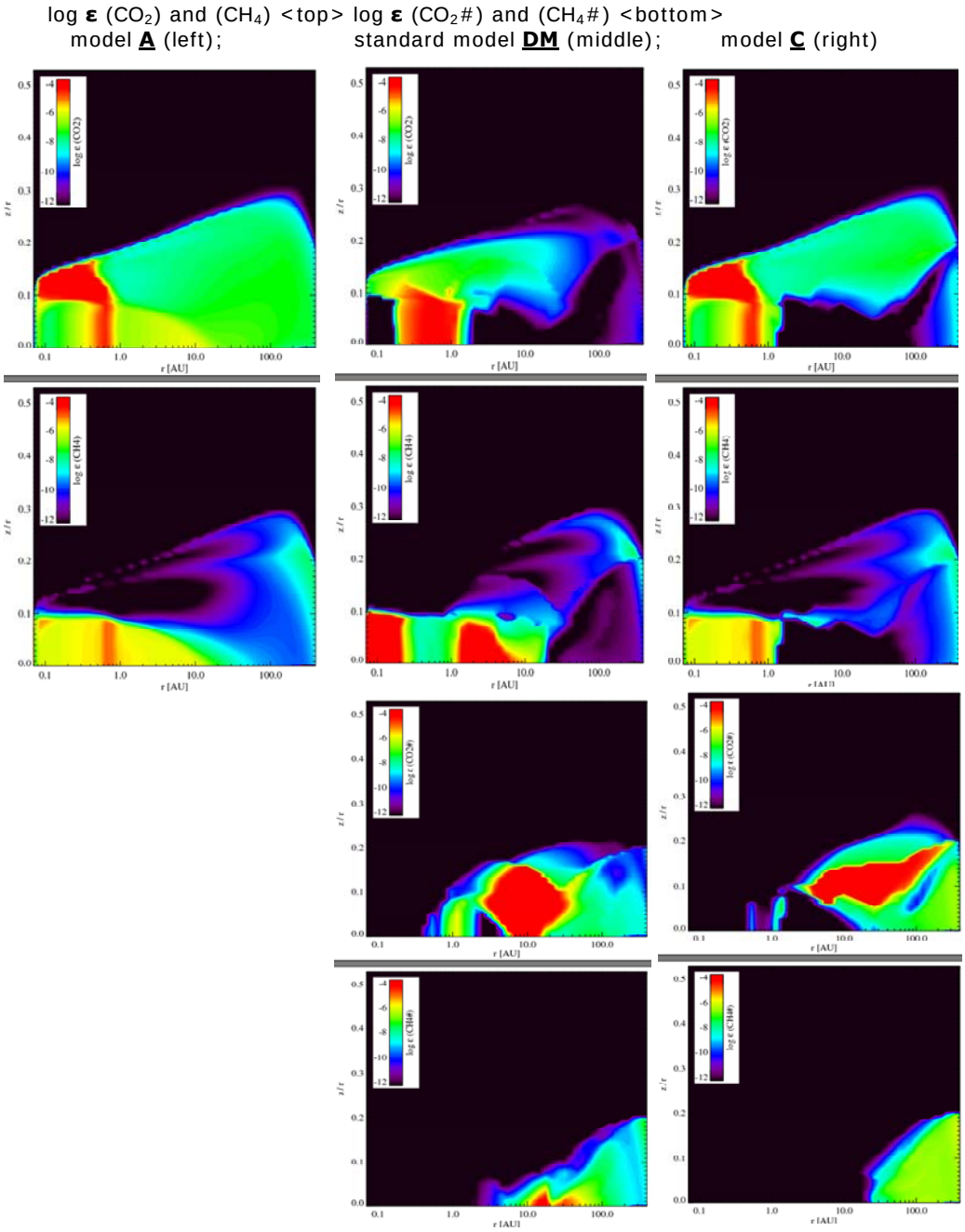

Fig.H.6.3.1.: Concentrations of carbon forms in the midplane of a PPD. CO_2 and CH_4 as gas (top) and the Condensates / ices thereof (bottom). Models **A** , **DM** and **C** were taken for comparison.

It is reported in the literature (e.g.: Kamp and Dullemond 2004; Woitke 2009), that carbon in the midplane can appear either in the form of carbon monoxide or as methane. To verify this fact, the reference model DM was compared with the minimised models A (without) and C (with condensates/ices). Carbon monoxide in high concentrations ~10^{-4} [cm^{-3}] was present in large areas (0-120AU/ 0-0.3 z/r) of models DM, A and C (q.v. Fig.H.6.1.1-4.).The exceptions, with much lower abundance, are the ice lines of DM and C and in model DM the region 0-0.2 AU/ 0-0.1 z/r.

For the thesis discussions, carbon dioxide CO_2 is chosen instead of CO, because the differences are more demonstrative.
In reference model DM, the area 0-0.2 AU/ 0-0.1 z/r, methane is prevalent with ~10^{-4} [cm^{-3}] where carbon dioxide is less concentrated (down to ~10^{-12} [cm^{-3}]). CO_2 is present with 10^{-4} [cm^{-3}] in the areas 0-1AU/ 0.1-0.18 z/r of the minimised models A and C; methane is not dominant there, because the reference model DM has much more methane related reactions than thesis models A and C (90 reactions in DM, 10 reactions in A, 15 reactions in C). DM shows high methane concentration of ~ ~10^{-4} [cm^{-3}] in two regions: 0-0.2 AU/ 0-0.1 z/r and 1.2-10 AU/0-0.08 z/r.

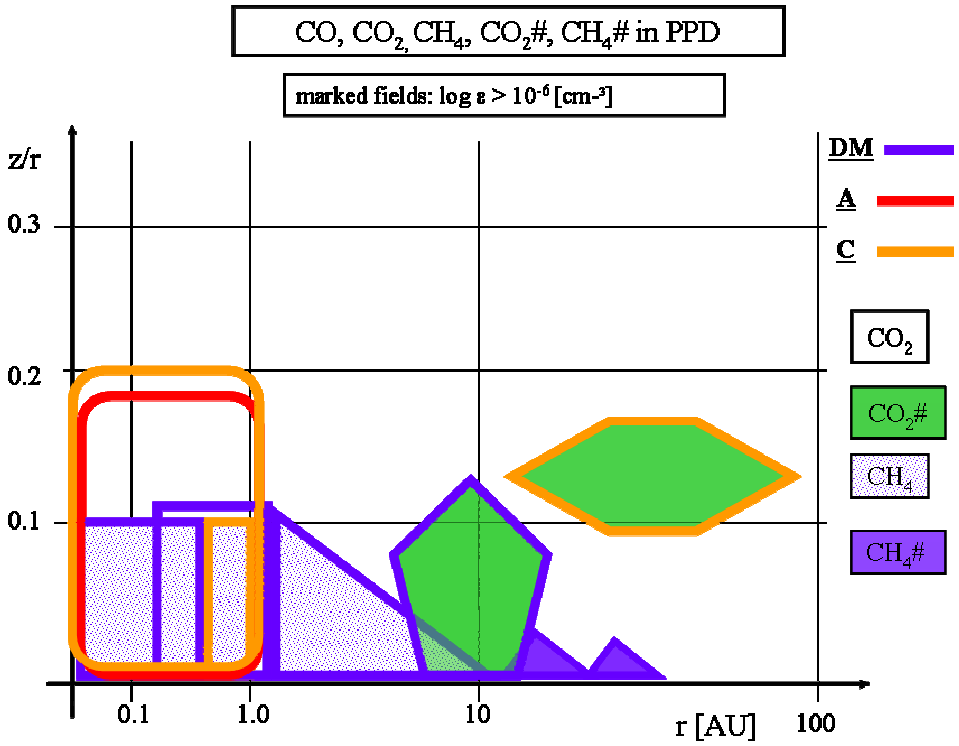

Fig.H.6.3.2: Distribution of CO, CO2, CH4, CO2# and CH4# in PPDs of models **A**, **C**, compared to **DM**

It can be stated that CO2# is a dominant C/O medium for the thesis models in regions of 4-100 AU//0.05-0.2 z/r.
The sketch in Fig.H.6.3.2. illustrates the above described distribution and makes the different areas more obvious.

I. Conclusion and Outlook

Conclusion:

This thesis presents new chemical models of a protoplanetary T Tauri star disc with special attention to carbon containing reactions and species. To reach necessary transparency the thesis has reduced drastically the number of elements, species and therefore reactions; target-oriented species and reactions have been introduced to form stable chemical networks. The subsequent reactions offer a comprehensible chain towards basic chemicals out of C, H, O and N. The construction of the desired chemical networks materialises in so called 'reaction trees' (RT), in which abundant and reactive molecules / atoms like H_3^+ and He^+ start and establish chemical reaction sequences.
After lots of proven and tested chemical networks, final versions of minimised test models A-E were compared among themselves and against the chosen reference model DIANA-SMALL (part of the DIANA project). Decisions for the reaction sequences were taken on the basis of chemically reasonable reactions which are also kinetically and thermodynamically feasible.

The reference model DM revealed several weak points: numerous elements with low abundances, only a small number of condensates/ices and some missing complex carbon/oxygen species. Consequently, the author of this thesis formulated suitable chemical reactions/species and ascertained they are available in the UMIST2012 data base. The thesis models were continuously improved to achieve consistent chemical networks; the choice and implementation of fitting chemical reactions made the model A stable with ~ 230 reactions, although A has no condensates or ices. The addition of 23 condensates resulted in the model C, containing ~ 400 reactions.

Compared with the reference model, the model D worked with 50% of the elements and achieved 85% of the sum of reactions with 90% of species; the elements and species comparison is expressed in numbers, because different elements and ices are involved. Model D performs equally well as the reference model; the stringent reaction selection leads to even better results, especially with regard to line fluxes of certain species.
The remaining discrepancies between the reference model and the thesis models, as well as among the thesis models themselves, are explained below.

The assessment of the model calculations and the resulting main formation and destruction reactions found 36 essential reactions commonly used in all models including the reference model and 28 other reactions shared among the thesis models only. The evaluations of the most important reactions allow the comparison with the proposed RT and offer the possibility to create new, corrected RTs.

CO, HCO^+ and HCN are generally selected as important species for the evaluation of PPD chemistry. The evaluation of the species concentrations in the models reveals an obvious difference of the CO abundance between the reference model and all thesis models: CO is less abundant in the reference model; even more noticeable is the lack of CO_2 on exactly the same spot close to the midplane. In all models HCO^+ is less abundant in the warm molecular layer areas. Only in photon dominated areas of the outer PPD regions at 10 to 100 AU, higher concentrations were recognised. It seems there is no correlation between the number of reactions and the resulting concentrations of HCO^+. In the region close to the midplane, the reference model has minimum concentrations of HCN, CO and CO_2, whereas all thesis models have maximum concentrations in this region. This phenomenon is one of the fundamental differences between the reference model and the thesis models.

Heating and cooling processes reflect the presence and abundance of molecules and/or condensates/ices in the various PPD layers. The answer to the fundamental question

"will heating and cooling processes alter, if chemical networks are minimised?" is: "in principle not". Generally there is a tendency to lower complexity in the thesis models. Since H_{2exc} is missing in the thesis models, it is compensated by other mechanisms: carbon photo-ionisation, absorption on dust/grain and formation of H_2 on dust.

The analysis of the temperature distributions in the models with and without condensates/ices leads to the conclusion that the models are almost identical; only small differences exist in the elevated midplane, due to the growing UV radiation influence. These regions become optically thin; T_{gas} increases and is uncoupled from T_{dust}.

Another important perception of the chemistry modelling around a star in the PPD are the resultant line fluxes of the species involved. Most of the species show no striking differences between the models, but a huge discrepancy was found in case of the diazenylium cation (N_2H^+). Compared to the reference model the values of thesis models are far off (~ $1 \cdot 10^{-22}$ [Wm^{-2}] compared to ~ 10^{-29} and ~10^{-25} [Wm^{-2}] resp.). However, one thesis model with condensates/ices and 85% (in number) of the reference model reactions shows an even higher line flux (~ $6 \cdot 10^{-22}$ [Wm^{-2}]) . Possibly the selection of the reactions in this model was more structured. Several attempts were made to increase the diazenylium cation line flux, e.g.: increase by factor 100 the Fe concentration and add Fe^0 reactions; it became evident, that iron/metal concentrations do not influence the extreme difference.

Carbon in the midplane can appear either in the form of carbon monoxide or as methane. To verify this fact, the reference model was compared with the minimised models without and with condensates / ices. Thus CH_4 appeared in the reference model as the important carbon carrier in the gas-phase; CO_2# was the respective carbon medium in the ice phase. CO_2 in the gas-phase and CO_2# ice were the dominant C/O medium in the thesis models

Outlook:

Based on the successful Model C new studies can develop even more minimised models for the PPD design: firstly with 36+28 reactions commonly used in the thesis models, secondly with either 71 gas phase or 94 gas plus ices reactions. Further considerations will select the necessary reactions to calculate the conditions of the disc with ProDiMo code correctly; alternatively, a way to rearrange the ProDiMo code for appropriate calculations to an even further minimised model have to be found.
Moreover, the most promising model C could be developed further by adding those species, which appear in RTs but are not available in the UMIST data base. In order to include the species and their chemical reactions in the ProDiMo calculation code, it is necessary to perform a kinetic data survey.

All these test runs could be the starting point of new aims: to verify with a small number of selected reaction sequences the design of functional networks. Subsequent reactions could produce molecules which would function as building blocks for relevant organic substances like sugars, amino acids, nucleotides and the like, thus creating all the basic chemicals out of C, H, N, O, whose observation in reality has already started.

The phenomenon of the CO, CO_2 and HCN minimum concentration of the reference model in an area, where all the thesis models have a maximum concentration is one of the fundamental differences between the reference model and the thesis models. Perhaps it is the bigger and different element portfolio of the reference model, which causes the difference; not the number of reactions as such. This presumption could be followed up in further test models.

The resultant line fluxes of the species involved are an important outcome of the chemistry modelling around a star in the PPD. One thesis model with condensates/ices has 85% reactions in number (not identical ones) of the reference model and shows even higher line flux of the critical diazenylium cation. The supposed reason is the more structural selection of the thesis reactions compared to the reference model. This could also be studied in more effective test models.

K. Annexe

Annex B.0. Chemical reactions in space and their classification (Schlemmer 2015)

	Process	Type of reaction	Typical example	Remarks
Ionic interaction	Cationic	Cation–neutral reactions	$N^+ + H_2 \rightarrow NH^+ + H$	Rearrangement
		Radiative associations (ion)	$C^+ + H_2 \rightarrow CH_2^+ + h\nu$	Bond formation
	Mixed	Chemi-ionization	$O + CH \rightarrow HCO^+ + e$	Bond formation
		Direct cosmic ray processes	$H_2 + \gamma \rightarrow H_2^+ + e^-$	Ionization, Heating
		Radiative recombination	$H_2CO^+ + e^- \rightarrow H_2CO + h\nu$	Neutralization
		Anion–cation recombination	$HCO^+ + H^- \rightarrow H_2 + CO$	Neutralization
		Dissociative recombination	$H_3^+ + e^- \rightarrow H_2 + H, 3H$	Neutralization, Rearrangement
	Anionic	Anion–neutral reactions	$C^- + NO \rightarrow CN^- + O$	Rearrangement
		Associative detachment	$H^- + H \rightarrow H_2 + e^-$	Bond formation
		Electron attachment	$C_6H + e^- \rightarrow C_6H^- + h\nu$	Ionization
	Neutral	Neutral–neutral reactions	$C + C_2H_2 \rightarrow C_3H + H$	Rearrangement
		Photodissociation	$H_2 + h\nu \rightarrow 2H$	Bond dissociation
		External photoprocesses	$C_3N + h\nu \rightarrow C_2 + CN$	Rearrangement
		Internal photoprocesses	$CO + h\nu \rightarrow C + O$	Bond dissociation
		Radiative association (neutral)	$C + H_2 \rightarrow CH_2 + h\nu$	Bond formation
	Nonreactive	Inelastic processes	$C^+(^2P_{1/2}) + M \rightarrow C^+(^2P_{3/2}) \rightarrow C^+(^2P_{1/2}) + h\nu$	Cooling
		Gas–grain interactions	$H + H + \text{grain} \rightarrow H_2 + \text{grain}$	Bond formation

Annex B.1 Calculation methods for PPDs; a selection out of 46 models (Henning &Semenov 2013)

Year	Ref.	Structure	Viscosity	High-energy radiation			Gas thermal balance	Dust grain sizes	Reactions	Chemistry Time-dep.	Dynamics
				UV	X-rays	CRP					
1996	Aikawa et al.[2]	MMSN,[288] steady	passive	no	no	10^{-17} s^{-1}	no	0.1μm	gas-grain	yes	no
2004	Glassgold et al.[1]	1+1D,[92] steady	$\alpha = 0.01-2.0$,	no	1+1D[52]	no	yes	power law	gas-phase	yes	no
2004	Kamp & Dullemond[9]	1+1D,[298] steady	passive	1+1D	no	yes	yes	0.1μm	gas-phase	no	no
2007	Willacy & Woods[21]	1+1D,[306] steady	$\alpha = 0.01, 0.025$	2D[40]	1+1D[96]	1D	yes	power law	gas-grain, D	yes	rad. advection
2009	Woitke et al.[1]	1D,[313] steady	α	2D	2D	1D	yes	power law	gas-grain	no	no

Annex E Tab. E.1.3.**:** 81 Additional reactions to operate the ProDiMo calculation system with out condensates / ices. in reference model DM and thesis models.(the dimerisation of H on dust has a different number for DM as in the thesis models).

Reaction no.										
1	10247/10274	H	+	H	-->	dust	+	H2	+	dust
2	10266	H2	+	PHOTON	-->	H	+	H		
3	10500	H	+	XPHOT	-->	H+	+	e-		
4	10501	He	+	XPHOT	-->	He+	+	e-		
5	10502	C	+	XPHOT	-->	C++	+	2e-		
6	10503	C+	+	XPHOT	-->	C++	+	e-		
7	10504	N	+	XPHOT	-->	N++	+	2e-		
8	10505	N+	+	XPHOT	-->	N++	+	e-		
9	10506	O	+	XPHOT	-->	O++	+	2e-		
10	10507	O+	+	XPHOT	-->	O++	+	e-		
11	10520	Fe	+	XPHOT	-->	Fe++	+	2e-		
12	10521	Fe+	+	XPHOT	-->	Fe++	+	e-		
13	10522	H2	+	XPHOT	-->	H+	+	H+	+	2e-
14	10523	CH	+	XPHOT	-->	C++	+	H	+	2e-
15	10524	NH	+	XPHOT	-->	N++	+	H	+	2e-
16	10525	OH	+	XPHOT	-->	O++	+	H	+	2e-
17	10526	CN	+	XPHOT	-->	C++	+	N	+	2e-
18	10527	CN	+	XPHOT	-->	C+	+	N+	+	2e-
19	10528	CN	+	XPHOT	-->	C	+	N++	+	2e-
20	10529	CO	+	XPHOT	-->	C++	+	O	+	2e-
21	10530	CO	+	XPHOT	-->	C+	+	O+	+	2e-
22	10531	CO	+	XPHOT	-->	C	+	O++	+	2e-
23	10532	N2	+	XPHOT	-->	N++	+	N	+	2e-
24	10533	N2	+	XPHOT	-->	N+	+	N+	+	2e-
25	10535	NO	+	XPHOT	-->	N++	+	O	+	2e-
26	10536	NO	+	XPHOT	-->	N+	+	O+	+	2e-
27	10537	NO	+	XPHOT	-->	N	+	O++	+	2e-
28	10538	O2	+	XPHOT	-->	O	+	O++	+	2e-
29	10539	O2	+	XPHOT	-->	O+	+	O+	+	2e-
30	10542	CH2	+	XPHOT	-->	C++	+	H2	+	2e-
31	10543	NH2	+	XPHOT	-->	N++	+	H2	+	2e-
32	10544	H2O	+	XPHOT	-->	O++	+	H2	+	2e-
33	10545	HCN	+	XPHOT	-->	C++	+	NH	+	2e-
34	10546	HCN	+	XPHOT	-->	N++	+	CH	+	2e-
35	10547	CO2	+	XPHOT	-->	C++	+	O2	+	2e-
36	10548	CO2	+	XPHOT	-->	O++	+	CO	+	2e-
37	10549	H	+	e-	-->	2e-	+	H+		
38	10550	He	+	e-	-->	2e-	+	He+		
39	10551	H2	+	e-	-->	2e-	+	H2+		
40	10552	H2	+	e-	-->	2e-	+	H	+	H+
41	10553	C	+	e-	-->	2e-	+	C+		
42	10554	C+	+	e-	-->	2e-	+	C++		
43	10555	N	+	e-	-->	2e-	+	N+		
44	10556	N+	+	e-	-->	2e-	+	N++		
45	10557	O	+	e-	-->	2e-	+	O+		
46	10558	O+	+	e-	-->	2e-	+	O++		

47	10571	Fe	+	e-	-->	2e-	+	Fe+		
48	10572	Fe+	+	e-	-->	2e-	+	Fe++		
49	10573	C++	+	e-	-->	C+				
50	10574	N++	+	e-	-->	N+				
51	10575	O++	+	e-	-->	O+				
52	10582	Fe++	+	e-	-->	Fe+				
53	10593	C+	+	H	-->	C	+	H+		
54	10594	C++	+	H	-->	C+	+	H+		
55	10595	C	+	H+	-->	C+	+	H		
56	10596	C+	+	H+	-->	C++	+	H		
57	10597	C+	+	H2	-->	C	+	H2+		
58	10598	C++	+	H2	-->	C	+	2H+		
59	10599	N+	+	H	-->	N	+	H+		
60	10600	N++	+	H	-->	N+	+	H+		
61	10601	N	+	H+	-->	N+	+	H		
62	10602	N+	+	H+	-->	N++	+	H		
63	10603	N+	+	H2	-->	N	+	H2+		
64	10604	N++	+	H2	-->	N+	+	H2+		
65	10605	N++	+	H2	-->	N+	+	H	+	H+
66	10606	N++	+	H2	-->	N	+	2H+		
67	10607	N++	+	H2	-->	NH+	+	H+		
68	10609	O++	+	H	-->	O+	+	H+		
69	10611	O+	+	H+	-->	O++	+	H		
70	10612	O+	+	H2	-->	O	+	H2+		
71	10613	O++	+	H2	-->	O+	+	H2+		
72	10614	O++	+	H2	-->	O+	+	H	+	H+
73	10615	O++	+	H2	-->	O	+	2H+		
74	10616	O++	+	H2	-->	OH+	+	H+		
75	10702	Fe+	+	H	-->	Fe	+	H+		
76	10703	Fe++	+	H	-->	Fe+	+	H+		
77	10705	Fe+	+	H+	-->	Fe++	+	H		
78	10706	Fe+	+	H2	-->	Fe	+	H2+		
79	10707	Fe++	+	H2	-->	Fe+	+	H2+		
80	10773	N	+	XPHOT	-->	N+	+	e-		
81	10774	O	+	XPHOT	-->	O+	+	e-		

Tab. E.1.4. : Screening of reactions in a 40/40 grid and their influence on chemical network

Model	Removed reactions and results		U12	PDM		Reaction Enthalpy		Photo reactions		no cross
	Number	Reaction	reactions	reactions	mult. T-fit	exotherm	endotherm	Diss.	Ioniz.	section
							//>10 eV			
Ch.40	nil	no 'white spots'	235	93	61	197	32//5	13	5	3
		= no irregularities on diagrams								
Ch.41	1258	H2CO+ + e- ---> CO + 2H	225	93	61	187	32//4	13	5	3
	1357	HCO+ + e- ---> CO + H								
	1358	HCO2+ + e- ---> CO2 + H								
	1359	HCO2+ + e- ---> CO + O + H								
	1360	HCO2+ + e- ---> CO + OH								
	5617	O + CN ---> CO + N								
	5235	CH2 + NO ---> HCN + OH								
	5327	CH + O ---> CO + H								
	488	H + CN+ ---> CN + H+								
	491	H + HCN+ ---> HCN + H+								
		rather many white spots								
	Added reactions to 41									
Ch.42	1357	HCO+ + e- ---> CO + H	226	93	61	188	32//3	13	5	3
		only one white spot								
Ch.43	491	H + HCN+ ---> HCN + H+	227	93	61	189?	32//5	13	5	3
		white spot disappeared								
Ch.43New		like Chemie 43 but reactions	239	81	61	187?	32//5	13	5	3
		shifted from PDM to U12								
Ch.43All		taking all U12 reactions for	986	81	11	809	85//8	34	9	12
		the selected species								
Ch.44	Added to 43new		242	81	3	190	32//5	13	5	3
	added because of double temperature reaction									
	1412	HN2+ + e- ---> N2 + H								
	5318	CH + O2 ---> CO2 + H								
	76	H- + H ---> H2 + e-								
	added because of more e- consumption									
	1286	H3+ + e- ---> 3 H								
	1247	H2+ + e- ---> 2 H								
	490	H + H2+ ---> H2 + H+								
		removed								
	5617	O + CN ---> CO + N								
Ch.45	Added to 44		242	81	3	190	32//5	13	5	3
	1428	NO+ + e- ---> O + N								
		removed								
	490	H + H2+ ---> H2 + H+								
		white spots increased								
Ch.46	Added to 45		242	81	3	190	32//5	13	5	3
	4948	H- + NO+ ---> H + NO								
	1247	H2+ + e- ---> 2 H								
	1286	H3+ + e- ---> 3 H								
		removed								
	5053	OH- + NO+ ---> OH + NO								
	Species H- and OH- removed		230	81	3	181	32//5	13	4	3
	Species OH- and reaction 5053 added									
	5053	OH- + NO+ ---> OH + NO								
	Reactions removed									
	5354	CN + O2 ---> NO + CO								
	2454	CH5+ + CO ---> HCO+ + CH4								
		many white spots								
	Reactions added back		233	81	3	184	32//5	13	4	3
	5354	CN + O2 ---> NO + CO								
		less white spots								
Ch.47		like Chemie 46	240	81	2	191	32//5	13	4	3
		whitout Species H-, OH-, O-								
		but added reactions to copy 40								
	1258	H2CO+ + e- ---> CO + 2H								
	1357	HCO+ + e- ---> CO + H								
	1358	HCO2+ + e- ---> CO2 + H								
	1359	HCO2+ + e- ---> CO + O + H								
	1360	HCO2+ + e- ---> CO + OH								
	5617	O + CN ---> CO + N								
	5235	CH2 + NO ---> HCN + OH								
	5327	CH + O ---> CO + H								
	488	H + CN+ ---> CN + H+								
	491	H + HCN+ ---> HCN + H+								
		no white spots								
Ch.48		like Chemie 47	236	81						
		removed								
	1357	HCO+ + e- ---> CO + H								
	1358	HCO2+ + e- ---> CO2 + H								
	1359	HCO2+ + e- ---> CO + O + H								
	1360	HCO2+ + e- ---> CO + OH								
		many white spots								
		*) irregularities on diagrams								

Annex F Tab.F.4.: Additional 94 reactions concerning condensates/ices.

11292 IC: CO + dust --> CO# + dust
11293 DT: CO# + dust --> CO + dust
11294 DC: CO# + CRP --> CO
11295 DP: CO# + PHOTON --> CO
11296 IC: H2O + dust --> H2O# + dust
11297 DT: H2O# + dust --> H2O + dust
11298 DC: H2O# + CRP --> H2O
11299 DP: H2O# + PHOTON --> H2O
11300 IC: CO2 + dust --> CO2# + dust
11301 DT: CO2# + dust --> CO2 + dust
11302 DC: CO2# + CRP --> CO2
11303 DP: CO2# + PHOTON --> CO2
11304 IC: CH4 + dust --> CH4# + dust
11305 DT: CH4# + dust --> CH4 + dust
11306 DC: CH4# + CRP --> CH4
11307 DP: CH4# + PHOTON --> CH4
11308 IC: NH3 + dust --> NH3# + dust
11309 DT: NH3# + dust --> NH3 + dust
11310 DC: NH3# + CRP --> NH3
11311 DP: NH3# + PHOTON --> NH3
11312 IC: HCN + dust --> HCN# + dust
11313 DT: HCN# + dust --> HCN + dust
11314 DC: HCN# + CRP --> HCN
11315 DP: HCN# + PHOTON --> HCN
11324 IC: H2CO + dust --> H2CO# + dust
11325 DT: H2CO# + dust -> H2CO + dust
11326 DC: H2CO# + CRP --> H2CO
11327 DP: H2CO# + PHOTON --> H2CO
11328 IC: HCO + dust --> HCO# + dust
11329 DT: HCO# + dust --> HCO + dust
11330 DC: HCO# + CRP --> HCO
11331 DP: HCO# + PHOTON --> HCO
11332 IC: CN + dust --> CN# + dust
11333 DT: CN# + dust --> CN + dust
11334 DC: CN# + CRP --> CN
11335 DP: CN# + PHOTON --> CN
11336 IC: N2 + dust --> N2# + dust
11337 DT: N2# + dust --> N2 + dust
11338 DC: N2# + CRP --> N2
11339 DP: N2# + PHOTON --> N2
11340 IC: CH + dust --> CH# + dust
11341 DT: CH# + dust --> CH + dust
11342 DC: CH# + CRP --> CH
11343 DP: CH# + PHOTON --> CH
11344 IC: OH + dust --> OH# + dust
11345 DT: OH# + dust --> OH + dust
11346 DC: OH# + CRP --> OH
11347 DP: OH# + PHOTON --> OH
11360 IC: NH + dust --> NH# + dust
11361 DT: NH# + dust --> NH + dust
11362 DC: NH# + CRP --> NH
11363 DP: NH# + PHOTON --> NH
11372 IC: C + dust --> C# + dust
11373 DT: C# + dust --> C + dust
11374 DC: C# + CRP --> C
11375 DP: C# + PHOTON --> C
11376 IC: N + dust --> N# + dust
11377 DT: N# + dust --> N + dust
11378 DC: N# + CRP --> N
11379 DP: N# + PHOTON --> N
11380 IC: O + dust --> O# + dust
11381 DT: O# + dust --> O + dust
11382 DC: O# + CRP --> O
11383 DP: O# + PHOTON --> O
11400 IC: Fe + dust --> Fe# + dust
11401 DT: Fe# + dust --> Fe + dust
11402 DC: Fe# + CRP --> Fe
11403 DP: Fe# + PHOTON --> Fe
11420 IC: NH2 + dust --> NH2# + dust
11421 DT: NH2# + dust --> NH2 + dust
11422 DC: NH2# + CRP --> NH2
11423 DP: NH2# + PHOTON --> NH2
11440 IC: CH2 + dust --> CH2# + dust
11441 DT: CH2# + dust --> CH2 + dust
11442 DC: CH2# + CRP --> CH2
11443 DP: CH2# + PHOTON --> CH2
11480 IC: HNC + dust --> HNC# + dust
11481 DT: HNC# + dust --> HNC + dust
11482 DC: HNC# + CRP --> HNC
11483 DP: HNC# + PHOTON --> HNC
11516 IC: NO + dust --> NO# + dust
11517 DT: NO# + dust --> NO + dust
11518 DC: NO# + CRP --> NO
11519 DP: NO# + PHOTON --> NO
11520 IC: NO2 + dust --> NO2# + dust
11521 DT: NO2# + dust --> NO2 + dust
11522 DC: NO2# + CRP --> NO2
11523 DP: NO2# + PHOTON --> NO2
11532 IC: O2 + dust --> O2# + dust
11533 DT: O2# + dust --> O2 + dust
11534 DC: O2# + CRP --> O2
11535 DP: O2# + PHOTON --> O2
11556 GG: O# + H --> OH#
11557 GG: OH# + H --> H2O#

Annex G **Tab.G.2.4.**

Model DM

1st main formation reactions				2nd main formation reactions			
	area	grid no.	reaction no. and type in DM	area	grid no.	reaction no. and type in DM	
CO	I	19	11293 DT: CO# + dust --> CO + dust				
	I	20	11295 DP: CO# + PHOTON --> CO		4	1357 DR: HCO+ + e- --> CO + H	
	II	1	489 CE: H + CO+ --> CO + H+				
HCN	I	16	11313 DT: HCN# + dust --> HCN + dust		4	3812 IN: NH3 + HCNH+ --> HCN + NH4+	
	I	10	5489 NN: N + CH3 --> HCN + H2				
	II	15	10299 NN: H2exc + CN --> HCN + H		8	5369 NN: H2 + CN --> HCN + H	
HCO+	I	15	2905 IN: H3+ + CO --> HCO+ + H2				
	I	5	2183 IN: CH+ + H2O --> HCO+ + H2		12	2613 IN: H2+ + CO --> HCO+ + H	
	II	3	1623 IN: C+ + H2O --> HCO+ + H				
CN	I	2	906 CR: HCN + CRPHOT --> CN + H		5	2776 IN: H2O + HCN+ --> CN + H3O+	
	I	4	1349 DR: HCNH+ + e- --> CN + H				
	II	1	488 CE: H + CN+ --> CN + H+		6	5202 NN: C + NH --> CN + H	
CO2	I	14	11301 DT: CO2# + dust --> CO2 + dust				
	I	15	11303 DP: CO2# + PHOTON --> CO2	II	10	5317 NN: CH + O2 --> CO2 + H	
	II	13	5692 NN: OH + CO --> CO2 + H		12	5636 NN: O + HCO --> CO2 + H	
CN+	I	7	3475 IN: He+ + HCN --> CN+ + He				
	II	3	1650 IN: C+ + NH --> CN+ + H		4	2191 IN: CH+ + N --> CN+ + H	
	II	8	6071 RA: C+ + N --> CN+ + PHOTON				
HCN+	I	6	2663 IN: H2 + CN+ --> HCN+ + H				
	II	3	1647 IN: C+ + NH2 --> HCN+ + H				
	II	8	3682 IN: N + CH2+ --> HCN+ + H				
H2O	I	16	11297 DT: H2O# + dust --> H2O + dust		6	3808 IN: NH3 + H3O+ --> NH4+ + H2O	
	I	17	11299 DP: H2O# + PHOTON --> H2O				
	II	15	10282 NN: H2exc + OH --> H2O + H		13	6141 RA: H + OH --> H2O + PHOTON	
H3O+	I	7	2914 IN: H3+ + H2O --> H3O+ + H2		2	2456 IN: CH5+ + H2O --> H3O+ + CH4	
	I	4	2672 IN: H2 + H2O+ --> H3O+ + H		6	2777 IN: H2O + HCO+ --> CO + H3O+	
	II	3	2616 IN: H2+ + H2O --> H3O+ + H				
C2H2+		not included					
NO	I	10	5549 NN: NH + O --> NO + H				
	I	8	5522 NN: N + SO --> S + NO				
	II	7	5514 NN: N + OH --> NO + H				
NO+	I	8	3574 IN: N+ + CO --> NO+ + C		5	629 CE: NO + O2+ --> O2 + NO+	
	I	13	3875 IN: O+ + HCN --> NO+ + CH				
	II	10	3697 IN: N + OH+ --> NO+ + H		3	404 CE: H+ + NO --> NO+ + H	
HN2+	I	3	2948 IN: H3+ + N2 --> HN2+ + H2		1	2621 IN: H2+ + N2 --> HN2+ + H	
	II	2	2690 IN: H2 + N2+ -> HN2+ + H		5	3694 IN: N + NH2+ --> HN2+ + H	
H3+	I/II	1	2614 IN: H2+ + H2 --> H3+ + H		3	2691 IN: H2 + NH+ --> N + H3+	
H	I	17	5367 NN: H2 + CH3 --> CH4 + H		20	5373 NN: H2 + NH2 --> NH3 + H	
	I	8	1427 DR: NH4+ + e- --> NH3 + H				
	II	2	407 CE: H+ + O -> O+ + H		33	6182 RR: H+ + e- --> H + PHOTON	

	1st main destruction reactions			2nd main destruction reactions		
	area	grid no.	reaction no. and type in DM	area	grid no.	reaction no. and type in DM
CO	I	17	11292 IC: CO + dust --> CO# + dust		8	2905 IN: H3+ + CO --> HCO+ + H2
	II	12	5914 PH: CO + PHOTON --> O + C		16	11169 XP: CO + XPHOT --> C + O++ +e-
	II	15	11167 XP: CO + XPHOT --> C++ + O + e-			
HCN	I	13	11312 IC: HCN + dust --> HCN# + dust		6	3036 IN: H3O+ + HCN --> HCNH+ + H2O
	I	12	5955 PH: HCN + PHOTON --> CN + H		10	5401 NN: H + HCN --> CN + H2
	II	1	389 CE: H+ + HCN --> HCN+ + H			
HCO+	I	5	2777 IN: H2O + HCO+ --> CO + H3O+		9	3814 IN: NH3 + HCO+ --> CO + NH4+
	I	3	1357 DR: HCO+ + e- --> CO + H			
	II	13	4941 MN: H- + HCO+ --> H + HCO		11	4032 IN: OH + HCO+ --> HCO2+ + H
CN	I	10	5369 NN: H2 + CN --> HCN + H		12	5533 NN: NH3 + CN --> HCN + NH2
	II	17	11164 XP: CN + XPHOT --> C++ + N			
	II	16	5910 PH: CN + PHOTON --> N + C			
CO2	I	27	11300 IC: CO2 + dust --> CO2# + dust		6	877 CR: CO2 + CRPHOT --> CO + O
	II	3	517 CE: He+ + CO2 --> CO2+ + He			
	II	23	5913 PH: CO2 + PHOTON --> CO + O		4	549 CE: N+ + CO2 --> CO2+ + N
CN+	I	5	2663 IN: H2 + CN+ --> HCN+ + H		6	2766 IN: H2O + CN+ --> HCN+ + OH
	II	2	488 CE: H + CN+ --> CN + H+		7	3686 IN: N + CN+ --> N2+ + C
HCN+	I	4	2680 IN: H2 + HCN+ --> HCNH+ + H		5	2776 IN: H2O + HCN+ --> CN + H3O+
	II	2	1348 DR: HCN+ + e- --> CN + H			
	II	1	491 CE: H + HCN+ --> HCN + H+			
H2O	I	16	11296 IC: H2O + dust --> H2O# + dust		2	891 CR: H2O + CRPHOT --> OH + H
	II	13	5934 PH: H2O + PHOTON --> H2O+ + e-	I	9	2914 IN: H3+ + H2O --> H3O+ + H2
	II	1	379 CE: H+ + H2O --> H2O+ + H			
H3O+	I	10	3808 IN: NH3 + H3O+ --> NH4+ + H2O			
	I	3	1304 DR: H3O+ + e- --> OH + H			
	II	7	3054 IN: H3O+ + SiH --> SiH2+ + H2O		1	1301 DR: H3O+ + e- --> H2O + H
C2H2+	not included					
NO	I	20	5724 NN: Si + NO --> SiO + N		12	5235 NN: CH2 + NO --> HCN + OH
	I	16	5510 NN: N + NO --> N2 + O		22	6002 PH: NO + PHOTON --> O + N
	II	3	404 CE: H+ + NO --> NO+ + H			
NO+	I	1	537 CE: Mg + NO+ --> NO + Mg+		2	621 CE: NO+ + Fe --> Fe+ + NO
	I	4	1428 DR: NO+ + e- --> O + N			
HN2+	I	6	2788 IN: H2O + HN2+ --> N2 + H3O+		5	2518 IN: CO + HN2+ --> HCO+ + N2
	I	1	1411 DR: HN2+ + e- --> N2 + H		9	3822 IN: NH3 + HN2+ --> N2 + NH4+
	II	4	2436 IN: CH4 + HN2+ --> N2 + CH5+			
H3+	I	8	2914 IN: H3+ + H2O --> H3O+ + H2			
	I	7	2905 IN: H3+ + CO --> HCO+ + H2			
	II	11	2960 IN: H3+ + O --> H2O+ + H			
H	I	6	5390 NN: H + CH4 --> CH3 + H2		5	5387 NN: H + CH2 --> CH + H2
	I	18	10274 HG: H + H + dust -> H2 + dust			
	II	2	493 CE: H + O+ --> O + H+		10	5413 NN: H + NH2 --> NH + H2

Model A

	1st main formation reactions			2nd main formation reactions		
	area	grid no.	reaction no. and type in DM	area	grid no.	reaction no. and type in DM
CO	I	8	2777 IN: H2O + HCO+ --> CO + H3O+		8	2777 IN: H2O + HCO+ --> CO + H3O+
	I	3	1357 DR: HCO+ + e- --> CO + H		12	5617 NN: O + CN --> CO + N
	II	13	6093 RA: C + O --> CO + PHOTON		6	1653 IN: C+ + O2 --> CO + O+
HCN	I	8	5405 NN: H + HNC --> HCN + H		5	3812 IN: NH3 + HCNH+ --> HCN + NH4+
	I	10	5497 NN: N + HCO --> HCN + O		9	5484 NN: N + CH2 --> HCN + H
	II	7	5369 NN: H2 + CN --> HCN + H			
HCO+	I	7	2905 IN: H3+ + CO --> HCO+ + H2		3	2321 IN: CH3+ + O --> HCO+ + H2
	II	6	2664 IN: H2 + CO+ --> HCO+ + H	I	2	1623 IN: C+ + H2O --> HCO+ + H
	II	1	64 AD: CH + O --> HCO+ + e-			
CN	I	4	5311 NN: CH + N --> CN + H		2	1230 DR: CH4N+ + e- --> CN + H2 +H2
	I	6	5955 PH: HCN + PHOTON --> CN + H		7	5971 PH: HNC + PHOTON --> CN + H
	II	1	488 CE: H + CN+ --> CN + H+			
CO2	I/II	5	5636 NN: O + HCO --> CO2 + H	I	2	2515 IN: CO + HCO2+ --> CO2 + HCO+
	I/II	6	5692 NN: OH + CO --> CO2 + H	I	4	5317 NN: CH + O2 -> CO2 + H
CN+	I	3	3475 IN: He+ + HCN --> CN+ + He			
	II	1	1650 IN: C+ + NH --> CN+ + H		4	6071 RA: C+ + N --> CN+ + PHOTON
	II	2	2191 IN: CH+ + N --> CN+ + H			
HCN+	I/II	3	2663 IN: H2 + CN+ --> HCN+ + H			
	I/II	1	389 CE: H+ + HCN -> HCN+ + H			
	I	4	3682 IN: N + CH2+ -> HCN+ + H			
H2O	I	3	3036 IN: H3O+ + HCN --> HCNH+ + H2O		6	5379 NN: H2 + OH -> H2O + H
	I	1	1301 DR: H3O+ + e- -> H2O + H		2	3029 IN: H3O+ + H2CO --> H3CO+ + H2O
	II	7	6141 RA: H + OH --> H2O + PHOTON			
H3O+	I	5	2914 IN: H3+ + H2O --> H3O+ + H2			
	I	4	2777 IN: H2O + HCO+ --> CO + H3O+			
	II	2	2672 IN: H2 + H2O+ --> H3O+ + H			
C2H2+	I/II	1	1613 IN: C+ + CH4 --> C2H2+ + H2			
	I/II	2	2473 IN: CH + CH3+ --> C2H2+ + H2			
NO	I/II	1	621 CE: NO+ + Fe --> Fe+ + NO	I	2	2499 IN: CN+ + CO2 --> C2O+ + NO
	I/II	4	5514 NN: N + OH --> NO + H	I	3	5354 NN: CN + O2 --> NO + CO
NO+	I	4	3574 IN: N+ + CO -> NO+ + C		6	3875 IN: O+ + HCN --> NO+ + CH
	I	7	6001 PH: NO + PHOTON --> NO+ + e-			
	II	5	3695 IN: N + O2+ -> NO+ + O		2	404 CE: H+ + NO --> NO+ + H
HN2+	I/II	2	2948 IN: H3+ + N2 --> HN2+ + H2		1	2621 IN: H2+ + N2 -> HN2+ + H
	I/II	3	3694 IN: N + NH2+ --> HN2+ + H			
H3+	I/II	1	2614 IN: H2+ + H2 --> H3+ + H		2	2698 IN: H2 + O2H+ --> O2 + H3+
H	I	17	5379 NN: H2 + OH --> H2O + H		16	5378 NN: H2 + O -> OH + H
	I	9	2614 IN: H2+ + H2 --> H3+ + H			
	II	1	407 CE: H+ + O --> O+ + H		23	6182 RR: H+ + e- --> H + PHOTON

	1st main destruction reactions			2nd main destruction reactions		
	area	grid no.	reaction no. and type in DM	area	grid no.	reaction no. and type in DM
CO	I	4	2905 IN: H3+ + CO --> HCO+ + H2			
	I	6	5692 NN: OH + CO -> CO2 + H			
	II	7	5914 PH: CO + PHOTON --> O + C	II	8	10529 XP: CO + XPHOT --> C++ + O + e-
HCN	I	3	3036 IN: H3O+ + HCN --> HCNH+ + H2O	I	3	3036 IN: H3O+ + HCN --> HCNH+ + H2O
	I	7	5955 PH: HCN + PHOTON --> CN + H			
	II	6	5401 NN: H + HCN -> CN + H2	II	1	389 CE: H+ + HCN --> HCN+ + H
HCO+	I/II	1	1357 DR: HCO+ + e- -> CO + H			
	I/II	3	2777 IN: H2O + HCO+ --> CO + H3O+			
	I/II	2	2134 IN: C + HCO+ --> CO + CH+			
CN	I	3	5369 NN: H2 + CN -> HCN + H	I	2	5354 NN: CN + O2 --> NO + CO
	I	4	5617 NN: O + CN -> CO + N	I	1	2305 IN: CH3+ + CN --> CH2CN+ + H
	II	5	5910 PH: CN + PHOTON --> N + C			
CO2	I	1	877 CR: CO2 + CRPHOT --> CO + O	I	5	2904 IN: H3+ + CO2 --> HCO2+ + H2
	I	2	1617 IN: C+ + CO2 --> CO+ + CO			
	II	9	5393 NN: H + CO2 -> CO + OH	II	8	3440 IN: He+ + CO2 --> O2 + C+ + He
CN+	I	4	2663 IN: H2 + CN+ -> HCN+ + H	I	2	2499 IN: CN+ + CO2 --> C2O+ + NO
	II	1	488 CE: H + CN+ -> CN + H+			
HCN+	I	2	2680 IN: H2 + HCN+ --> HCNH+ + H			
	II	1	491 CE: H + HCN+ -> HCN + H+			
H2O	I	9	3682 IN: N + CH2+ -> HCN+ + H	II	1	379 CE: H+ + H2O --> H2O+ + H
	I	8	2777 IN: H2O + HCO+ --> CO + H3O+			
	II	11	5935 PH: H2O + PHOTON --> OH + H	II	10	5399 NN: H + H2O --> OH + H2
H3O+	I/II	4	3036 IN: H3O+ + HCN --> HCNH+ + H2O	II	1	1301 DR: H3O+ + e- --> H2O + H
	I/II	2	1304 DR: H3O+ + e- -> OH + H			
C2H2+	I	1	1005 DR: C2H2+ + e- --> CH + CH	I	3	3837 IN: NH + C2H2+ --> CH2CN+ + H
	I	4	3919 IN: O + C2H2+ --> HCO+ + CH			
	II	2	3619 IN: N + C2H2+ --> HCN + CH+			
NO	I	4	5235 NN: CH2 + NO --> HCN + OH			
	I	5	5708 NN: OH + NO --> NO2 + H			
	II	7	6002 PH: NO + PHOTON --> O + N	II	6	6001 PH: NO + PHOTON --> NO+ + e-
NO+	I/II	1	621 CE: NO+ + Fe -> Fe+ + NO			
	I/II	2	1428 DR: NO+ + e- -> O + N			
HN2+	I	3	2518 IN: CO + HN2+ --> HCO+ + N2	I	2	2436 IN: CH4 + HN2+ --> N2 + CH5+
	II	1	1411 DR: HN2+ + e- -> N2 + H			
H3+	I	5	2914 IN: H3+ + H2O --> H3O+ + H2			
	I	4	2905 IN: H3+ + CO --> HCO+ + H2			
	II	1	1285 DR: H3+ + e- --> H2 + H	II	8	2961 IN: H3+ + O --> OH+ + H2
H	I	5	5399 NN: H + H2O --> OH + H2	I	6	5405 NN: H + HNC --> HCN + H
	I	11	10247 HG: H + H + dust --> H2 + dust	I	9	5429 NN: H + OH --> O + H2
	II	1	493 CE: H + O+ --> O + H+			

Model B

	1st main formation reactions			2nd main formation reactions		
	area	grid no.	reaction no. and type in DM	area	grid no.	reaction no. and type in DM
CO	I	6	2777 IN: H2O + HCO+ -> CO + H3O+		12	5244 NN: CH2 + O --> CO + H
	I	3	1357 DR: HCO+ + e- -> CO + H			
	II	1	489 CE: H + CO+ -> CO + H+		19	6093 RA: C + O --> CO + PHOTON
HCN	I	7	3812 IN: NH3 + HCNH+ -> HCN + NH4+		15	5533 NN: NH3 + CN --> HCN + NH2
	I	5	1350 DR: HCNH+ + e- -> HCN + H		12	5405 NN: H + HNC --> HCN + H
	II	11	5369 NN: H2 + CN -> HCN + H		2	491 CE: H + HCN+ --> HCN + H+
HCO+	I	12	2905 IN: H3+ + CO -> HCO+ + H2		8	2518 IN: CO + HN2+ --> HCO+ + N2
	I	2	1623 IN: C+ + H2O -> HCO+ + H	II	1	64 AD: CH + O -> HCO+ + e-
	II	4	2221 IN: CH2+ + O -> HCO+ + H		9	2613 IN: H2+ + CO --> HCO+ + H
CN	I	3	906 CR: HCN + CRPHOT -> CN + H		5	1230 DR: CH4N+ + e- --> CN + H2 +H2
	I	9	5204 NN: C + NO -> CN + O		13	5955 PH: HCN + PHOTON --> CN + H
	II	1	488 CE: H + CN+ -> CN + H+		15	6091 RA: C + N --> CN + PHOTON
CO2	I/II	7	5317 NN: CH + O2 -> CO2 + H		4	2778 IN: H2O + HCO2+ --> CO2 + H3O+
	I/II	10	5636 NN: O + HCO -> CO2 + H		3	2515 IN: CO + HCO2+ --> CO2 + HCO+
	I/II	11	5692 NN: OH + CO -> CO2 + H			
CN+	I	4	3475 IN: He+ + HCN -> CN+ + He		5	3491 IN: He+ + HNC -> CN+ + He
	I	1	1650 IN: C+ + NH -> CN+ + H			
	II	6	6071 RA: C+ + N -> CN+ + PHOTON		2	2191 IN: CH+ + N -> CN+ + H
HCN+	I	5	2663 IN: H2 + CN+ -> HCN+ + H		3	1649 IN: C+ + NH3 -> HCN+ + H2
	I	2	1647 IN: C+ + NH2 -> HCN+ + H		7	3571 IN: N+ + CH4 -> HCN+ + H2
	II	8	3682 IN: N + CH2+ -> HCN+ + H			
H2O	I	4	5379 NN: H2 + OH -> H2O + H		2	H3O+ + HCN --> HCNH+ + H2O
	I	3	3808 IN: NH3 + H3O+ -> NH4+ + H2O		7?	5707 NN: OH + NH3 --> H2O + NH2
	II	9	6141 RA: H + OH -> H2O + PHOTON			
H3O+	I/II	8	2914 IN: H3+ + H2O -> H3O+ + H2		6	2777 IN: H2O + HCO+ --> CO + H3O+
	I/II	4	2672 IN: H2 + H2O+ -> H3O+ + H		5	2739 IN: H2O+ + H2O --> H3O+ + OH
					3	2616 IN: H2+ + H2O -> H3O+ + H
C2H2+	I	1	1613 IN: C+ + CH4 -> C2H2+ + H2		2	2170 IN: CH+ + CH4 --> C2H2+ + H2
	II	3	2473 IN: CH + CH3+ -> C2H2+ + H2			
NO	I	1	621 CE: NO+ + Fe -> Fe+ + NO		2	2499 IN: CN+ + CO2 --> C2O+ + NO
	I	9	5549 NN: NH + O -> NO + H			
	II	7	5514 NN: N + OH -> NO + H			
NO+	I	6	3574 IN: N+ + CO -> NO+ + C		10	3714 IN: NH+ + CO2 --> NO+ + HCO
	I	4	629 CE: NO + O2+ -> O2 + NO+			
	II	9	3697 IN: N + OH+ -> NO+ + H		2	404 CE: H+ + NO -> NO+ + H
HN2+	I	2	2948 IN: H3+ + N2 -> HN2+ + H2		1	2621 IN: H2+ + N2 -> HN2+ + H
	II	4	3694 IN: N + NH2+ -> HN2+ + H		3	3583 IN: N+ + NH3 -> HN2+ + H2
					5	3726 IN: NH+ + N2 -> HN2+ + N
H3+	I/II	1	2614 IN: H2+ + H2 -> H3+ + H		3	2691 IN: H2 + NH+ -> N + H3+
					4	2698 IN: H2 + O2H+ -> O2 + H3+
H	I	8	2614 IN: H2+ + H2 -> H3+ + H		7	1427 DR: NH4+ + e- -> NH3 + H
	I	13	5368 NN: H2 + CH -> CH2 + H		15	5373 NN: H2 + NH2 -> NH3 + H
	II	2	407 CE: H+ + O -> O+ + H		25	6182 RR: H+ + e- --> H + PHOTON

	1st main destruction reactions			2nd main destruction reactions	
	area	grid no.	reaction no. and type in DM	grid no.	reaction no. and type in DM
CO	I	6	2905 IN: H3+ + CO -> HCO+ + H2	11	5692 NN: OH + CO -> CO2 + H
	I	12	5914 PH: CO + PHOTON -> O + C		
	II	14	10529 XP: CO + XPHOT --> C++ + O	15	10531 XP: CO + XPHOT --> C + O++ +e-
HCN	I	11	5401 NN: H + HCN -> CN + H2		
	I	7	3036 IN: H3O+ + HCN --> HCNH+ + H2O		
	I/II	12	5955 PH: HCN + PHOTON --> CN + H	10	4011 IN: OH+ + HCN --> HCNH+ + O
HCO+	I	4	2777 IN: H2O + HCO+ --> CO + H3O+		
	I	2	1357 DR: HCO+ + e- -> CO + H	8	5957 PH: HCO+ + PHOTON --> CO+ + H
	II	7	4032 IN: OH + HCO+ --> HCO2+ + H		
CN	I	6	5369 NN: H2 + CN -> HCN + H	8	5533 NN: NH3 + CN --> HCN + NH2
	I	5	5354 NN: CN + O2 -> NO + CO	7	5491 NN: N + CN -> N2 + C
	II	13	10526 XP: CN + XPHOT --> C++ + N	14	10528 XP: CN + XPHOT --> C + N++ +e-
CO2	I	1	877 CR: CO2 + CRPHOT -> CO + O	9	2904 IN: H3+ + CO2 --> HCO2+ + H2
	I	19	5913 PH: CO2 + PHOTON --> CO + O		
	II	8	2612 IN: H2+ + CO2 --> HCO2+ + H	16	4006 IN: OH+ + CO2 --> HCO2+ + O
CN+	I	8	2663 IN: H2 + CN+ -> HCN+ + H	9	2766 IN: H2O + CN+ --> HCN+ + OH
	II	1	488 CE: H + CN+ -> CN + H+	7	2506 IN: CN+ + O2 -> OCN+ + O
				2	682 CE: O + CN+ -> CN + O+
HCN+	I	4	2680 IN: H2 + HCN+ --> HCNH+ + H	1	481 CE: H2O + HCN+ --> HCN + H2O+
	II	3	1348 DR: HCN+ + e- -> CN + H	5	2776 IN: H2O + HCN+ --> CN + H3O+
H2O	I	7	2914 IN: H3+ + H2O -> H3O+ + H2	11	5399 NN: H + H2O -> OH + H2
	I	13	5935 PH: H2O + PHOTON --> OH + H		
	II	1	379 CE: H+ + H2O -> H2O+ + H	12	5934 PH: H2O + PHOTON --> H2O+ + e-
H3O+	I	7	3808 IN: NH3 + H3O+ --> NH4+ + H2O	5	3036 IN: H3O+ + HCN --> HCNH+ + H2O
	I	3	1304 DR: H3O+ + e- -> OH + H		
	II	1	1301 DR: H3O+ + e- -> H2O + H		
C2H2+	I	1	1005 DR: C2H2+ + e- -> CH + CH		
	I	4	3919 IN: O + C2H2+ --> HCO+ + CH		
	II	3	3837 IN: NH + C2H2+ --> CH2CN+ + H		
NO	I	5	943 CR: NO + CRPHOT --> NO+ + e-	19	6002 PH: NO + PHOTON --> O + N
	I	17	5708 NN: OH + NO -> NO2 + H		
	II	18	6001 PH: NO + PHOTON --> NO+ + e-	2	404 CE: H+ + NO -> NO+ + H
NO+	I/II	1	621 CE: NO+ + Fe -> Fe+ + NO		
	I/II	2	1428 DR: NO+ + e- -> O + N		
HN2+	I	6	2788 IN: H2O + HN2+ --> N2 + H3O+	7	3111 IN: HCN + HN2+ --> HCNH+ + N2
	I	5	2518 IN: CO + HN2+ --> HCO+ + N2		
	II	1	1411 DR: HN2+ + e- -> N2 + H	4	2436 IN: CH4 + HN2+ --> N2 + CH5+
H3+	I	8	2914 IN: H3+ + H2O -> H3O+ + H2		
	I	6	2905 IN: H3+ + CO -> HCO+ + H2	10	2948 IN: H3+ + N2 -> HN2+ + H2
	II	1	1285 DR: H3+ + e- -> H2 + H	12	2959 IN: H3+ + O2 -> O2H+ + H2
H	I	5	5387 NN: H + CH2 -> CH + H2	9	5413 NN: H + NH2 -> NH + H2
	I	19	10247 HG: H + H + dust -> H2 + dust		
	II	2	493 CE: H + O+ -> O + H+	15	6140 RA: H + O --> OH + PHOTON

Model C

	1st main formation reactions			2nd main formation reactions		
	area	grid no.	reaction no. and type in DM	area	grid no.	reaction no. and type in DM
CO	I	15	11293 DT: CO# + dust --> CO + dust	8		2777 IN: H2O + HCO+ --> CO + H3O+
	I	3	1357 DR: HCO+ + e- --> CO + H	11		5393 NN: H + CO2 --> CO + OH
	II	13	6093 RA: C + O --> CO + PHOTON	6		1653 IN: C+ + O2 --> CO + O+
HCN	I	9	11313 DT: HCN# + dust --> HCN + dust	6		5405 NN: H + HNC --> HCN + H
	I	7	5484 NN: N + CH2 --> HCN + H			
	II	1	491 CE: H + HCN+ --> HCN + H+	5		5369 NN: H2 + CN --> HCN + H
HCO+	I	7	2905 IN: H3+ + CO --> HCO+ + H2	3		2321 IN: CH3+ + O --> HCO+ + H2
	II	6	2664 IN: H2 + CO+ --> HCO+ + H			
	II	2	1623 IN: C+ + H2O --> HCO+ + H			
CN	I	4	5311 NN: CH + N --> CN + H	2		1230 DR: CH4N+ + e- --> CN + H2 + H2
	I	6	5955 PH: HCN + PHOTON --> CN + H	6		5955 PH: HCN + PHOTON --> CN + H
	II	1	488 CE: H + CN+ --> CN + H+			
CO2	I	7	11301 DT: CO2# + dust --> CO2 + dust			
	I	5	5636 NN: O + HCO --> CO2 + H			
	II	6	5692 NN: OH + CO --> CO2 + H	4		5317 NN: CH + O2 --> CO2 + H
CN+	I	3	3475 IN: He+ + HCN --> CN+ + He			
	II	1	1650 IN: C+ + NH --> CN+ + H	4		6071 RA: C+ + N --> CN+ + PHOTON
	II	2	2191 IN: CH+ + N --> CN+ + H			
HCN+	I/II	1	389 CE: H+ + HCN --> HCN+ + H			
	I/II	3	2663 IN: H2 + CN+ --> HCN+ + H			
	II	4	3682 IN: N + CH2+ --> HCN+ + H			
H2O	I	7	11297 DT: H2O# + dust --> H2O + dust	3		3036 IN: H3O+ + HCN --> HCNH+ + H2O
	I	9	11299 DP: H2O# + PHOTON --> H2O			
	II	6	6141 RA: H + OH --> H2O + PHOTON	1		1301 DR: H3O+ + e- --> H2O + H
H3O+	I/II	2	2672 IN: H2 + H2O+ --> H3O+ + H			
	I/II	5	2914 IN: H3+ + H2O --> H3O+ + H2			
	I	4	2777 IN: H2O + HCO+ --> CO + H3O+			
C2H2+	I	1	1613 IN: C+ + CH4 --> C2H2+ + H2			
	II	2	2473 IN: CH + CH3+ --> C2H2+ + H2			
NO	I/II	5	11517 DT: NO# + dust --> NO + dust	1		621 CE: NO+ + Fe --> Fe+ + NO
	I/II	4	5514 NN: N + OH --> NO + H			
NO+	I	4	3574 IN: N+ + CO --> NO+ + C	6		3875 IN: O+ + HCN --> NO+ + CH
	I	7	6001 PH: NO + PHOTON --> NO+ + e-			
	II	5	3695 IN: N + O2+ --> NO+ + O	2		404 CE: H+ + NO --> NO+ + H
HN2+	I/II	2	2948 IN: H3+ + N2 --> HN2+ + H2	1		2621 IN: H2+ + N2 --> HN2+ + H
	I/II	3	3694 IN: N + NH2+ -> HN2+ + H			
H3+	I/II	1	2614 IN: H2+ + H2 --> H3+ + H	2		2698 IN: H2 + O2H+ --> O2 + H3+
H	I	8	1427 DR: NH4+ + e- --> NH3 + H	10		2614 IN: H2+ + H2 -> H3+ + H
	I	4	1286 DR: H3+ + e- --> H + H			
	II	1	407 CE: H+ + O --> O+ + H	25		6182 RR: H+ + e- --> H + PHOTON

	1st main destruction reactions			2nd main destruction reactions	
	area	grid no.	reaction no. and type in DM	area grid no.	reaction no. and type in DM
CO	I	11	11292 IC: CO + dust --> CO# + dust		
	I	4	2905 IN: H3+ + CO --> HCO+ + H2		
	II	8	5914 PH: CO + PHOTON --> O + C	9	10529 XP: CO + XPHOT --> C++ + O + e-
HCN	I	9	11312 IC: HCN + dust --> HCN# + dust	3	3036 IN: H3O+ + HCN --> HCNH+ + H2O
	I	1	389 CE: H+ + HCN --> HCN+ + H	6	5401 NN: H + HCN -> CN + H2
	II	7	5955 PH: HCN + PHOTON --> CN + H		
HCO+	I	3	2777 IN: H2O + HCO+ --> CO + H3O+		
	II	1	1357 DR: HCO+ + e- --> CO + H	2	2134 IN: C + HCO+ --> CO + CH+
CN	I	3	5369 NN: H2 + CN --> HCN + H		
	I	4	5617 NN: O + CN --> CO + N		
	II	5	5910 PH: CN + PHOTON --> N + C		
CO2	I	12	11300 IC: CO2 + dust --> CO2# + dust	1	877 CR: CO2 + CRPHOT --> CO + O
	I	5	2904 IN: H3+ + CO2 --> HCO2+ + H2	12	11300 IC: CO2 + dust --> CO2# + dust
	II	2	1617 IN: C+ + CO2 --> CO+ + CO	8	3440 IN: He+ + CO2 -> O2 + C+
CN+	I	4	2663 IN: H2 + CN+ --> HCN+ + H	2	2499 IN: CN+ + CO2 --> C2O+ + NO
	II	1	488 CE: H + CN+ --> CN + H+	5	2768 IN: H2O + CN+ --> HNCO+ + H
HCN+	I	2	2680 IN: H2 + HCN+ --> HCNH+ + H		
	II	1	491 CE: H + HCN+ --> CN + H+		
H2O	I	13	11296 IC: H2O + dust --> H2O# + dust		
	I	9	2914 IN: H3+ + H2O --> H3O+ + H2		
	II	11	5935 PH: H2O + PHOTON--> OH* + H	10	5399 NN: H + H2O -> OH + H2
H3O+	I/II	4	3036 IN: H3O+ + HCN --> HCNH+ + H2O	1	1301 DR: H3O+ + e- -> H2O + H
	I/II	2	1304 DR: H3O+ + e- --> OH* + H		
C2H2+	I	1	1005 DR: C2H2+ + e- --> CH + CH	3	3837 IN: NH + C2H2+ --> CH2CN+ + H
	I	4	3919 IN: O + C2H2+ --> HCO+ + CH		
	II	2	3619 IN: N + C2H2+ --> HCN + CH+		
NO	I	10	11516 IC: NO + dust --> NO# + dust	4	5235 NN: CH2 + NO --> HCN + OH
	I	5	5708 NN: OH + NO --> NO2 + H		
	II	6	6001 PH: NO + PHOTON --> NO+ + e-	7	6002 PH: NO + PHOTON --> O + N
NO+	I/II	1	621 CE: NO+ + Fe --> Fe+ + NO		
	I/II	2	1428 DR: NO+ + e- --> O + N		
HN2+	I	3	2518 IN: CO + HN2+ --> HCO+ + N2		
	II	1	1411 DR: HN2+ + e- --> N2 + H		
H3+	I	6	2914 IN: H3+ + H2O --> H3O+ + H2	5	2905 IN: H3+ + CO --> HCO+ + H2
	I	2	1286 DR: H3+ + e- --> H + H		
	II	1	1285 DR: H3+ + e- --> H2 + H	9	2961 IN: H3+ + O --> OH+ + H2
H	I	13	10247 HG: H + H + dust --> H2 + dust	6	5399 NN: H + H2O --> OH + H2
	I	4	3067 IN: H + CH3+ --> CH2+ + H2	7	5405 NN: H + HNC --> HCN + H
	II	1	493 CE: H + O+ --> O + H+		

Model D

	1st main formation reactions			2nd main formation reactions		
	area	grid no.	reaction no. and type in DM	area	grid no.	reaction no. and type in DM
CO	I	16	11293 DT: CO# + dust --> CO + dust	6		2777 IN: H2O + HCO+ --> CO + H3O+
	I	3	1357 DR: HCO+ + e- --> CO + H	11		5393 NN: H + CO2 --> CO + OH
	II	1	89 CE: H + CO+ -> CO + H+	15		6093 RA: C + O --> CO + PHOTON
HCN	I	16	11313 DT: HCN# + dust --> HCN + dust	11		5405 NN: H + HNC --> HCN + H
	I	5	1350 DR: HCNH+ + e- --> HCN + H	7		3812 IN: NH3 + HCNH+ --> HCN + NH4+
	II	10	5369 NN: H2 + CN --> HCN + H	2		491 CE: H + HCN+ --> HCN + H+
HCO+	I	12	2737 IN: H2O+ + CO --> HCO+ + OH	2		1623 IN: C+ + H2O --> HCO+ + H
	I	13	2905 IN: H3+ + CO --> HCO+ + H2	6		2454 IN: CH5+ + CO --> HCO+ + CH4
	II	4	2221 IN: CH2+ + O --> HCO+ + H	10		2613 IN: H2+ + CO --> HCO+ + H
CN	I	3	906 CR: HCN + CRPHOT --> CN + H	5		1230 DR: CH4N+ + e- --> CN + H2 + H2
	I	10	5311 NN: CH + N -> CN + H	9		5204 NN: C + NO --> CN + O
	II	1	488 CE: H + CN+ -> CN + H+	15		6091 RA: C + N --> CN + PHOTON
CO2	I	13	11301 DT: CO2# + dust --> CO2 + dust			
	I	14	11303 DP: CO2# + PHOTON --> CO2 +	8		5317 NN: CH + O2 --> CO2 + H
	II	12	5692 NN: OH + CO --> CO2 + H	11		5636 NN: O + HCO --> CO2 + H
CN+	I	5	3475 IN: He+ + HCN --> CN+ + He	6		3491 IN: He+ + HNC --> CN+ + He
	I	2	1650 IN: C+ + NH --> CN+ + H	3		2191 IN: CH+ + N --> CN+ + H
	II	7	6071 RA: C+ + N --> CN+ + PHOTON			
HCN+	I	5	2663 IN: H2 + CN+ --> HCN+ + H	3		1649 IN: C+ + NH3 --> HCN+ + H2
	I	6	2901 IN: H3+ + CN --> HCN+ + H2			
	II	8	3682 IN: N + CH2+ --> HCN+ + H			
H2O	I	13	11297 DT: H2O# + dust --> H2O + dust	12		6199 CL: H + OH --> H2O + M
	I	14	11299 DP: H2O# + PHOTON --> H2O	6		3808 IN: NH3 + H3O+ --> NH4+ + H2O
	II	11	6141 RA: H + OH --> H2O + PHOTON	7		5379 NN: H2 + OH --> H2O + H
H3O+	I	9	2914 IN: H3+ + H2O --> H3O+ + H2	6		2739 IN: H2O+ + H2O --> H3O+ + OH
				7		2777 IN: H2O + HCO+ --> CO + H3O+
	II	5	2672 IN: H2 + H2O+ --> H3O+ + H	4		2616 IN: H2+ + H2O --> H3O+ + H
C2H2+	I	1	1613 IN: C+ + CH4 --> C2H2+ + H2	2		2170 IN: CH+ + CH4 --> C2H2+ + H2
	II	3	2473 IN: CH + CH3+ --> C2H2+ + H2			
NO	I	8	11517 DT: NO# + dust --> NO + dust			
	I	6	5549 NN: NH + O --> NO + H			
	II	5	5514 NN: N + OH --> NO + H			
NO+	I	7	3574 IN: N+ + CO --> NO+ + C	5		629 CE: NO + O2+ -> O2 + NO+
	I	16	6001 PH: NO + PHOTON --> NO+ + e-	12		3714 IN: NH+ + CO2 --> NO+ + HCO
	II	11	3697 IN: N + OH+ --> NO+ + H	2		404 CE: H+ + NO -> NO+ + H
HN2+	I	2	2948 IN: H3+ + N2 --> HN2+ + H2	1		2621 IN: H2+ + N2 -> HN2+ + H
	II	4	3694 IN: N + NH2+ --> HN2+ + H	3		3583 IN: N+ + NH3 -> HN2+ + H2
H3+	I	1	2614 IN: H2+ + H2 --> H3+ + H			
	II	3	2691 IN: H2 + NH+ --> N + H3+	4		2698 IN: H2 + O2H+ -> O2 + H3+
H	I	15	5368 NN: H2 + CH --> CH2 + H	17		5373 NN: H2 + NH2 -> NH3 + H
	I	8	1427 DR: NH4+ + e- --> NH3 + H	9		2614 IN: H2+ + H2 -> H3+ + H
	II	2	407 CE: H+ + O --> O+ + H	29		6182 RR: H+ + e- --> H + PHOTON

	1st main destruction reactions			2nd main destruction reactions		
	area	grid no.	reaction no. and type in DM	area	grid no.	reaction no. and type in DM
CO	I	18	11292 IC: CO + dust --> CO# + dust		13	5692 NN: OH + CO --> CO2 + H
	I	7	2905 IN: H3+ + CO --> HCO+ + H2			
	II	16	10529 XP: CO + XPHOT --> C++ + O			
HCN	I	17	11312 IC: HCN + dust --> HCN# + dust		7	3036 IN: H3O+ + HCN --> HCNH+ + H2O
	I	14	5955 PH: HCN + PHOTON --> CN + H		13	5401 NN: H + HCN --> CN + H2
	II	1	389 CE: H+ + HCN --> HCN+ + H			
HCO+	I	5	2777 IN: H2O + HCO+ --> CO + H3O+			
	I	2	1357 DR: HCO+ + e- --> CO + H			
	II	11	4032 IN: OH + HCO+ --> HCO2+ + H			
CN	I	7	5369 NN: H2 + CN --> HCN + H		9	5533 NN: NH3 + CN --> HCN + NH2
	I	13	5910 PH: CN + PHOTON --> N + C			
	II	8	5491 NN: N + CN --> N2 + C		11	5619 NN: O + CN -> NO + C
CO2	I	17	11300 IC: CO2 + dust --> CO2# + dust		1	877 CR: CO2 + CRPHOT --> CO + O
	I	16	5913 PH: CO2 + PHOTON --> CO + O		8	2904 IN: H3+ + CO2 --> HCO2+ + H2
	II	7	2612 IN: H2+ + CO2 --> HCO2+ + H		13	4006 IN: OH+ + CO2 --> HCO2+ + O
CN+	I	8	6071 RA: C+ + N --> CN+ + PHOTON		9	2766 IN: H2O + CN+ --> HCN+ + OH
				I	10	2768 IN: H2O + CN+ --> HNCO+ + H
	II	1	488 CE: H + CN+ --> CN + H+		2	682 CE: O + CN+ --> CN + O+
HCN+	I	3	1348 DR: HCN+ + e- --> CN + H		5	2776 IN: H2O + HCN+ --> CN + H3O+
	II	4	2680 IN: H2 + HCN+ --> HCNH+ + H		2	491 CE: H + HCN+ --> HCN + H+
H2O	I	16	11296 IC: H2O + dust --> H2O# + dust		12	5399 NN: H + H2O -> OH + H2
	I	14	5935 PH: H2O + PHOTON --> OH + H		8	2914 IN: H3+ + H2O -> H3O+ + H2
	II	1	379 CE: H+ + H2O --> H2O+ + H		13	5934 PH: H2O + PHOTON --> H2O+ + e-
H3O+	I	4	1304 DR: H3O+ + e- -> OH + H		10	3808 IN: NH3 + H3O+ --> NH4+ + H2O
	I	8	3036 IN: H3O+ + HCN --> HCNH+ + H2O			
	II	1	1301 DR: H3O+ + e- -> H2O + H			
C2H2+	I	1	1005 DR: C2H2+ + e- --> CH + CH			
	I	4	3919 IN: O + C2H2+ --> HCO+ + CH			
	II	3	3837 IN: NH + C2H2+ --> CH2CN+ + H			
NO	I	22	11516 IC: NO + dust --> NO# + dust			
	I	19	6002 PH: NO + PHOTON --> O + N		4	943 CR: NO + CRPHOT --> NO+ + e-
	II	18	6001 PH: NO + PHOTON --> NO+ + e-		2	3588 IN: N+ + O2 -> NO + O+
NO+	I	1	621 CE: NO+ + Fe --> Fe+ + NO			
	II	2	1428 DR: NO+ + e- --> O + N			
HN2+	I	7	2788 IN: H2O + HN2+ --> N2 + H3O+		8	3111 IN: HCN + HN2+ --> HCNH+ + N2
	I	6	2518 IN: CO + HN2+ --> HCO+ + N2		9	3602 IN: HN2+ + CO2 --> HCO2+ + N2
	II	1	1411 DR: HN2+ + e- --> N2 + H		4	2436 IN: CH4 + HN2+ --> N2 + CH5+
H3+	I	8	2914 IN: H3+ + H2O --> H3O+ + H2			
	I	6	2905 IN: H3+ + CO --> HCO+ + H2			
	II	1	1285 DR: H3+ + e- --> H2 + H		13	2959 IN: H3+ + O2 --> O2H+ + H2
H	I	5	5387 NN: H + CH2 --> CH + H2		9	5413 NN: H + NH2 --> NH + H2
	I	19	10247 HG: H + H + dust --> H2 + dust			
	II	2	493 CE: H + O+ --> O + H+			

Model E

	1st main formation reactions			2nd main formation reactions	
	area	grid no.	reaction no. and type in DM	grid no.	reaction no. and type in DM
CO	I	15	11293 DT: CO# + dust --> CO + dust	3	1357 DR: HCO+ + e- --> CO + H
	I	6	1653 IN: C+ + O2 --> CO + O+	8	2777 IN: H2O + HCO+ --> CO + H3O+
	II	13	6093 RA: C + O --> CO + PHOTON	12	5617 NN: O + CN --> CO + N
HCN	I	5	5369 NN: H2 + CN -> HCN + H	6	5405 NN: H + HNC --> HCN + H
	I	9	11313 DT: HCN# + dust --> HCN + dust		
	II	1	491 CE: H + HCN+ --> HCN + H+	3	1350 DR: HCNH+ + e- --> HCN + H
HCO+	I	6	2664 IN: H2 + CO+ --> HCO+ + H	2	1623 IN: C+ H2O --> HCO+ + H
	I	7	2905 IN: H3+ + CO --> HCO+ + H2	3	2321 IN: CH3+ + O --> HCO+ + H2
	II	1	64 AD: CH + O --> HCO+ + e-		
CN	I	4	5311 NN: CH + N --> CN + H	2	1230 DR: CH4N+ + e- --> CN + H2 + H2
	I	6	5955 PH: HCN + PHOTON --> CN + H	5	5401 NN: H + HCN --> CN + H2
	II	1	488 CE: H + CN+ --> CN + H+		
CO2	I	7	11301 DT: CO2# + dust --> CO2 + dust	5	5636 NN: O + HCO -> CO2 + H
	I	9	11303 DP: CO2# + PHOTON --> CO2		
	II	6	5692 NN: OH + CO --> CO2 + H	4	5317 NN: CH + O2 -> CO2 + H
CN+	I	3	3475 IN: He+ + HCN --> CN+ + He		
	I	1	1650 IN: C+ + NH --> CN+ + H		
	II	2	2191 IN: CH+ + N --> CN+ + H	4	6071 RA: C+ + N --> CN+ + PHOTON
HCN+	I	3	2663 IN: H2 + CN+ --> HCN+ + H		
	I	4	3682 IN: N + CH2+ --> HCN+ + H		
	II	1	389 CE: H+ + HCN --> HCN+ + H		
H2O	I	7	11297 DT: H2O# + dust --> H2O + dust	3	3036 IN: H3O+ + HCN --> HCNH+ + H2O
	I	9	11299 DP: H2O# + PHOTON --> H2O		
	II	6	6141 RA: H + OH --> H2O + PHOTON	1	1301 DR: H3O+ + e- --> H2O + H
H3O+	I	5	2914 IN: H3+ + H2O --> H3O+ + H2		
	I	4	2777 IN: H2O + HCO+ --> CO + H3O+		
	II	2	2672 IN: H2 + H2O+ --> H3O+ + H		
C2H2+	I	2	2473 IN: CH + CH3+ --> C2H2+ + H2		
	II	1	1613 IN: C+ + CH4 --> C2H2+ + H2		
NO	I	5	11517 DT: NO# + dust --> NO + dust	1	621 CE: NO+ + Fe --> Fe+ + NO
	II	4	5514 NN: N + OH --> NO + H	7	11519 DP: NO# + PHOTON --> NO
NO+	I	4	3574 IN: N+ + CO --> NO+ + C	6	3875 IN: O+ + HCN --> NO+ + CH
	I	7	6001 PH: NO + PHOTON --> NO+ + e-		
	II	5	3695 IN: N + O2+ -> NO+ + O	2	404 CE: H+ + NO --> NO+ + H
HN2+	I	2	2948 IN: H3+ + N2 -> HN2+ + H2		
	II	3	3694 IN: N + NH2+ -> HN2+ + H	1	2621 IN: H2+ + N2 --> HN2+ + H
H3+	I	1	2614 IN: H2+ + H2 -> H3+ + H	2	2698 IN: H2 + O2H+ --> O2 + H3+
H	I	8	1427 DR: NH4+ + e- -> NH3 + H	17	5378 NN: H2 + O -> OH + H
	I	4	1286 DR: H3+ + e- -> H + H	10	2614 IN: H2+ + H2 -> H3+ + H
	II	1	407 CE: H+ + O -> O+ + H	24	6182 RR: H+ + e- --> H + PHOTON

	1st main destruction reactions			2nd main destruction reactions	
	area	grid no.	reaction no. and type in DM	grid no.	reaction no. and type in DM
CO	I	11	11292 IC: CO + dust --> CO# + dust	4	2905 IN: H3+ + CO --> HCO+ + H2
	II	8	5914 PH: CO + PHOTON --> O + C	9	10529 XP: CO + XPHOT --> C++ + O
HCN	I	9	11312 IC: HCN + dust --> HCN# + dust	3	3036 IN: H3O+ + HCN --> HCNH+ + H2O
	I	6	5401 NN: H + HCN --> CN + H2		
	II	7	5955 PH: HCN + PHOTON --> CN + H	1	389 CE: H+ + HCN --> HCN+ + H
HCO+	I	3	2777 IN: H2O + HCO+ --> CO + H3O+		
	II	1	1357 DR: HCO+ + e- --> CO + H	2	2134 IN: C + HCO+ --> CO + CH+
CN	I	3	5369 NN: H2 + CN --> HCN + H	4	5617 NN: O + CN --> CO + N
	I	8	11332 IC: CN + dust --> CN# + dust		
	II	5	5910 PH: CN + PHOTON --> N + C		
CO2	I	9	5393 NN: H + CO2 --> CO + OH	1	877 CR: CO2 + CRPHOT --> CO + O
	I	12	11300 IC: CO2 + dust --> CO2# + dust	5	2904 IN: H3+ + CO2 --> HCO2+ + H2
	II	2	1617 IN: C+ + CO2 --> CO+ + CO	8	3440 IN: He+ + CO2 --> O2 + C+ + He
CN+	I	4	2663 IN: H2 + CN+ --> HCN+ + H	5	2768 IN: H2O + CN+ --> HNCO+ + H
	II	1	488 CE: H + CN+ --> CN + H+		
HCN+	I	2	2680 IN: H2 + HCN+ --> HCNH+ + H		
	II	1	491 CE: H + HCN+ --> HCN + H+		
H2O	I	10	5399 NN: H + H2O --> OH + H2	9	2914 IN: H3+ + H2O --> H3O+ + H2
	I	14	11296 IC: H2O + dust --> H2O# + dust		
	II	11	5935 PH: H2O + PHOTON --> OH + H	1	379 CE: H+ + H2O -> H2O+ + H
H3O+	I	4	3036 IN: H3O+ + HCN --> HCNH+ + H2O		
	II	2	1304 DR: H3O+ + e- --> OH + H	1	1301 DR: H3O+ + e- -> H2O + H
C2H2+	I	1	1005 DR: C2H2+ + e- --> CH + CH	3	3837 IN: NH + C2H2+ --> CH2CN+ + H
	I	4	3919 IN: O + C2H2+ --> HCO+ + CH		
	II	2	3619 IN: N + C2H2+ --> HCN + CH+		
NO	I	10	11516 IC: NO + dust --> NO# + dust	4	5235 NN: CH2 + NO --> HCN + OH
	I	7	6002 PH: NO + PHOTON --> O + N		
	II	6	6001 PH: NO + PHOTON --> NO+ + e-	2	404 CE: H+ + NO -> NO+ + H
NO+	I	1	621 CE: NO+ + Fe --> Fe+ + NO		
	II	2	1428 DR: NO+ + e- --> O + N		
HN2+	I	3	2518 IN: CO + HN2+ --> HCO+ + N2	2	2436 IN: CH4 + HN2+ --> N2 + CH5+
	II	1	1411 DR: HN2+ + e- --> N2 + H		
H3+	I	6	2914 IN: H3+ + H2O --> H3O+ + H2		
	I	5	2905 IN: H3+ + CO --> HCO+ + H2		
	II	1	1285 DR: H3+ + e- --> H2 + H	9	2961 IN: H3+ + O --> OH+ + H2
H	I	13	10247 HG: H + H + dust --> H2 + dust	6	5399 NN: H + H2O --> OH + H2
	I	4	3067 IN: H + CH3+ --> CH2+ + H2	7	5405 NN: H + HNC --> HCN + H
	II	1	493 CE: H + O+ --> O + H+	10	5429 NN: H + OH --> O + H2

L. Methods and ProDiMo - program handling

L.1. Program steps

Installation of the last version of the ProDiMo (PDM) program after receiving online permission and introduction: The PDM code can be downloaded from https://forge.roe.ac.uk/trac/ProDiMo, start at
https://forge.roe.ac.uk/trac/ROEforge/wiki/NewUserForm
to get a ProDiMo user account

Input program

```
pohl@flavius:~$ cd Models
pohl@flavius:~/Models$ ls –l
```

list of models constructed follows ; a small selection is given below (leaving out the 10, 20 and 30 series) :

```
drwxr-xr-x 2 pohl pohl    4096 2014-08-18 11:47 Chemie40
drwxr-xr-x 2 pohl pohl    4096 2014-08-19 12:30 Chemie41
drwxr-xr-x 2 pohl pohl    4096 2014-08-19 14:28 Chemie42
drwxr-xr-x 2 pohl pohl    4096 2014-08-22 12:32 Chemie43
drwxr-xr-x 2 pohl pohl    4096 2014-08-25 11:11 Chemie43ALL
drwxr-xr-x 2 pohl pohl    4096 2014-09-03 13:32 Chemie43new
drwxr-xr-x 2 pohl pohl    4096 2014-09-04 15:12 Chemie44
drwxr-xr-x 2 pohl pohl    4096 2014-09-08 15:41 Chemie45
drwxr-xr-x 2 pohl pohl    4096 2014-09-11 15:28 Chemie46
drwxr-xr-x 2 pohl pohl    4096 2014-09-15 16:31 Chemie47
drwxr-xr-x 2 pohl pohl    4096 2014-09-29 14:27 Chemie48
drwxr-x--- 2 pohl pohl    4096 2015-03-09 11:42 DIANA_SMALL
```

to insert a new model

```
cp –r TTauriChem [name new model]
cd [name new model]
pohl@flavius:~/Models/[name of new model]$
```

to change parameters of the star or the program

```
kate Parameters/ or species or reactions.in
```

change and save!

```
-rw-r--r-- 1 pohl pohl      6083 2014-04-08 12:18 Parameter.in
-rw-r--r-- 1 pohl pohl      1197 2014-04-08 12:23 Reactions.in
-rw-r--r-- 1 pohl pohl      1199 2014-04-08 12:20 Species.in
```

to implement changes of reactions into the program

```
-rw-r--r-- 1 pohl pohl      2664 2014-06-24 15:37 RobertUmistNo.txt
```

to start the supporting standard programs

```
drwxr-xr-x 2 pohl pohl    4096 2013-04-12 14:50 TTauri
drwxr-xr-x 2 pohl pohl    4096 2013-09-18 11:42 TTauriChem
drwxr-xr-x 2 pohl pohl    4096 2015-07-22 11:50 UmistChemie
```

the conditioned models ready for calculation

```
drwxr-x--- 2 pohl pohl    4096 2015-03-09 11:42 DIANA_SMALL       = DM
drwxr-x--- 2 pohl pohl    4096 2015-07-22 10:03 Robert_UMIST47    = A
drwxr-x--- 2 pohl pohl    4096 2014-10-28 14:39 Robert_UMIST47_SO = B
drwxr-x--- 2 pohl pohl    4096 2014-10-01 16:51 Robert_UMIST48
drwxr-xr-x 2 pohl pohl    4096 2014-11-21 12:04 Robert_UMIST50    = C
drwxr-x--- 3 pohl pohl    4096 2014-10-31 12:38 Robert_UMIST50_SO = D
drwxr-x--- 2 pohl pohl    4096 2014-11-21 12:03 Robert_UMIST51    = E
drwxr-x--- 2 pohl pohl    4096 2015-03-12 13:15 Robert_UMIST52    =“F“
```

to start the selected model with the ProDiMo program in an on-line monitoring version

```
pohl@flavius:~/Models/Robert_UMIST50$ ./prodimo ./prodimo > prodimo.log &
```

to visit the results

```
>IDL
.run prodimo.pro
```

to change reactions using the UMIST2012 database

```
pohl@flavius:~/Models$
cd UmistChemie
pohl@flavius:~/Models/UmistChemie$
>kate RobertUmistNo.txt
```

change or insert new reaction number out of the UMIST2012 data base, save and close

```
>IDL
.run filterUmist
>exit
pohl@flavius:~/Models/UmistChemie$cp.RobertUmist2012.dat
../../ProDiMo/data/UMIST2012.dat
pohl@flavius:~/Models/[name of new model] ./prodimo ./prodimo > prodimo.log
&
>IDL
.run prodimo.pro
```

read-out z/r / r [AU] diagrams

```
pohl@flavius:~/Models/[name of model]$
>out.ps
```

to start chemistry analysis

```
>IDL
.run chemanalyse
chemanalyse,”XY”,/readdata or chemanalyse,”XX” (for the following)
```

.

L.2. Parameter input for the selected star and the calculatory steps and conditions :

Parameter.in
Robert_UMIST47 = model A

***** Parameter Input-File for ProDiMo *****

```
0.7        ! M_star     [M_sun]      : stellar mass
1.0        ! Lstar      [Lsun]       : stellar luminosity
4000.0     ! Teff       [K]          : stellar effective temperature
0.01       ! fUV        [-]          : LUV/Lstar
1.0        ! pUV        [-]          : UV powerlaw exponent
.true.     ! Xrays      [-]          : use Xray chemistry and heating?
1.E+30     ! Xray_Lum   [erg/s]      : X-ray luminosity
0.1        ! Xray_Emin  [keV]        : X-ray min. photon energy
2.E+7      ! Xray_Temp  [K]          : X-ray emission temperature
0.01       ! Mdisk      [Msun]       : disk mass
0.01       ! dust_to_gas [-]         : the dust-to-gas mass ratio
0.01       ! fPAH       [-]          : PAH abundance with respect to ISM
0.0        ! ChemHeatFac [-]         : efficiency of chemical heating
1.3E-17    ! CRI        [1/s]        : cosmic ray ionisation of H2
1.0        ! CHI_ISM    [-]          : strength of incident vertical UV
0.0        ! alpha_vis  [-]          : viscous heating parameter
0.15       ! v_turb     [km/s]       : turbulent Doppler width

------ dust parameters ------
2.094      ! rho_gr     [g/cm^3] : dust grain material mass density
0.05       ! amin       [mic]       : minimum dust particle size
3000.0     ! amax       [mic]       : maximum dust particle size
3.5        ! apow       [-]         : dust size distr f(a)~a^-apow
2          ! settle_method          : dust settling (Dubrulle et al. 1995)
1.E-3      ! a_settle               : turbulence alpha
0.8        ! hollow_sphere          : max hollow volume ratio
dust_opacity_list2X.txt           ! dust_opacity_list_file
3          ! NDUST                  : number of selected dust species
  0.60     Mg0.7Fe0.3SiO3[s]
  0.15     amC-Zubko[s]
  0.25     vacuum[s]

------ disk shape ------
.false.    ! soft_edges             : add confining boundary layers?
.false.    ! solve_diskstruc        : solve the vertical hydrostatic eq.?
.true.     ! MCFOST_LIKE            : fixed disk structure like in MCFOST?
0.07       ! Rin        [AU]        : inner disk radius
200.0      ! Rtaper     [AU]        : tapering-off radius
400.0      ! Rout       [AU]        : outer disk radius
1.0        ! epsilon    [-]         : column density exponent
1.0        ! gtaper     [-]         : tapering-off exponent
10.0       ! MCFOST_H0  [AU]   : scale height ...
100.0      ! MCFOST_RREF [AU]  : ... belonging to reference radius
1.15       ! MCFOST_BETA        : flaring power

------ the big molecules ------
.false.    ! UV_H2                  : electronic levels for H2?
.false.    ! custom_COrovib         : big ro-vibronic CO model?
.true.     ! H2O_rovibration        : big ro-vib H2O models?
.true.     ! H2O_Daniel2011         : new H2O collision rates
.false.    ! CO2_LTE_cooling
.false.    ! HCNrovib_LTE_cooling
.false.    ! CH4_LTE_cooling
```

```
.false.       ! NH3rovib_LTE_cooling
.false.       ! OHrovib_LTE_cooling
.false.       ! C2H2_LTE_cooling
.false.    ! Hatom_bb
.false.    ! Hatom_bf
------ dimensions ------
70         ! NXX
70         ! NZZ
26         ! NLAM
5          ! NUV
2          ! N1UV
21         ! Ntheta
13         ! Nphi
50         ! RTitmax
30.0       ! tau_cutoff
------ accelerations ------
.true.     ! parallel_chem
.false.    ! parallel_debug
.false.    ! ignore_Tg_midplane
.false.    ! use_chemsol
------ image and SED parameters ------
.true.     ! calcSED             : calculate SED and images?
.true.     ! monoSED             : use monochromatic mode?
300        ! NlamSED             : number of lambda gridpoints
0.1        ! lminSED             : minimum lambda[mic]
3000.0     ! lmaxSED             : maximum lambda[mic]
140.0      ! dist     [pc]       : distance
45.0       ! incl     [deg]      : inclination (0=face-on)
------ line transfer? ------
.true.     ! line_transfer       : calculate line transfer?
.false.    ! immediate_lines     : line RT directly after init?
.false.    ! line_cube
8          ! line_Nstar
40         ! line_Nhole
300        ! line_Ndisk
40         ! line_Npuff
360        ! line_Ntheta
501        ! line_image_side_Npix

------ tolerances ------
0.05         ! tol_convergence   : convergence criterion for global interation
1.0E-8       ! tol_diskstruc     : rel.&abs. tolerance for vertical disk struc
1.0E-8       ! temp_precis       : rel. precision in T-determination
1.0E-9       ! chem_precis       : precision in solve_chemistry

------ switches ------
0          ! verbose_level       : how much output? (-1...4)
.true.     ! solve_temp          : solve the heating/cooling balance?
.false.    ! conserve_pressure   : conserve pgas instead of n<H>?
.true.     ! pseudo_aniso_scat   : ignore forward scattering
.true.     ! chi_from_RT         : calculate chi from UV rad. transfer?
.true.     ! Td_from_RT          : calculate dust temp. from rad. transfer?
.true.     ! Jback_from_RT       : calculate background Jnu from rad. transfer?
.true.     ! UVpumping           : use large model atoms?
.true.     ! PAH_from_RT         : PAH heating from cross-sections?
.true.     ! Rphoto_from_RT      : calculate photorates from rad. transfer?
.false.    ! Rphoto_bandint      : use band-integrated photo-rates?
.false.    ! write_pop           : write output for line transfer?
.true.     ! NewChemScan         : new initial abund. from down-right scan?
.false.    ! freeze_RT           : freeze radiative transfer results Td/Jv?
.false.    ! freeze_diskstruc    : freeze density/pressure structure?
.false.    ! freeze_Tgas         : freeze gas temperature?
```

```
.false.    ! freeze_chemistry  : freeze chemical concentrations?
.false.    ! perfect_ice       : use long integration time for ices?
.false.    ! OSU_rates
.true.     ! UMIST2012
.true.     ! Eads_from_file    : UMIST2012 adsorption energies
onlyadd    ! handle_UMIST      : handle UMIST-data (erase/overwrite/onlyadd)
0          ! num_noerase       : exceptions from erasing UMIST data

------ start from MCMax? --------
.false.     ! restart
.true.     ! radtrans
.false.    ! readMCFOST  forProDiMo.fits.gz

------ FLitS ---------------------
.false.    ! FLiTs

.true.         ! chemanalysis
```

L.3. Chemanalyse opened as described in L.2. **CO** as an example

Chemanalyse

```
IDL> .run chemanalyse
% Compiled module: READ_CHEMANALYSIS.
% Compiled module: READ_SPECIES.
% Compiled module: READ_REACTIONS.
% Compiled module: FIND_REACTIONS.
% Compiled module: GET_MAJOR_REACTIONS.
% Compiled module: REACTION_NETWORK.
% Compiled module: CHEMANALYSE.
IDL> chemanalyse,"CO",/readdata
===============================================
  reading ./ProDiMo.out ...
===============================================
reading ProDiMo.out, VERSION=8
dimension  70 x 70
unit=         100
% Compiled module: READCOL.
% Compiled module: REMCHAR.
% Compiled module: GETTOK.
% Compiled module: STRSPLIT.
% READCOL: 68 valid lines read
Reading chemanalysis.out
% Compiled module: STRNUMBER.
% READCOL: 1462989 valid lines read
Species :CO
( Explanations: indenture number// PDM reaction number // reaction type as in section 'references' listed // reaction )

All the formation reactions :      19
     14     479 CE: H2O    + CO+            -> CO     + H2O+
     30     877 CR: CO2    + CRPHOT         -> CO     + O
     48    1258 DR: H2CO+  + e-             -> CO     + H
     59    1357 DR: HCO+   + e-             -> CO     + H
     61    1359 DR: HCO2+  + e-             -> CO     + O
     62    1360 DR: HCO2+  + e-             -> CO     + OH
     63    1376 DR: HNCO+  + e-             -> CO     + NH
     73    1617 IN: C+     + CO2            -> CO+  + CO
     74    1620 IN: C+     + H2CO           -> CO     + CH2+
     79    1653 IN: C+     + O2             -> CO     + O+
     81    2134 IN: C      + HCO+           -> CO     + CH+
```

```
 124   2777 IN: H2O    + HCO+           -> CO     + H3O+
 142   3438 IN: He+    + CO2            -> CO     + O+     + He
 172   5327 NN: CH     + O              -> CO     + H
 173   5354 NN: CN     + O2             -> NO     + CO
 179   5393 NN: H      + CO2            -> CO     + OH
 191   5617 NN: O      + CN             -> CO     + N
 217   6093 RA: C      + O              -> CO     + PHOTON
 268  10548 XP: CO2    + XPHOT          -> O++    + CO     + e-
```

All the destruction reactions : 11

```
  22    550 CE: N+     + CO             -> CO+    + N
 102   2515 IN: CO     + HCO2+          -> CO2    + HCO+
 103   2518 IN: CO     + HN2+           -> HCO+   + N2
 127   2905 IN: H3+    + CO             -> HCO+   + H2
 145   3441 IN: He+    + CO             -> O      + C+     + He
 152   3574 IN: N+     + CO             -> NO+    + C
 194   5692 NN: OH     + CO             -> CO2    + H
 200   5914 PH: CO     + PHOTON         -> O      + C
 252  10529 XP: CO     + XPHOT          -> C++    + O      + e-
 253  10530 XP: CO     + XPHOT          -> C+     + O+     + e-
 254  10531 XP: CO     + XPHOT          -> C      + O++    + e-
```

Write chemistry analysis output to chemistry_analsyis_CO.ps
% LOADCT: Loading table Rainbow + white
% Stop encountered: CHEMANALYSE 866 /scratch/pohl/ProDiMo/idl/chemanalyse.pro
% Program caused arithmetic error: Floating underflow

Chemanalyse .txt

Main formation and destruction reactions
species :**CO**

Formation reactions

```
  1     30    877 CR: CO2    + CRPHOT       -> CO     + O
  2     48   1258 DR: H2CO+   + e-          -> CO     + H
  3     59   1357 DR: HCO+    + e-          -> CO     + H
  4     61   1359 DR: HCO2+   + e-          -> CO     + O
  5     73   1617 IN: C+      + CO2         -> CO+    + CO
  6     79   1653 IN: C+      + O2          -> CO     + O+
  7     81   2134 IN: C       + HCO+        -> CO     + CH+
  8    124   2777 IN: H2O     + HCO+        -> CO     + H3O+
  9    142   3438 IN: He+     + CO2         -> CO     + O+     + He
 10    172   5327 NN: CH      + O           -> CO     + H
 11    179   5393 NN: H       + CO2         -> CO     + OH
 12    191   5617 NN: O       + CN          -> CO     + N
 13    217   6093 RA: C       + O           -> CO     + PHOTON
 14    268  10548 XP: CO2     + XPHOT       -> O++    + CO  + e-
```

Destruction reactions

```
  1     22    550  CE: N+     + CO          -> CO+    + N
  2    102   2515 IN: CO     + HCO2+       -> CO2    + HCO+
  3    103   2518 IN: CO     + HN2+        -> HCO+   + N2
  4    127   2905 IN: H3+    + CO          -> HCO+   + H2
  5    145   3441 IN: He+    + CO          -> O      + C+     + He
  6    194   5692 NN: OH     + CO          -> CO2    + H
  7    200   5914 PH: CO     + PHOTON      -> O      + C
  8    252  10529 XP: CO     + XPHOT       -> C++    + O  + e-
```

L. 4. Program run (example model A)

Example: Model A

```
This is PRODIMO
Version: 1.0,  Revision: 2124|
home/lv70473/rabc6/ProDiMoHEAD/src_devel |
(c) 2012 Peter Woitke, Inga Kamp & Wing-Fai Thi |

 Reading additional Paramterfile:
 ParameterA.in
beta_mag is not set. deltaMRI value is ignored

 'ProDiMo_datapath' =
 /home/lv70473/rabc6/ProDiMoHEAD/data/
INIT_ELEMENTS: ...
 selected elements   6                  H   He  C   N   O   Fe

 INIT_PAH: ...
 circumcoronene
        54  carbon atoms
        18  hydrogen atoms
 PAH particle radius          =   4.87E-08 cm
 PAH mass/macromolecule       =     666.74 amu
 NC=  54 charge=-1 IP[eV]=  3.103
 NC=  54 charge= 0 IP[eV]=  6.243
 NC=  54 charge= 1 IP[eV]=  9.384
 NC=  54 charge= 2 IP[eV]= 12.524

 mass normalization factor =   1.20927486207672
 Zone  1  fPAH =      1.00E-02,  PAH  mass =      1.53E-08  Msun,  mass(PAH)/mass(solid)=      1.53E-04,
mass(solid)=   1.00E-04
 total mass of PAH in the disk =   1.53E-08 Msun
 mass of PAH/total solid mass  =   1.53E-04
 PAH excitation maximum wavelength =   4.35E-01 micron
 GET_PAH_HC_RATIO=  0.340206908719886
 Maximum PAH temperature :1152.1 K
 The chosen PAH is stable against photodissociation

 INIT_SPECIES: ...
 selected species   68 +  9
 He     He+    C      C+     C++    O      O+     O++    Fe     Fe+    CO     CO+    OH     OH+    CH
CH+    CH2    CH2+   CH3+   CH4    CH5+   O2     O2+    H2+    H3+    HCO    HCO+   H2O
H2O+   H3O+   H      H+     H2     CO2    N      N+     N++    NH+    NH2    NH2+   NH3    NH3+
N2     HN2+   CN     CN+    HCN    HCN+   NO     NO+    H2CO   Fe++   HNC    O2H+   HCO2+
HCNH+  NH4+   H3CO+  H2CO+  CH2CN+ CH4N+  CH3OH2+ C2H2+  HNCO+  OCN+   C2O+
NO2    NH     PHOTON CRP    CRPHOT e-     M      dust   XPHOT  XUVPHOT RDP

 INIT_REACTIONS: ...

 reading  reactions  from  /home/lv70473/rabc6/ProDiMoHEAD/data/RobertUmist2012_Chemie47.dat     =
model A
 having included  232 UMIST chemical reactions
 no of reactions with multiple T-fits:  2

 reading additional reactions from Reactions.in ... 3 columns

 having included   81 additional reactions
 altogether   313 chemical reactions
 no of reactions with multiple T-fits:  2
 ****************************************
 ***      check form/dest in UMIST      ***
```

```
 *** and write results to CheckChem.log ***
 ***                           ***
 ***   done check form/dest in UMIST    ***
*********************************************
 *** check chemical network for consistency ***
 *** for reactions in Reactions.in only     ***
 *** and write results to CheckNetwork.log  ***
 *********************************************

 Reading photoprocesses master list ...
 found detailed cross-sections for  17 photo-reactions
 N(photo-dissociation), N(photo-ionisation)  13   4
 could not find cross-sections for   2 photo-reactions
 Use default CO self-shielding

 Reading ice photoabsorption data from /home/lv70473/rabc6/ProDiMoHEAD/data//COi
 ce_photodesoprtion_Lu2005.dat
 CO#: 700 wavelength points between  912.00 and 1611.00 Angstrom

 INIT_HEATCOOL: ...
 allocating SYS ...

Reactions for chemical heating/cooling ...
...    0 exothermic reactions
...    0 endothermic reactions

 INIT_GRID: ...

 INIT_STAR: ...
 Teff  [K]    =  4000.0000
 Lstar [Lsun] =     1.0000
 Mstar [Msun] =     0.7000
 Rstar [Rsun] =     2.0862
 logg         =     3.6441
 Mdisk [Msun] =   1.00E-02 (3.33E+03 Mearth)
 R_in  [AU]   =     0.0700
 R_out [AU]   =   400.0000
 v(Rin)[km/s] =    94.1876
 P(Rin)[days] =     8.0853

 interpolating Phoenix stellar spectrum ...
test integrated star spectrum    4000.00000000000       3999.94286347427
 adding extra UV as powerlaw fUV=0.01000 pUV=  1.000 ...
 intersection of UV powerlaw with stellar spectrum is at 398.20 nm
 adding Xray input spectrum Emin[keV]= 0.10 Emax[keV]= 61.99 TXray[K]= 2.0E+07 ...
 Lstar =    1.0000   Ltotal =   1.0264
 fUV =  0.010000  LUV/Lstar = 0.010001  Ladded/Lstar = 0.026430
 Teff from StarSpectrum.in is    4026.2
 UV-flux between 111.00nm - 145.00nm = 2.635E-12 erg/cm2/s
 L_UV1          between  91.20nm  - 250.00nm  = 3.846E+31 erg/s
 L_UV2          between 111.00nm  - 145.00nm  = 6.179E+30 erg/s
 L_FUV          between  91.20nm  - 205.00nm  = 2.393E+31 erg/s
 L_EUV          between  91.20nm  -   0.10keV = 5.803E+30 erg/s
 L_X (total)    between   0.10keV -  61.99keV = 1.000E+30 erg/s
 L_X (0.1-10)   between   0.10keV -  10.00keV = 9.998E+29 erg/s
 L_X (Very hard) between  10.00keV -  61.99keV = 1.943E+26 erg/s
 L_X (Soft)     between   0.10keV -   1.00keV = 7.956E+29 erg/s
 L_X (Soft)     between   0.30keV -   1.00keV = 3.705E+29 erg/s
 L_X (Hard)     between   1.00keV -  10.00keV = 2.031E+29 erg/s
 ratio Very Hard/total LX          :   1.9432E-04
 X-Hardness (Hard/Soft)            :   5.4805E-01
 X-Hardness2 (Hard-Soft)/(Hard+Soft):  -2.9195E-01
```

```
 photon particle fluxes ...
 - UV band 1 (912-1110)Ang: 2.19115E+18 1/cm^2/s  (chi=1.041E+11)
 - UV band 2 (912-2050)Ang: 2.82600E+19 1/cm^2/s  (chi=1.471E+11)
 -    1000 Ang photon flux: 1.07937E+14 1/cm^2/s/(cm^-1)
 -    1000 Ang   lam*u_lam: 7.15201E-03 erg/cm^3
 -     stellar chi at 1 AU: 2.45102E+06 3.46401E+06
 - ISM irradiation (UV band 1) may dominate >  1.566E+03 AU

 INIT_DUST: ...
 amin[mic], amax[mic], apow =     0.050  3000.000     3.500
 <a>, <a^2>^1/2, <a^3>^1/3  = 8.333E-06 1.116E-05 5.342E-05
 <a>,    <a^2>,    <a^3>  = 8.333E-06 1.245E-10 1.525E-13
 surface area/H-nucleus [cm^2] =  2.663562942763451E-023

 Readig dust opacity list file dust_opacity_list2X.txt

name                    filename          mass density [g/cm^3
MgSiO3[s]              nk2_MgSiO3-Jena_X.dat          2.80
Mg0.7Fe0.3SiO3[s]      nk2_Mg07Fe03SiO3_X.dat         3.04
Mg0.5Fe0.5SiO3[s]      nk2_Mg0.5Fe0.5SiO3_X.dat       3.20
Mg2SiO4[s]             nk_Mg2SiO4-Jena_X.dat          3.33
MgFeSiO4[s]            nk2_MgFeSiO4-Jena_X.dat        3.71
SiO2[s]               nk2_SiO2-Posch_X.dat           2.21
Al2O3[s]              nk2_Al2O3-Jena_X.dat           3.89
TiO2[s]               nk2_TiO2-Posch_X.dat           3.90
SiC[s]                nk_SiC-Anja_X.dat              3.20
Fe[s]                 nk2_iron_X.dat                 7.87
FeO[s]                nk2_FeO_X.dat                  2.40
FeS[s]                nk2_FeS_X.dat                  4.83
amorphC[s]            nk2_Carbon-Jena800_X.dat       1.80
amorphC_M[s]          nk2_amorphC_M_X.dat            1.80
amC-Zubko[s]          nk_amC-zb1_X.dat               1.80
amC-Zubko-ACAR[s]      nk2_amC-zb2-ACAR_X.dat        1.95
AstroSilicate_Draine[s]  nk2_AstroSilicate_Draine_X.dat  3.50
AstroSilicate_MW89[s]    nk_AstroSilicate_MW89_X.dat    3.50
Oss_Draine[s]          nk_Oss_Draine.dat              3.50
cryst_silicate[s]      nk_mg2_0.33_0000_037_X.dat     3.33
H2Oice[s]             nk_H2OiceWarren_X.dat          0.92
amorphous_H2Oice[s]    nk_H2O_Li_X.dat                1.20
vacuum[s]             nk_vacuum_X.dat                0.00

 chosen dust volume mix consists of ...
 Mg0.7Fe0.3SiO3[s]        Vs= 60.00%  rho_gr = 3.040 g/cm^3
 amC-Zubko[s]             Vs= 15.00%  rho_gr = 1.800 g/cm^3
 vacuum[s]                Vs= 25.00%  rho_gr = 0.000 g/cm^3
             dust material density of mix = 2.094 g/cm^3
  CPU-time=      0.17 sec
     time=      0.45 sec

 auto-adjust beta_max=   27.8519199462411

 FIXED DISK_STRUCTURE: ...
muH =  2.277005167537201E-024
 fac=  0.998695995120060

 DUST STRUCTURE: ...
  calculating dust settling according to ...
  method=2, alpha= 1.00E-03
  (parameter values may depend on zones)
   Vol[cm^3] =   4.755010508892508E+047  4.742492468570887E+047
   Mgas[Msun] =   1.000183458851792E-002
```

```
 Mdust[Msun] =   1.000183458851792E-004

 INIT XRAY CROSS SECTIONS: ...
 ********************************************
 *** check chemical network for consistency ***
 *** for reactions in Reactions.in only     ***
 *** and write results to CheckNetwork.log  ***
 ********************************************
 INIT_LINE_TRANSFER: ...

 CALCULATE DUST AND GAS OPACITIES ...

  *** WARNING: having partly reduced ndust_RT() in
     the midplane regions by up to a fac =  6.721630886414147E-002
     to improve convergence in radiative transfer

 CALCULATE OPTICAL DEPTHS ...
 ... tau_rad(visual,1AU)=1 at z/r =  0.192857753395199
 ...       estimated LnearIR/Lsun =  0.157550534966160

 INCIDENT INTENSITIES ...
 ... parameters CHI_ISM=1.000E+00,  Tback= 2.7,  IR_ISRF=F
 before: chi=   1.09734068435247
   norm: chi=   1.00000000000000
 ... min dust temperature (opt.thick limit)=  2.90K
 ... min dust temperature (opt. thin limit)=  3.70K

 SOLUTION OF CONTINUUM RADIATIVE TRANSFER ...

 ESTIMATE MEAN INTENSITIES ...
maxtau=  5.31080E+04 band(wl,idx):   1.05727E-01   2

 RT total time consumption=   2308.7 sec

 CALCULATING MONOCHROMATIC FACE-ON SED ...
   applying energy-conserving Jnu-interpolation ...
   ... finished Jnu-interpolation. time= 7.04 sec,  max. bg-err= 0.0000
 CALCULATING MONOCHROMATIC SED incl= 45.0 ...
   RT_GRID: NZONES=1  R1in=   0.07  Ntot= 225
 Nrays=  15148  steps/ray= 71.49  fcalls/step= 2.431
 time= 147.02 sec

expected near-IR excess ...
 ... from star light conversion:   0.1576 Lsun
 ... from viscous heating:         0.0000 Lsun
IR excesses as measured from the model SED ...
 ... ( 2 - 7   ) mic:              0.1075 Lsun
 ... ( 7 - 30  ) mic:              0.0836 Lsun
 ... (30 - 1000) mic:              0.0500 Lsun

 CHEMISTRY AND ENERGY BALANCE ...
 67 .........t.....................................................
 64 .......t.....................................................
 43 .......t.....................................................
  3 ................................t.....................................
    12345678901234567890123456789012345678901234567890123456789012345678901234567890
             1        2        3        4        5        6        7

  CPU-time=  18188.22 sec
     time=   1206.09 sec
   max element conservation error   :   1.53E-04
   max chemical equilibrium error   :   9.97E-05
```

```
  max heating/cooling balance error:   1.00E-03
  non-LTE calls, %sparse, <it>     :   1295340   0.000%  2.2802
  solve_chemistry calls            :     35120
  advance_chemistry calls          :       215
  NR converged after advance_chem  :       178
  NR failed after advance_chem     :        37
  advance_chemistry failed         :         0

 SOUNDSPEED ...

 FIXED DISK_STRUCTURE: ...
 muH =  2.277005167537201E-024
 fac=   1.00000207633019

 DUST STRUCTURE: ...
  calculating dust settling according to ...
  method=2, alpha= 1.00E-03
  (parameter values may depend on zones)
   Vol[cm^3] =   4.755010508892508E+047  4.742492468570887E+047
  Mgas[Msun] =   1.000183458949390E-002
 Mdust[Msun] =   1.000183458949386E-004

 LINE TRANSFER:
 Starting line ray-tracing...
   RT_GRID: NZONES=1  R1in=   0.07  Ntot= 389
 requested line image FOV =   800.00 AU
        actual image FOV =   870.92 AU

  line#02   CO   097->052 lam[mic]=     5.0   flux[W/m^2]= 3.255E-20 cont[Jy]= 2.94E-01 FWHM[km/s]=
 124.16
  line#04   CO   003->002 lam[mic]= 1300.4   flux[W/m^2]= 9.726E-20 cont[Jy]= 4.60E-02 FWHM[km/s]=
 2.69
  line#05  13CO 003->002 lam[mic]= 1360.2   flux[W/m^2]= 4.548E-20 cont[Jy]= 4.03E-02 FWHM[km/s]=
 2.65
  line#06  C18O 003->002 lam[mic]= 1365.4   flux[W/m^2]= 2.859E-20 cont[Jy]= 3.98E-02 FWHM[km/s]=
 2.59
  line#08  13CO 004->003 lam[mic]=  906.8   flux[W/m^2]= 1.320E-19 cont[Jy]= 1.06E-01 FWHM[km/s]=
 2.70
  line#09  C18O 004->003 lam[mic]=  910.3   flux[W/m^2]= 8.103E-20 cont[Jy]= 1.05E-01 FWHM[km/s]=
 2.66
  line#11   CO   052->048 lam[mic]=    72.8   flux[W/m^2]= 3.226E-22 cont[Jy]= 9.63E-01 FWHM[km/s]=
 30.40
  line#12   OI   002->001 lam[mic]=    63.2   flux[W/m^2]= 2.303E-17 cont[Jy]= 9.41E-01 FWHM[km/s]=
 7.05
  line#14   OI   004->001 lam[mic]=     0.6   flux[W/m^2]= 8.372E-18 cont[Jy]= 1.39E-01 FWHM[km/s]=
 24.34
  line#15   CII  002->001 lam[mic]=   157.7   flux[W/m^2]= 5.978E-18 cont[Jy]= 9.67E-01 FWHM[km/s]=
 2.74
  line#17   C    003->002 lam[mic]=   370.4   flux[W/m^2]= 4.112E-19 cont[Jy]= 5.13E-01 FWHM[km/s]=
 2.26
  line#18   Fe+  002->001 lam[mic]=    26.0   flux[W/m^2]= 3.851E-21 cont[Jy]= 7.72E-01 FWHM[km/s]=
 8.90
  line#20   OH    015->011 lam[mic]=    71.2   flux[W/m^2]= 4.596E-19 cont[Jy]= 9.58E-01 FWHM[km/s]=
 30.23
  line#22   OH   005->001 lam[mic]=    79.2   flux[W/m^2]= 6.032E-20 cont[Jy]= 9.71E-01 FWHM[km/s]=
 10.43
  line#23   OH   003->001 lam[mic]=   119.4   flux[W/m^2]= 3.590E-19 cont[Jy]= 9.96E-01 FWHM[km/s]=
 14.20
  line#24   OH   004->002 lam[mic]=   119.2   flux[W/m^2]= 3.176E-19 cont[Jy]= 9.96E-01 FWHM[km/s]=
 16.26
  line#27  o-H2O  024->019 lam[mic]=   63.3   flux[W/m^2]= 5.725E-20 cont[Jy]= 9.41E-01 FWHM[km/s]=
 30.44
```

```
 line#28  o-H2O  010->006 lam[mic]=   78.7  flux[W/m^2]= 7.587E-20 cont[Jy]= 9.71E-01 FWHM[km/s]=
15.57
 line#29  p-H2O 007->004 lam[mic]=   90.0  flux[W/m^2]= 1.028E-19 cont[Jy]= 9.82E-01 FWHM[km/s]=
10.82
 line#30  p-H2O 009->008 lam[mic]=  187.1  flux[W/m^2]= 3.676E-21 cont[Jy]= 9.17E-01 FWHM[km/s]=
15.81
 line#32  o-H2  002->001 lam[mic]=   17.0  flux[W/m^2]= 6.360E-20 cont[Jy]= 5.39E-01 FWHM[km/s]=
16.93
 line#33  p-H2  003->002 lam[mic]=   12.3  flux[W/m^2]= 1.646E-20 cont[Jy]= 3.68E-01 FWHM[km/s]=
16.96
 line#35  o-H2  006->001 lam[mic]=    2.1  flux[W/m^2]= 1.434E-20 cont[Jy]= 5.75E-01 FWHM[km/s]=
5.37
 line#37  p-H2 007->001 lam[mic]=    2.2  flux[W/m^2]= 9.345E-20 cont[Jy]= 5.52E-01 FWHM[km/s]=
2.68
 line#38  o-H2  009->007 lam[mic]=    4.7  flux[W/m^2]= 4.047E-21 cont[Jy]= 3.03E-01 FWHM[km/s]=
9.04
 line#40  CN  005->003 lam[mic]= 1321.4  flux[W/m^2]= 5.171E-20 cont[Jy]= 4.40E-02 FWHM[km/s]=
2.43
 line#41  HCN  005->004 lam[mic]=  845.7  flux[W/m^2]= 1.105E-19 cont[Jy]= 1.26E-01 FWHM[km/s]=
2.76
 line#42  HCN 004->003 lam[mic]= 1127.5  flux[W/m^2]= 6.367E-20 cont[Jy]= 6.53E-02 FWHM[km/s]=
2.67
 line#43  CH+  006->005 lam[mic]=   72.1  flux[W/m^2]= 1.541E-21 cont[Jy]= 9.61E-01 FWHM[km/s]=
33.06
 line#44  CH+  005->004 lam[mic]=   90.0  flux[W/m^2]= 9.082E-22 cont[Jy]= 9.82E-01 FWHM[km/s]=
27.48
 line#45  CH+   003->002 lam[mic]=  179.6  flux[W/m^2]= 1.285E-22 cont[Jy]= 9.30E-01 FWHM[km/s]=
7.24
 line#46  HCO+  002->001 lam[mic]= 3361.3  flux[W/m^2]= 5.969E-22 cont[Jy]= 3.35E-03 FWHM[km/s]=
2.31
 line#47  HCO+  004->003 lam[mic]= 1120.5  flux[W/m^2]= 2.698E-20 cont[Jy]= 6.63E-02 FWHM[km/s]=
2.49
 line#48  HCO+  005->004 lam[mic]=  840.4  flux[W/m^2]= 4.287E-20 cont[Jy]= 1.27E-01 FWHM[km/s]=
2.66
 line#49     N2H+        004->003   lam[mic]=   1072.6     flux[W/m^2]=   6.692E-29   cont[Jy]=   7.24E-02
FWHM[km/s]=   3.56
  Nrays=  65214  steps/ray=184.48  fcalls/step= 2.325
  CPU-time=24840.95 sec
     time= 1665.65 sec
/----------------------------------------------\
| finished disk structure after iter =    1  |
| convergence = 0.0000E+00                    |
\----------------------------------------------/
```

M. Acronyms and formulae

ProDiMo	calculation program of DIANA
PPD	proto planetary disk
DIANA	is an European Framework Seven (FP7) project, SPACE-2011 collaboration, project no 284405,
DM	DIANA*_SMALL - one reference model for ProDiMo *[Disk analysis and modelling of multi-wavelengths observational data from proto-planetary disks]
CR	cosmic ray
CRP	cosmic ray particles
RT	Reaction tree - reaction possibilities of a species in a gas phase
UMIST	release 2012 – a chemical data base for Astro-chemistry
UCDP	"university-cluster" data processing system
XPHOT	x-ray photons
PAH	polycyclic aromatic hydrocarbons
z/r	relative height from the midplane of the disk
r	distance from rotational centre of the disk (=star centre)
$[X^{0/+/-}]$	means concentration of $X^{0/+/-}$ mainly expressed in $[cm^{-3}]$
$\boldsymbol{\varepsilon}$	relative concentration of a species to hydrogen : $\boldsymbol{\varepsilon_i} = n_i / n_{(H)}$ mainly expressed in the diagrams as log $\boldsymbol{\varepsilon}$ $(X^{0/+/-})$

note:
HN_2^+ equals to N_2H^+ , which is the chemical correct notation form of the diazenylium cation

Abbreviations of reaction types in reaction spreadsheets:

AD	Associative Detachment
CD	Collisional Dissociation
CE	Charge Exchange
CP	Cosmic-Ray Proton (CRP)
CR	Cosmic-Ray Photon (CRPHOT)
DR	Dissociative Recombination
IN	Ion-Neutral
MN	Mutual Neutralisation
NN	Neutral-Neutral
PH	Photo process
RA	Radiative Association
REA	Radiative Electron Attachment
RR	Radiative Recombination

N. References:

Aikawa Y. et al. (1996), Evolution of molecular abundances in gaseous disks around young stars: depletion of CO molecules, Astrophys. Journ., 467, p.684-697

Blagojevic V. et al. (2003), Gas-phase syntheses for interstellar carboxylic and amino acids, Monthly Notat.Royal Astron. Soc.'MNRAS',339,1 , pp. L7-L11.

Danger G. et al. (2011), Experimental investigation of aminoacetonitrile formation through the Strecker synthesis in astrophysical-like conditions: reactivity of methanimine, ammonia and hydrogen cyanide, A&A 535, A47, DOI: 10.1051/0004-6361/201117602

Henning T. and Semenov D. (2013), Chemistry in Protoplanetary Disks, arXiv:1310.3151v1 [astro-ph.GA] 11 Oct 2013

Herbst E. and Klemperer W. (1973), The formation and depletion of molecules in dense interstellar clouds, Astrophys. Journ. 185, p.505-534

Herbst E. and Leung, C. M. (1989), Gas-phase production of complex hydrocarbons, cyanopolyynes and related compounds in dens interstellar clouds, Astrophys. J. Suppl.Series, 69, p.271-300

Kamp I. & Dullemond C.P. (2004), The gas temperature in the surface layers of PPD's, The Astrophysical Journal, 615, p.991–999

KInetic Database for Astrochemistry (KIDA): http:// kida.obs.u-bordeaux1.fr/

McElroy D. et al., (2013), The UMIST database for astrochemistry 2012, A&A 550, A36

McEwan M.J. and Scott G.B.I. (1999), New H and H_2 reactions with small hydrocarbon ions and their roles in benzene synthesis in dense interstellar clouds, The Astrophys, Journ., 513, p.287-293

Meijerink R. and Glassgold A.E. (2007), Atomic diagnostics of X-ray irradiated protoplanetary disks, arXiv:0712.0112v1 [astro-ph] 1 Dec 2007

ProDiMo references: The PDM code can be downloaded from https:// forge.roe.ac.uk/trac/ ProDiMo, start at https:// forge.roe.ac.uk/trac/ROEforge/wiki/NewUserForm to get a ProDiMo user account

Prasad S.S. and Huntress jr.W.T. (1980), A Model for gas-phase chemistry in interstellar clouds: I. The basic model, library of chemical reactions and chemistry among C, N, and O compounds, The Astrophys. Journ. Suppl. Series, 43, p.1-35

Reboussin L. et al. (2015), Chemistry in Protoplanetary Disks: the gas-phase CO/H_2 ratio and
the Carbon reservoir, arXiv:1505.01309v1 [astro-ph.SR] 6 May 2015

Schlemmer S. ed. (2015), Laboratory Astrochemistry, Wiley-VCH, ISBN:978-527-40889-4, p.109 et seqq.

Semenov D., Wiebe D. and Henning T. (2004), Reduction of chemical networks; II. Analysis of the fractional ionisation in protoplanetary discs, arXiv:astro-ph/0403555v1 23 Mar 2004

Smith D. et al.(1992), The ion chemistry of interstellar clouds. Chem.Rev.,92, p.1473-1485 [mod. S. Schlemmer, Laboratory Astrochemistry, Wiley-VCH (2015)]

Stancil P.C. and Dalgarno A. (1998), Chemical processes in astrophysical radiation-fields, Faraday Discuss., 109, p.61-69

Turner B.E. (1997), The physics and chemistry of small translucent molecular clouds, VIII: HCN and HNC, The Astrophys. Journ., 483, p.235-261

Walsh C. et al. (2014), Complex organic molecules in protoplanetary disks, arXiv:1403.0390v1 [astro-ph.EP] 3 Mar 2014

Woitke P., Kamp I. & Thi W.F.(2009) , Radiation thermo-chemical models of protoplanetary disks I. Hydrostatic disk structure and inner rim, 2009, A&A 501, p.383-406

Woods P.M. and Willacy K. (2008), Carbon isotope fractionation in protoplanetary disks, arXiv:0812.0269v1 [astro-ph] 1 Dec 2008]

udfa.ajmarkwick.net/downloads/rate13_code.pdf, an Introduction to Astrochemical Modelling , Catherine Walsh (with some additions from Tom Millar), June 2009, June 2013, July 2014

UMIST (University of Manchester Institute of Science and Technology) 2012: http:// udfa.ajmarkwick.net/

Further reading :

Aguńdez M. and Wakelam V. (2013), Chemistry of Dark Clouds: databases, networks, and models, arxiv.org/pdf/1310.3651

Aresu G. et al. (2010), X-ray impact on the protoplanetary disks around T Tauri stars, arXiv:1011.5623v2 [astro-ph.SR] 29 Nov 2010

Armitage P.J. (2014), Lecture notes on the formation and early evolution of planetary systems, arXiv:astro-ph/0701485v4 26 Aug 2014

Barone V. et al. (2015), Gas phase formation of the prebiotic molecule formamide:insights from new quantum computations, Mon. Not. R. Astron. Soc. 000, p.1-6, arXiv:1507.03741v2 [astro-ph.GA] 15 Jul 2015

Bergin E.A. et al. (2006), The Chemical Evolution of protoplanetary Disks, arXiv preprint arXiv:0908.3708, 2009

Carrasco E. et al. (2013), Proton transfer chains in cold plasmas of H2 with small amounts of N_2. The prevalence of NH_4^+, Phys. Chem. Chem. Phys.,15, p.1699-1706

Dalgarno A. & Black J.H. (1976), Molecule formation in the interstellar gas, Rep. Prog. Phys. 39 573 (http://iopscience.iop.org/0034-4885/39/6/002)

Dullemond C. P. and Monnier J. D. (2010), The inner regions of protoplanetary disks, arXiv:1006.3485v1 [astro-ph.SR]17 June 2010

Geers V.C. et al. (2008), Lack of PAH emission toward low-mass embedded young stellar objects?, arXiv:0812.3664v1 [astro-ph] 18 Dec 2008

Herbst E. (1985), An update of and suggested increase in calculated radiative association rate coefficients, The Astrophys.Journ., 291, p.226-229

Herbst E. (2001), The chemistry of interstellar space, Chem. Soc. Rev.,vol.30, p.168–176

Herbst E. and van Dishoeck E.F.(2009), Complex Organic Interstellar Molecules, Annu. Rev. Astron. Astrophys., vol.47, p.427–480

Hogerheijde M. et al. (2011), The water ortho-to-para ratio in a protoplanetary disk, Leiden Observatory, http://www.lorentzcenter.nl/lc/web/2011/469/presentations/Hogerheijde.pdf

Hudson R.L. & Loeffler M.J. (2013), Ketene formation in interstellar ices: a laboratory study, The Astrophys.Journ., 773, pp.109-119

Jaber A.A. et al. (2014), The census of complex organic molecules in the solar type protostar IRAS16293-2422, arXiv:1406.7195v1 [astro-ph.SR] 27 Jun 2014

Jørgensen J.K. et al. (2005), H_2CO and CH_3OH abundances in the envelopes around low-mass protostars, arXiv:astro-ph/0503599v1 28 Mar 2005

Klippenstein S.J. et al. (2010), Temperature dependence of two key interstellar reactions of H_3^+: O (^{3}P) + H_3^+ and CO + H_3^+, J. Phys. Chem.A, 114, p.278–290

Kwok S. (2009), Organic matter in space: from star dust to the Solar System, Astrophys Space Sci., 319, p.5–21

Loison J.-C. (2014), The interstellar gas-phase chemistry of HCN and HNC, MNRAS, 443 (1), p.398-410

Lüttjohann E., Inaugural Dissertation zur Erlangung der Doktorwürde der Math.-Nat. Gesamtfakultät der Ruprecht-Karls-Universität Heidelberg (2011),Chemische und mineralogische Entwicklung Protoplanetarer Scheiben.

Mathis J.S., Rumpl W. and Nordsieck K.H. (1977), The size distribution of interstellar grains, The Astrophys.Journ., 217, p.425-433

Martinez_Jr.O. , (2008), Gas phase study of C^+-reactions of interstellar relevance, The Astrophysical Journal, vol.686, p.1486-1492

Natta A. and Testi L. (2007), Dust in protoplanetary disks: properties and evolution, in: "Protostars and Planets VI", Ed.: Reipurth B., Jewitt D., Keil K., University of Arizona Press

Öberg K. et al. (2010), The Spitzer ice legacy: Ice evolution from cores to protostars, arXiv:1107.5825v1 [astro-ph.GA] 28 Jul 2011 July 14th

Öberg K.I. et al. (2010), A cold complex chemistry toward the low mass protostar B1-B: evidence for complex molecule production in ices, arXiv:1005.0637v1 [astro-ph.GA] 4 May 2010

Richthofen J. Freiherr von (2002), Untersuchung der Bildung, des Isotopenaustausches und der Isomerisierung des Ionensystem HCO^+/HOC^+, Dissertation zur Erlangung des Dr. rer. nat., Fakultät für Naturwissenschaften der TU Chemnitz, Deutschland

Roberge W.G. et al. (1991), Interstellar photodissoziation and photoionisation rates, The Astrophys.Journ.Suppl.Series, 77, p.287-297

Semenov D., Wiebe D. and Henning T. (2002), Reduction of chemical networks; I. The case of molecular clouds, arXiv:astro-ph/0212096v1 4 Dec 2002

Smith M.A., Schlemmer S. et al. (2002), $HOC^+ + H_2$ isomerisation rate at 25K:implications for the observed $[HCO^+]/[HOC^+]$ ratios in the ISM, The Astrophys.Journ., 578:L87–L90

Smith I.W.M. et al.(2004), Rapid neutral-neutral reactions at low temperatures: a new network
and first results for TMC-1, Mon.not. R. Astron. Soc. 350, p.323-330

van Dishoeck E.F. (2004), ISO Spectroscopy of Gas and Dust: From Molecular Clouds to Protoplanetary Disks, arXiv:astro-ph/0403061v1 2 Mar 2004

van Dishoeck E.F. (2006), Chemistry in low-mass protostellar and protoplanetary regions, PNAS, vol. 103, no.33, p.12249–12256

Vidali G. et al. (2006), Syracuse University N.Y.(USA), A summary of experimental results on H_2 formation on dust grain analogues, http://physics.syr.edu/research/astro

Viggiano A.A. et al. (1980), Laboratory studies of some ion-atom reactions related to interstellar molecular synthesis, The Astrophys.Journ., 236, p.492-497

Woitke P. et al. (2009), Hot and cool water in Herbig Ae protoplanetary disks: a challenge for Herschel, arXiv:0906.0448v2 [astro-ph.EP] 3 Jun 2009

O.1. List of Figures

Frontispiece: IRAS 04302+2247 edge-on disc 3

Fig. B.1.: Schematic diagram of a protoplanetary disc 10
Fig .B.2.: Three chemically distinct zones in a PPD 13

Fig.D.3.1.: Pattern of the Reaction Trees 18
Fig.D.3.2.: Reactions of formation and destruction of H_3^+ 19
Fig.D.3.3.: Reactions of formation and destruction of He^+ 19
Fig.D.3.4.: Reactions of formation and destruction of N_2H^+ 20
Fig.D.3.5.: Reactions of formation and destruction of CO 21
Fig.D.3.6.: Reactions of formation and destruction of HCO^+ 23
Fig.D.3.7.: Reactions of formation and destruction of C^+ 24
Fig.D.3.8.: Reactions of formation and destruction of CH^+ 25
Fig.D.3.9.: Reactions of formation and destruction of CH_2^+ 26
Fig.D.3.10.: Reactions of formation and destruction of CH_3^+ 27
Fig.D.3.11.: Reactions of formation and destruction of CH_5^+ 28
Fig.D.3.12.: Reactions of formation and destruction of HCN 29
Fig.D.3.13.: Reactions of formation and destruction of CN^+ 30
Fig.D.3.14.: Reactions of formation and destruction of O^+ 31
Fig.D.3.15.: Reactions of formation and destruction of O_2H^+ 32
Fig.D.3.16.: Reactions of formation and destruction of *OH 33

Fig.E.1.4.1.: Development of a chemical network improvement 37
Fig.E.1.4.2.: Development of a chemical network in a 30/30 grid point matrix 37
Fig.E.1.4.3.: Chemical network in a 40/40 grid point matrix ..... .38

Fig. F.3.1.-4.: log ε (CO) of the models DM, C , E and "F" 46

Fig. G.2.1.: Definition of the areas I and II 48
Fig. G.12.: RTs with the most important reactions in thesis models A and C 57

Fig. H.2.1.: Comparison log ε (CO) of models DM , A , B, C, D and E 61
Fig. H.2.2.: Comparison log ε (HCO^+) of models DM , A , B, C, D and E 62
Fig. H.2.3.: Comparison log ε (HCN) of models DM , A , B, C, D and E 63
Fig.H.3.1.: Heating processes vs.Cooling Processes of models DM, A and C 65
Fig.H.4.1.: log T_{gas} ; T_{gas} / T_{dust} of the models A, DM and C 66
Fig.H.5.2.: Line fluxes of some species in model DM, A, C and D. 68
Fig.H.6.1.1.: Chemical composition of the gas in the reference model DM 70
Fig.H.6.1.2.: Chemical composition of the gas in the model A. 71
Fig.H.6.1.3.: Chemical composition of the gas in the model B. 72
Fig.H.6.1.4.: Chemical composition of the gas in the model C. 73
Fig.H.6.2.1.: Chemical composition of condensates/ ices in the model DM. 74
Fig.H.6.2.2.: Chemical composition of condensates / ices in the model C. 75
Fig.H.6.3.1.: CO_2 and CH_4 as gas and condensates / ices in models A , DM and C 76
Fig.H.6.3.2: Distribution of CO, CO2, CH4, CO2#, CH4# in models A, C, and DM 77

O.2. List of tables

Tab.D.1.1.: Stellar and disk standard parameter for the model calculations 16

Tab.E.1.1.: Elements and abundances of the reference model DM 35
Tab.E.1.2.: 90 UMIST2012 species of the reference model DM....35
Tab.E.1.2.: Condensates / ices for the reference model DM....36
Tab.E.1.3.: 81 Non-UMIST reactions used in ProDiMo code....82
Tab.E.1.5.: Overview of the reference model DM....36
Tab.E.1.6.: Test model "Ch.41" created out of model "Ch.40"....38
Tab.E.1.7.: Overview of the interim model "Ch.43New"....39

Tab.F.1.: Elements and abundances of the thesis models A – E....42
Tab.F.2.: 68 UMIST2012 species of the thesis models A – E....42
Tab.F.2.1.: Overview of the thesis models A – E ("F")....43
Tab.F.3.: Condensates / ices for the thesis models C – E (and "F")....43
Tab.F.4.: Additional 94 reactions concerning condensates/ices....85

Tab.G.2.2.-3.: Main and second main reactions of CO for model C....48
Tab.G.2.4.: 1^{st} and 2^{nd} formation and destruction reactions....86
Tab.G.3.1.: Formation and destruction reactions of CO, CO^+ and CO#....50
Tab.G.3.2.: Formation and destruction reactions of HCO^+....50
Tab.G.3.3.: Formation and destruction reactions of CO_2, and CO_2#....51
Tab.H.3.4.: Formation and destruction reactions of $HCO2^+$....51
Tab.G.3.5.: Formation and destruction reactions of HCN, HCN^+ and HCN#....52
Tab.G.3.6.: Formation and destruction reactions of CN and CN^+....52
Tab.G.3.7.: Formation and destruction reactions of $C_2H_2^+$....53
Tab.G.3.8.: Formation and destruction reactions of dust....53
Tab.G.3.9.: Formation and destruction reactions of e^-....54
Tab.G.3.10.: Commonly used reactions in models A-E and DM....55
Tab.G.3.11.: Important reactions used in the thesis models A – E....56

Tab.H.5.1.: Line fluxes, of atoms and molecules in PPDs....67